University of Zurich[UZH]

Department of Informatics

Explorations on the role of robot morphology in legged locomotion

A dissertation submitted to the Faculty of Economics, Business Administration and Information Technology of the University of Zurich

for the degree of
Doctor of Science (Ph.D.)

by

Farrukh Iqbal Sheikh

from Pakistan

Accepted on the recommendation of

Prof. Dr. Rolf Pfeifer
Prof. Dr. phil. Andre Seyfarth

2014

The Faculty of Economics, Business Administration and Information Technology of the University of Zurich herewith permits the publication of the aforementioned dissertation without expressing any opinion on the views contained therein.

Zurich, June 13, 2014

Head of the Ph.D. program in informatics: Prof. Dr. Abraham Bernstein

Acknowledgements

I am indebted to the assistance and feedback of the dissertation committee. A special thanks to my supervisor **Prof. Dr. Rolf Pfeifer**, who gave me the opportunity to work in an exciting EU-project "Locomorph FP7-231688". Sincere thanks to Prof. Dr. phil. Andre Seyfarth and Dr. Helmut Hauser for their constructive feedback. Their reviews, suggestions and guidance helped me a lot in order to improve the thesis material and compiling interesting results.

I would like to extend my thanks to all my friends, especially Sheraz dar, Syed Guffran Ul Haq, Vu Quy Hung, Tao Li, Qian Zaho, Dr. Nathan Labhart and Dr. Lijin Aryananda for their help, corporation and encouragement during the work. In addition, I am very thankful to all my national friends from Zurich, Dr. Zeeshan Zia, Sarmad Rashid, Qasim Imtiaz, Assad. Without their selfless support and help, I might not be able to extend my research to the four-legged system.

Last but not least, I would like to express my special thanks to my *Ammi, Abbu*, my *wife* and my brothers, who have always been supporting, motivating and encouraging me throughout my stay at abroad. With yours prays, I am able to cope with difficult situations and accomplish all the goals. Finally, I appreciate the selfless support of the IFI-UZH staff members during my stay at the Artificial Intelligence Laboratory (Ai-Lab), University of Zurich.

Zusammenfassung

Tiere mit Beinen können sich agil, vielseitig, anpassungsfähig und energieeffizient in unstrukturierten Geländearten fortbewegen. Diese Eigenschaften sind mit dem heutigen Stand der Beinrobotik noch unerreicht. Viele Forschende haben Beinroboter mit unterschiedlichen Morphologien konzipiert, um diese Eigenschaften zu studieren; es ist jedoch eine grosse Herausforderung, nachgiebige Roboterbeine zu konstruieren, welche die gleichen Anforderungen wie Tierbeine erfüllen. Zudem macht es die hochgradig nichtlineare Interaktion von nachgiebigen, passiven Roboterbeinen mit der Umwelt sehr schwierig, deren Eigenschaften zu verstehen. Konventionelle Gestaltungsansätze zielten darauf ab, eine festgelegte nachgiebige Bein-Funktionen zu erreichen, aber Nachgiebigkeit und die Ruhelänge der Bein-Federn sind in der Biologie keine konstanten Parameter. Es ist deshalb interessant zu untersuchen, wie Variationen solcher morphologischen Parameter die Bewegung beeinflussen. In der vorliegenden Arbeit liegt der Fokus auf der Einstellbarkeit der Beinlänge.

In dieser Dissertation präsentieren wir einen neuartigen rekonfigurierbaren Mechanismus, der es uns erlaubt, die Beinlänge in Echtzeit zu ändern. Diese Eigenschaft wird benötigt, um die Funktion eines Beinstreckmuskels zu simulieren, der sich während der Bewegung zusammenzieht (Faser-Kontraktion) und ausdehnt (Faser-Verlängerung). Zusätzlich erlaubt er uns, ein Roboterbein mit unterschiedlichen Längen zu erstellen (willenliche Morphose). Indem wir diese Eigenschaft mit einer seriellen passiven Feder einbinden, konstruierten wir zwei Typen von Beinrobotern: Einen einbeinigen Hüpfroboter mit rekonfigurierbarer Beinlänge (RLLH) und einen vierbeinigen Roboter, der sich unterschiedlichen Terrains anpassen kann (DTAR). Um Prinzipien der dynamischen Bein-Fortbewegung zu untersuchen, haben wir jeweils Experimente mit open-loop Ansteuerung durchgeführt.

Die Forschung mit RLLH zielte darauf ab, Prinzipien der energieeffizienten, adaptiven und schnellen Fortbewegung zu untersuchen. Zuerst studierten wir die Ähnlichkeit der robotischen Beinfunktionen mit federartigen Beinfunktionen im Modell des Masse-Feder Modells (SLIP). Im zweiten Schritt erkundeten wir die Vorteile unterschiedlicher Beinlänge bei der Anpassung an verschiedene Untergründe. Drittens entwickelten wir Steuerprogramme zur Änderung der Geschwindigkeit und zum Wechsel zwischen Gangformen (von vorwärts- zu rückwärtsgerichteter Bewegung) von schnellem einbeinigen Rennen (0.8 – 1.2 m/sec) mit open-loop Ansteuerung. Viertens steigerten wir die Leistungsfähigkeit unseres Roboterbeines, indem wir die Rolle zweier unterschiedlicher Fuss-Morphologien untersuchten. Unsere Resultate legen nahe, dass ein nachgiebiger, gelenkiger Fuss die Energieeffizienz beim einbeinigen Rennen steigern kann.

Da eine einbeinige Roboterplattform nur eine beschränkte Anzahl Gangarten zeigen kann, erweiterten wir unsere Forschung zu einem vierbeinigen System (DTAR). Dieser Roboter verwendet vier Module mit unterschiedlichen Beinlängen. Er wurde eingesetzt, um Manövrierfähigkeit und verschiedene Gangarten zu untersuchen. Wir zeigen, dass die Manövrierbarkeit eines vierbeinigen Systems durch Veränderungen der ipsilateralen Beinpaare kontrolliert werden kann. Diese Eigenschaft ist nützlich, um die Stabilität zu erhöhen und gleichzeitig den Kontrollaufwand,

um den Roboter in verschiedene Richtungen zu steuern, zu minimieren. Zudem zeigen die vorläufigen Resultate von dynamischen Gangarten (Gangart Pronk und Gangart Bound) bei vierbeinigen Systemen einen starken Zusammenhang mit denjenigen von einbeinigen Systemen, d.h. das Design von selbst-stabilisierenden Hüpf- und Springarten des vierbeinigen Systems kann auf dem Verständnis des einbeinigen Systems aufbauen.

Die vorliegende Forschung zeigt auf, dass es unerlässlich ist, die natürlichen Dynamiken von Beinrobotern zu untersuchen, um die Rolle der Morphologie als Basis effizienter, schneller und vielseitiger Fortbewegung zu verstehen. Die aktive Veränderung der Beinmorphologie (z.B. Ruhelänge und Fuss-Nachgiebigkeit) ist eine sinnvolle Strategie, um sich effizient in unstrukturierten Geländearten fortzubewegen.

Abstract

Legged animals are capable of agile, versatile, adaptive, and energy-efficient locomotion over unstructured terrain. These attributes are still unmatched by today's legged robots. Many researchers have been studying these properties by designing legged machines of various morphologies. However, it is very challenging to design compliant robotic legs that encompass all of the aforementioned properties. Moreover, understanding each of these characteristics in the context of passive compliant legged locomotion is even more difficult because of highly non-linear interactions of the passive compliant robotic leg with its environment. Conventional design approach was aimed at achieving fixed compliant leg function, but compliance and rest length of leg spring are not fixed parameters in biology. Thus, it is of interest to study how such morphological parameter variations can influence locomotion. Here, the primary focus is on changed leg length.

In this thesis, we present a novel reconfigurable mechanism that allows us to alter the leg length in real-time. This feature is realized to mimic the function of a leg extensor muscle that contracts (fiber contraction) and extends (fiber lengthening) during locomotion to perform the required work on tendons (passive spring). In addition, it enables us to produce a robotic leg of various lengths (voluntary morphosis). By embedding this feature in series with a passive spring, we constructed two types of legged robots: a single-legged reconfigurable leg length hopper (RLLH) and a four-legged differential terrain adaptive robot (DTAR). Each was experimented with open-loop control to investigate principles of dynamic legged locomotion.

The research conducted using the single-legged RLLH was aimed at exploring principles of energy-efficient, adaptive, and rapid locomotion. First, we studied the similarity of the robotic leg function to the spring-like leg function as assumed in the spring loaded inverted pendulum (SLIP) model. Second, we explored the advantage of the variable leg length feature in adapting to different ground conditions. Third, we developed the speed and transition (from forward to backward direction) control of fast single-legged running (0.8 – 1.2 m/sec) using open-loop control. Fourth, we improved the performance of our robotic leg by investigating the role of two different foot morphologies. Our results suggest that a compliant articulated foot can enhance the energy efficiency of a single-legged running.

Knowing the fact that the single-legged platform can only exhibit a limited number of gaits, we extended our research to a four-legged system (DTAR). The DTAR robot uses four variable leg length modules. It was used to study maneuverability and different gaits. We report that the maneuverability of a four-legged system can be controlled by introducing a change in ipsilateral pairs of legs. We found that this feature is very useful to increase stability and minimize control effort for steering the robot in different directions. Furthermore, the preliminary results of dynamic gaits (pronk and bound) in a four-legged system show a strong relation to the single-legged system, i.e., the self-stable pronk and bound gaits of the four-legged system can be designed based on the understanding gained by the single-legged control.

The research presented here shows that it is essential to explore the natural dynamics of the legged robot system as it can help us to understand the role of a robot morphology and identify

the basis of efficient, fast, and versatile locomotion. The active change in leg morphology (e.g., rest leg length and foot compliance) is a useful strategy for legged robots to efficiently deal with unstructured environments.

Contents

List of Figures

Chapter 1

Introduction

Legged animals can traverse many conceivable terrains that vary in nature such as soft as swamp, hard as rock, rough as pebble, discrete as stair, steep as mountain, etc. Animals adapted such skills over evolutionary time-scale by varying their morphology and learning through trial and error [Alexander, 2003]. By exploiting both (morphology and control) animals are able to demonstrate fast and energy efficient locomotion in various types of terrains. However, legged robots that are built and programmed to achieve similar levels of performance as animals, are still at their earlier stage regarding fast, adaptive and energy-efficient locomotion. Legged robots targeting to produce animals-like performance can help us to advance our understanding of the principles of animals and humans locomotion in general. In this research, we aim at identifying optimal robot morphologies (shape and material) and control mechanisms that enable fast and energy-efficient legged robots for unstructured environments.

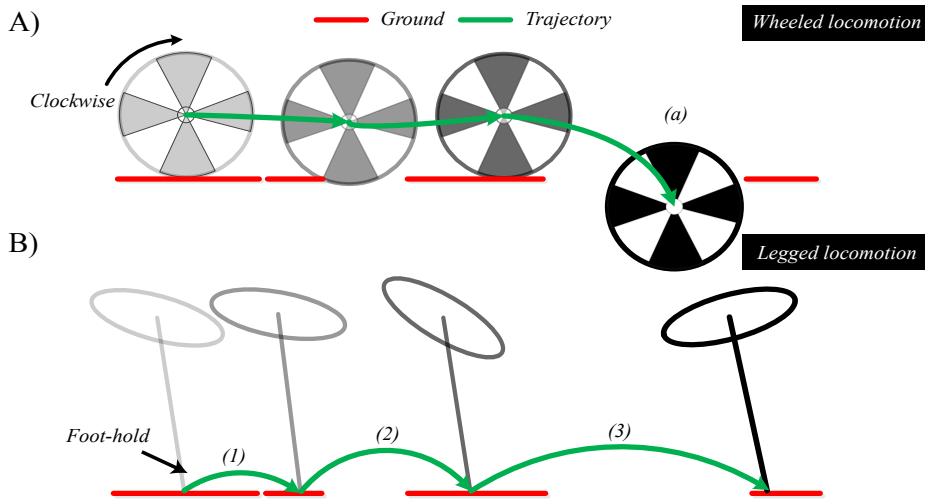

Figure 1.1: A comparison between wheeled and legged locomotion. A) shows a scenario where wheeled locomotion fails. B) indicates how the legged locomotion can overcome the same challenging ground as in A. Label (1)-(3) indicate various steps: (1) short step, (2) moderate step, and (3) leap.

Legged robots can better negotiate uneven terrains than wheeled robots because they have the ability to place their legs at discrete locations (foot-fall pattern). At the same time, they may

have flight phases, which is advantageous in dealing with different types of terrains. Imagine a situation where a robot has to deal with a terrain that consists of isolated ground patches as shown in Fig. 1.1. In this case, wheeled robot locomotion may fail when the distance of separation between two consecutive ground patches is too large. On the other hand, a legged robot has the potential to jump over the gap between the two consecutive ground patches. This particular feature makes the legged robot suitable for traversing highly unstructured terrain.

In the past, many legged robots have been built aiming at efficiently handling rough terrains. They can be grouped into two categories based on the number of active and passive joints: fully actuated legged robots and under actuated legged robots. Fully actuated legged robots were previously built to enhance robot mobility by increasing the number of active joints [Kimura and Fukuoka, 2000; Tsujita et al., 2001; Rebula et al., 2007], whereas under actuated legged robots were constructed to improve agility and energy efficiency by replacing some active joints by the passive joints [Papadopoulos and Buehler, 2000; Iida et al., 2009]. Many fully actuated legged robots (no passive compliance) turned out to be slower in exhibiting dynamic legged locomotion, i.e., unable to exhibit running gaits (pronk, bound and gallop) and mainly move forward on walking gaits. This may be due to several reasons: stiff leg design, increase in overall weight (more motors), limited actuation power, and employing complex control approaches. Despite the limitation of dynamic gaits in the fully-actuated robots, they are increasingly popular in the development and testing of control strategies for handling rough terrain [Vernaza et al., 2009], where the careful placement of the foot at a particular foot-hold is important to ensure stability while walking. On the other hand, under-actuated robots have more passive compliant joints to target energy-efficient locomotion. However, this particular feature also limits the under-actuated robot's performance to handle rough terrain. By considering the merits of these two different approaches (see chapter 2), we designed and constructed a novel robotic leg mimicking the function of biological muscles and tendons. This robotic leg uses a reconfigurable (variable) joint, which functions in series with a passive mechanical spring. By utilizing this mechanism, we built two types of modular legged robots (single-legged and four-legged), which can be positioned in between the aforementioned categories of legged robots. In addition, we define three design goals for our robots to be fulfilled before exploring several characteristics of legged locomotion, e.g., energy-efficient, adaptive, maneuverability and gait versatility:

1. Mimicking the dynamics of the leg spring as described by the SLIP (spring loaded inverted pendulum) model.
2. Online voluntary morphosis, i.e., able to adjust the rest leg length for mimicking a robotic leg of various heights.
3. Gait versatility, i.e., able to produce animal-like gaits (walk, trot, bound, and gallop).

1.1 Dynamics of the SLIP (spring loaded inverted pendulum) Model

The dynamics of running animals and humans are frequently described by the SLIP model [Blickhan et al., 2007]. The SLIP model consists of a point mass (body), a mass-less spring (leg) and an infinitesimal point contact (foot) (see Fig. 1.2B). This mechanical model is able to capture the underlying dynamic of a running animal by describing/predicting the excursion of the animal body's center of gravity (CoG) during periodic cycles of running. As can be seen in Fig. 1.2, despite the musculo-skeletal complexity of a Kangaroo (see Fig. 1.2A), its hopping and running behavior can be described by the spring-mass model (see Fig. 1.2B). This model is also known as a reduced parameter model for animal locomotion because it essentially describes the dynamics

of large groups of animals by producing similar ground reaction forces, as observed in kangaroo hopping [Kram and Dawson, 1998] and human running [Blum et al., 2009].

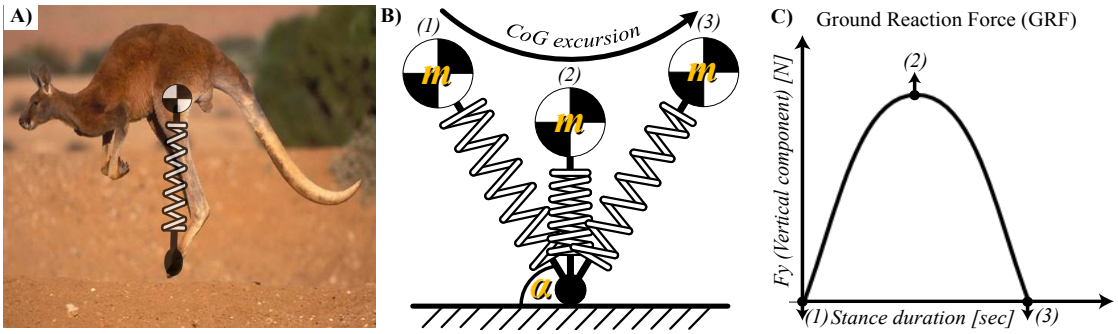

Figure 1.2: Mechanics of running. A) hopping locomotion of a kangaroo (adapted from [BBC, 2014]). B) 2D illustration of the spring mass model. C) approximate vertical ground reaction force pattern predicted by the SLIP model during ground contact phase. The GRF in (C) is similar to the ground reaction force observed in human and animal locomotion. Label (1), (2) and (3) in (B) and (C) describe following sequence of events during ground contact phase: (1) - touch down, (2) - mid stance and (3) - lift-off. The curved arrow in B) above indicates the excursion of body center of gravity (CoG).

The SLIP model is considered to be a good representation of legged locomotion as it requires only a small number of parameters (angle of attack and leg-stiffness) to describe certain types of animal locomotion, e.g., walking and running. Therefore, it can be considered as a template, i.e., minimalistic model to describe a given behavior [Full and Koditschek, 1999]. However, this model needs to be advanced further to gain additional insights into the mechanics and control of a physical legged robot. Physical legged robots face real-world constraints, such as limited power to weight ratio actuators, leg masses, shape of the foot, compliance in the joints, etc. By considering these real-world constraints, building a legged robot based on template models is challenging.

1.2 Online Voluntary Morphosis

Legged animals self-adjust their morphology to increase adaptivity to current tasks and environments. This particular attribute of legged animal locomotion, where animals actively change their morphology (shape) is defined as voluntary morphosis as considered in the EU project "Locomorph". Some situations, where this attribute enhances locomotion performance, are illustrated in Fig. 1.3. As can be seen in Fig. 1.3A, a four-legged goat is stepping down a steep mountain. While climbing down it changes the proportion of leg length of its front and hind pair of limbs that allows the goat to gain stability over an inclined surface. Similarly, in Fig. 1.3B, where a bonobo first reduces the length of its hind-limbs to shift its body mass to the hind limbs before making the complete transition from quadruped to biped walking. Finally, Fig. 1.3C shows the dynamic maneuverability of a cheetah that clearly inclined its body to the left by changing the leg length of its lateral pair of legs to achieve high-speed turning.

Fig. 1.3 highlights that animals often change the nominal length of individual legs to achieve stable, versatile and adaptive locomotion. Thus, by varying leg length online in a robot may increase stability, versatility and adaptivity over unstructured terrain. The concept of change in

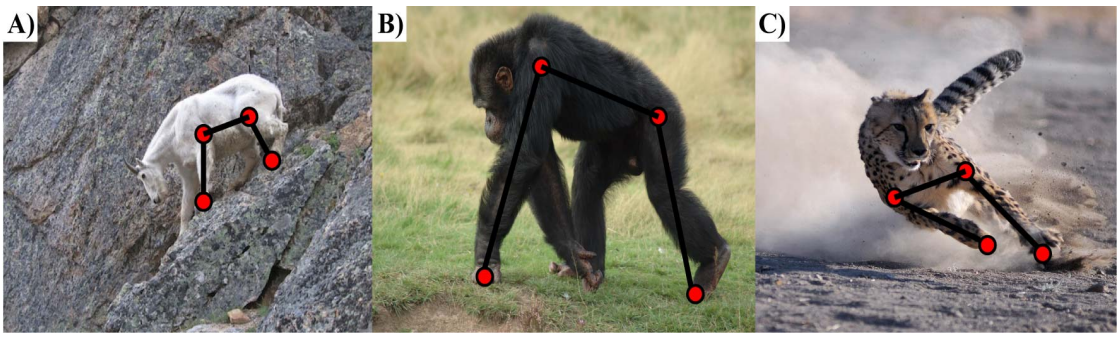

Figure 1.3: Voluntary morphosis in four-legged animals. A) Mountain goat stepping down from the inclined mountain, B) Bonobo locomotion on level ground before transition from quadruped to biped walking and C) dynamic maneuverability in a cheetah. Overlaid stick figures indicate connecting lines between feet and hip/shoulder joints.

leg length can be interpreted in different ways. Suppose that the leg length is defined as the distance from the hip to toe joint. By this definition, human can change its leg length by moving the lower leg segment (shank) relative to the upper leg segment (thigh) about the knee joint. This way of manipulating the leg length can be achieved by having a multi-segmented leg. It allows human to change its leg length during a "single" stride (short period), e.g., walking with the actuated knee. However, if we want to simulate the leg length of two or more humans of different heights then we need to physically construct two or more robotic legs. In this thesis, the ability to produce different legs is considered as "voluntary morphosis". This feature is implemented by the reconfigurable leg length mechanism. This mechanism allows us to mimic various lengths without compromising the angular range of leg oscillation. We will study how this design feature can enhance the locomotor function of the robot (see chapter 3).

1.3 Gait Versatility

Four-legged animals can locomote with a wide range of gaits. These gaits are classified as "symmetrical" or "asymmetrical" based on the temporal relation of the gait-specific foot-fall pattern. In symmetrical gaits, the movement of a pair of legs, e.g., (left hind and right fore legs) is repeated by the movement of the other pair of legs (left fore and right hind legs). For example, trotting is a symmetrical gait in which the opposite diagonal pairs of legs move $180\,\mathrm{deg}$ out of phase from each other. In contrast in asymmetrical gaits, like bound and gallop, the movement of one pair of legs is not followed by another pair of legs. More importantly, asymmetrical gaits also have a single aerial phase during a stride [Alexander, 2003]. It is potentially useful for running fast and for jumping over gaps. Most of the four-legged animals that use asymmetrical gaits are capable of running faster than animals of same size moving with a symmetrical gait. Therefore, it is important to implement both kinds of gaits in a four-legged robot to achieve versatile (slow and fast) locomotion. We built a four-legged robot to better understand the interplay between body morphology and control required for achieving different gaits.

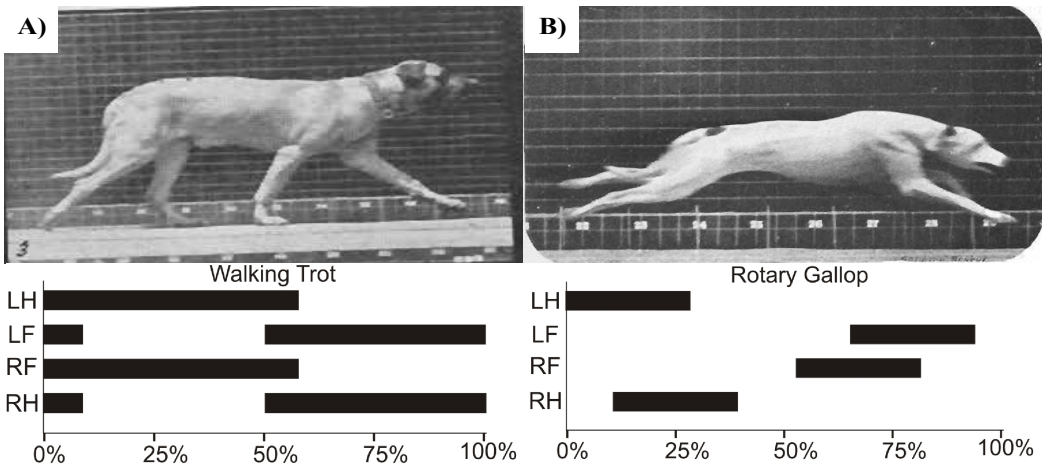

Figure 1.4: Dynamic gaits of a four-legged dog. A) and B) are the pictures taken from [Muybridge, 2007]. A) trot of a walking dog. B) gallop of a running dog that has an aerial phase during the single stride. In A), there is no aerial phase, whereas in B) there is a clear aerial phase that enables fast locomotion. The foot-fall patterns of trotting and galloping are indicated below.

1.4 Research Questions

Previously described three synthetic design requirements are very challenging to be realized in a physical legged robot platform. In this work, we built two legged robots: a single-legged reconfigurable leg length hopper (RLLH) and a four-legged differential terrain adaptive robot (DTAR). Both are designed to meet our synthetic design requirements for the following characteristics of legged locomotion: energy-efficiency, adaptability, high speeds, maneuverability, and gait versatility. Based on each of these characteristics of legged locomotion, we formulate the following research questions.

1. Is our designed robotics able to generate the SLIP-like ground reaction forces?
2. Which approach should we employ to understand dynamic legged locomotion?
3. Which criteria do we use to quantify the performance of our robot?
4. How can energy-efficient running be realized in a compliant robotic leg?
5. Can this robotic leg adapt to the changes in ground surfaces without changing the mechanical spring?
6. How can we control speed and direction of single-legged locomotion using a simple open-loop control?
7. Can we improve speed and energy efficiency in a legged robot by modifying morphology?
8. How can we achieve maneuverability by adjusting robot morphology in an open-loop control?
9. Can a four-legged robot achieve versatility in dynamic gaits, e.g., trot, pronk, bound, etc?

In order to answer the research questions listed above, we designed our research methodology by which we analyzed and evaluated the performance of our robots. Here, we follow a bio-mechanical approach. To study locomotion in the field of bio-mechanics, it is common to use the following motion analysis techniques: 3D force plate, optical motion capture and video recording. These measurement systems provide an accurate measurement of the subject's body dynamics. For example, 3D force plate can accurately measure the ground reaction forces (GRF) and the optical motion capture measures the motion of individual joints. These measurements are usually obtained from an observer perspective, i.e., they are external sensory measurements, which are unable to provide information about the activities of different muscle and tendon groups. However, the internal sensory information is equally important as the external sensory measurements to quantify the overall dynamic of human and animal locomotion. Though, it is hard to state, which sensory information is more important than the other as it seems to be a frame of reference problem. For example, the frame of reference problem explains that the continuous change in the environment with respect to an observer or vice versa changes the representation of a problem [Pfeifer and Scheier, 1999]. According to this concept, it is important to have both types of sensory measurements. We designed our experimental setup to support this idea such that we can study the complex dynamic behavior of our physical legged robot systems as accurately as possible. In this thesis, we gathered both internal and external sensory measurements of our robot such that we can understand and evaluate behaviors. As a result of this, our 2D single-legged hopper can run at a speed of about 0.8 – 1.2 m/sec without any global sensory feedback. Furthermore, we demonstrate that the single-legged control can be used to create different gaits of the four-legged robot. This means that the control approach of the single-legged system can be extended to control the four-legged system.

1.5 Thesis Outline

Each chapter of this thesis is designed to provide a conclusion of its respective research question. The organization of the chapters is as follows:

Chapter 2 reviews the previous work on legged robots. Section 2.1 provides a review on the bio-mechanical approach and introduces the spring-mass model. Section 2.2 compares existing robot designs and their control approaches to demonstrate the potential of different legged robots. Section 2.3 describes the implication of the embodiment framework in our research methodology that may bridge the gap between an experimental and a theoretical approach.

Chapter 3 addresses research question 1. For this, we introduce the key design features of our novel single-legged robot (RLLH). This robot can successfully hop in-place by generating SLIP-like ground reaction forces that are also similar in magnitude to the normalized ground reaction forces observed in human in-place hopping experiments.

Chapter 4 focuses on the research questions 2–5. It explains the concept of energy efficiency in compliant robotic leg locomotion during in-place hopping. In addition, it illustrates the concept of adapting to the ground properties like stiffness, damping and friction, by using the reconfigurable leg length mechanism in a passive compliant robot.

Chapter 5 extends the simple open-loop control by exploiting the intrinsic body dynamics of our single-legged robot. In this work, we demonstrate that the simple open-loop control can be used to control speed and changes in direction of fast single-legged running. In addition, it enables us to characterize the in-place hopping gait further into vertical in-place hopping and

oscillatory in-place running.

Chapter 6 is focused on exploring the effect of foot morphologies. In this chapter, we investigated two foot morphologies to enhance running speed and energy efficiency of our existing single-legged robot system (RLLH).

Chapter 7 provides the concept of maneuvering our four-legged system. In this chapter, we show that by changing the robot morphology through leg reconfiguration, we can achieve dynamic maneuverability using a simple open-loop control. This demonstrates how the morphology may contribute to simplifying the control of turning.

Chapter 8 provides the summary and discussion of the results presented in this thesis and draws the conclusions.

Chapter 9 highlights the future directions of this work.

Chapter 2

Background

In this chapter, we provide the background of our research methodology. We have reviewed related work from the field of bio-mechanics, robotics and embodied AI, to extract three synthetic design requirements that are essential for a dynamical fast legged robot. Section 2.1 provides a brief review on the work done in the field of bio-mechanics that have strengthened our understanding of the locomotor behavior of animals and humans. Section 2.2 discusses some state of the art legged robots that were successful in some aspects of achieving basic legged locomotion tasks, such as moving with a particular gait, coping with rough terrain, etc. Section 2.3 highlights the implications of the embodiment concept in the context of this work. Finally, we describe our research methodology.

2.1 Bio-mechanics

In the field of bio-mechanics, principles of human and animal locomotion are studied by the two types of mechanical models: complex and simple mechanical models. Complex models are developed based on the complexity of human and animal anatomy such that behaviors can be studied in greater detail, whereas simple models can explain the same behavior by abstracting the complexity of the system. Inspired by the fact that simple models are easier to comprehend, Alexander presented two simple models to describe the maximum walking speed and optimal jumping in humans [Alexander, 1992]. The walking model (inverted pendulum) consists of a body center of mass (COM) located at the hip and a straight stick (stiff) leg. With the help of this inverted pendulum model, the maximum speed of human walking was estimated. This estimation was simply described by the body COM vaulting over the stiff leg such that the body moves along a circular arc (see Fig. 2.1 top). In this way, the body exerts a centripetal acceleration towards the ground for speed below this threshold $v \leq (gr)^{1/2}$. In this equation, v represents the walking speed, g is the gravity constant, and r is the length of the rigid leg. It describes the speed limits of human walking. Later, by extending this simple model, the concept of jumping in athletes was described. This model consists of a body center of mass located at the hip and two mass-less segmented leg. One upper leg segment connects the hip joint to the knee and the lower leg segment connects the knee to the foot. By considering the force-velocity characteristics of a knee extensor muscle, an optimal jumping distance and jumping height were predicted. These two very simple models describe effects of the underlying leg mechanics of walking and jumping in humans. However, the direct application of these models in designing a robot is not straight forward due to their simplicity. Similarly, the spring-mass model [Blickhan, 1989; McMahon and Cheng, 1990] describes the dynamics of running and hopping in animals and humans (see Fig. 2.1 bottom). Although, the musculo-skeletal systems of animals and humans are enormously complex, during running and hopping, their overall behavior can be explained by the bouncing motion of a

point mass (representing as an animal body) in series with a mass-less spring (representing as a leg) [Blickhan, 1989]. Despite the simplifications, the results from this model were surprisingly similar to the dynamics of running animals [Blickhan, 1989; Blum et al., 2009]. Nowadays, this model is known as the SLIP (Spring Loaded Inverted Pendulum) model.

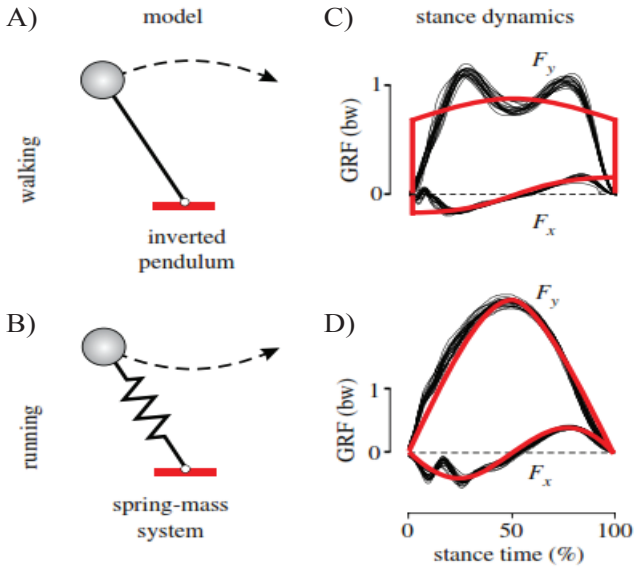

Figure 2.1: Simple models for walking and running (adapted from [Geyer et al., 2006]). A) is the inverted pendulum model for walking (top) in which the body CoG moves along the circular arc; B) is the running model (bottom), which is represented by the spring-mass model. C) are the vertical (upper graph) and horizontal (lower graph) ground reaction force (GRF) patterns for walking and B) is the GRF pattern for running.

In early studies, walking was described by the inverted pendulum model in which the body vaults over the stiff leg during stance, i.e., the trajectory of the body center of mass (COM) follows a circular arc [Alexander, 1992], and running was described by the spring-mass [Blickhan, 1989], where the trajectory of the body COM nearly follows the behavior of a mass supported by a spring-like leg. However, both walking and running are behaviors of the same human body, then why their mechanical models are significantly different? This was experimentally studied by Lee et al., [Lee and Farley, 1998]. They ran experiments with humans whose stance-limb deflection or compression of the leg length (the distance from hip to toe) was measured during walking and running. They showed that the leg compression in human walking is only 26% less than the leg compression in human running. In order to overcome the discrepancy in walking and running models, [Geyer et al., 2006] demonstrated that the ground reaction force pattern of human walking cannot be accurately described by the inverted pendulum model, but can be comprehended better by the spring loaded inverted pendulum model (see Fig. 2.2). As a result of this study [Geyer et al., 2006], the SLIP model has now become a standard model to study both human walking and running.

The running behavior of a legged machine can also be described by the SLIP model. Inspired by this, the SLIP model has been increasingly investigated in the field of legged robot locomotion. The conventional SLIP model is a conservative mechanical model, i.e., total energy (sum of kinetic and potential energy) remains constant during each stride of locomotion. However, in

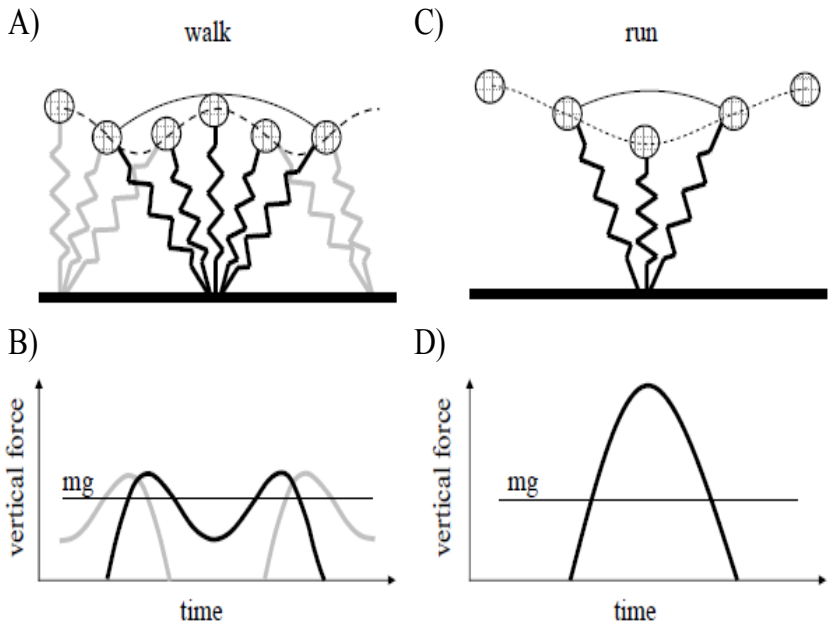

Figure 2.2: Spring-mass model for walking and running (adapted from [Blickhan et al., 2007]). A) and B) describe walking using the spring-mass model. C) and D) described running using the spring-mass model. It is important to note that the GRF pattern of walking and running was matched by the spring-mass model.

a physical system input energy (supplied energy) is never equal to the output energy. In other words, physical systems dissipate some of the supplied energy in the form of heat due to the presence of mechanical friction or electrical resistance (e.g. in robots). Therefore, the role of energy losses and supply has to be taken into account. In order to address this issue, the SLIP model was advanced further by incorporating damper and rotary actuator (see Fig. 2.3). These advanced variants of the SLIP model are known as TD-SLIP (Torque-Actuated Dissipative Spring Loaded Inverted Pendulum) [Ankarali and Saranli, 2010], and the CT-SLIP (Clock Torque Spring Loaded Inverted Pendulum Model) [Seipel and Holmes, 2007]. In these models, the damper represents the amount of energy loss per stride and the actuator serves as an active source to re-supply that lost energy back into the system; thereby the stable hopping and running more similar to the real system can be simulated. Recently, [Sebastian and Seyfarth, 2011] showed that changing the rest length of the leg spring may support energy stability to running gaits by compensating energy losses (e.g. due to leg damping or changing leg stiffness). This is an alternative approach to the torque-based energy supply mechanisms described with the TD-SLIP and CT-SLIP models. However, it is not yet fully understood, how energy supply and dissipation is generally organized in human and animal locomotion.

In summary, different variants of the SLIP models are useful tools to understand the mechanics of walking and running. However, these models cannot capture each and every single detail of the real system that deals with the real environment. For example, legged robots are composed of complex arrangements of electromechanical subsystems: motor, spring, gears, motor drivers, amplifiers, controllers, low-level control, high level control, sensors, mass in the legs [Peuker et al., 2012], different materials, etc. How each of these subsystems work in connection with other in real physical environments can be very difficult to model accurately. Therefore, the SLIP model is considered as a template in [Full and Koditschek, 1999] that can be used as a basic requirement

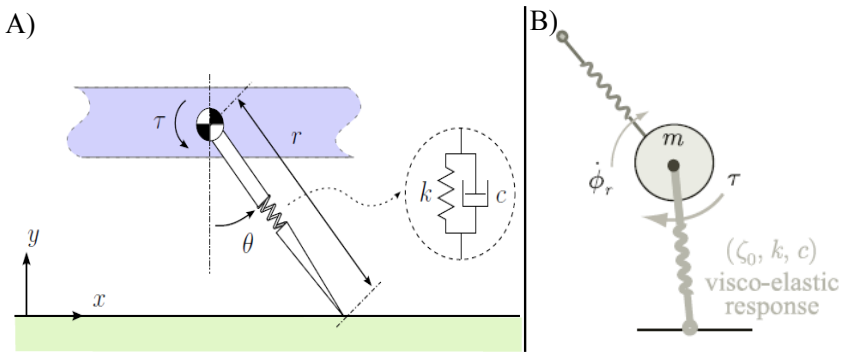

Figure 2.3: Advancement in the spring loaded inverted pendulum models. A) is the TD-SLIP model (adapted from [Ankarali and Saranli, 2010]), and B) is the CT-SLIP model (adapted from [Seipel and Holmes, 2007]). Both, TD and CT SLIP model incorporate actuator and damper to make the SLIP model bit more realistic.

for building legged systems. Then, by building and experimenting with the legged robots that exhibit SLIP like properties, we can advance these models further and their applicability in building physical legged systems. In this thesis, we consider the SLIP model as the underlying design principle for our legged robot system to demonstrate running. Furthermore, we experimented with our legged robots based on a bio-mechanical approach. This means that our experimental results may contribute to some extent to the advancement of these mechanical models. For example, if our robot is able to mimic running and walking dynamics of human and animal then an accurate simulation model of our robot can be a good starting point for improving the existing SLIP model.

2.2 Legged Robots

Research in the field of designing, controlling and modeling legged robots has been progressing rapidly for over three decades. The aim of this research is as follows: First to seek new legged robot morphologies, control methods and experimental approaches that may help to increase agility and mobility of man-made machines to handle very challenging terrains. Second, this research may also lead us to a better understanding of some of the characteristics of animal and human locomotion. Normally legged robots vary in size, number of legs, segments in legs, type of actuators used in legs and compliance (mechanical spring) in legs, etc. Therefore, there are potentially many ways by which existing legged robots can be distinguished and categorized. In this thesis, we grouped existing legged robots in to two categories: under-actuated and fully-actuated. This categorization can be achieved by looking at the number of active joints and passive joints in a particular design of the robotic leg. For example, if a robotic leg consists of 3 active joints (no passive joint or mechanical spring) then this particular robotic leg falls in to the category of the fully-actuated robot. Similarly, if the legged robot consists of 1 active and 1 passive joint (mechanical spring) then this robotic leg is under-actuated. Furthermore, this review only covers existing single-legged (hopper), two-legged (biped) and four-legged (quadruped) robotic systems.

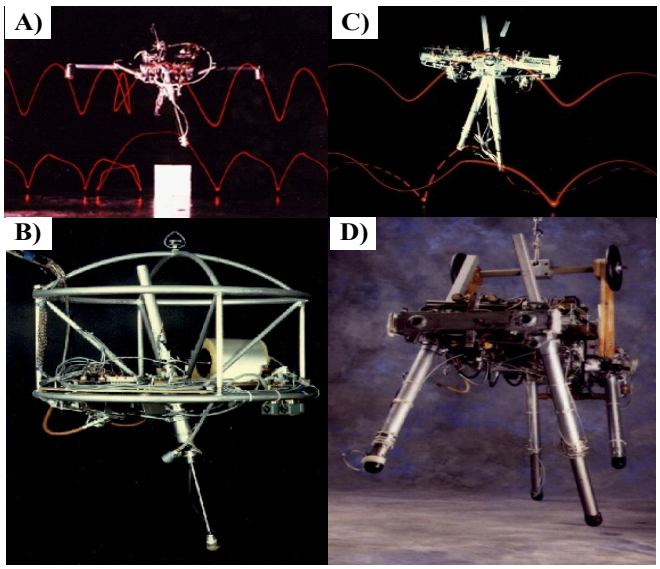

Figure 2.4: Legged robots built in the 80's (adapted from [Raibert, 1986a]). A) is the 2D single-legged planar hopper. B) is the bipedal planar runner. C) is the 3D single-legged hopper. D) is the four-legged runner.

2.2.1 State of the Art in Legged Robots

In the field of legged robots, Marc H. Raibert and his colleagues [Raibert, 1986b] studied the role of actively balanced locomotion in physical legged robots in the 80's. Their work was pioneering in the field of legged robot locomotion. They built number of prototypes: single legged planer hopper [Raibert, 1986a], 3D single legged hopper [Raibert et al., 1984], biped [Hodgins and Raibert, 1991] and quadruped [Raibert, 1990]. In all these prototypes, the leg design was kept telescopic comprising hydraulic and pneumatic actuators. The hydraulic actuator swung the leg in fore and aft direction, while the pneumatic actuator created a variable air-spring along the leg axis that can be controlled by regulating the pressure of compressed air. In addition, the switching valves were used to excite the leg spring by controlling the flow of compressed air in a cylindrical tube along the leg axis.

The control approach to actively balance and run these legged machines [Raibert, 1986b] consisted of three closed-loop control levels: one regulates the hopping height, the second one controls the body attitude and third one controls the forward speed. By this arrangement, they demonstrated that these machines were able to hop in-place and jump over obstacles, while maintaining the balance against small mechanical perturbation [Raibert, 1986a]. Moreover, the balance of most complex movements, such as somersault, was also successfully controlled [Playter and Raibert, 1992]. They showed that the same approach worked nicely in controlling the locomotion of the 3D single legged hopper, biped and quadruped robot [Hodgins and Raibert, 1991; Raibert, 1990]. However, the powerful pneumatic actuator limits the use of such machines to the laboratory, because pneumatic actuator usually works on a pressured air that can either be supplied by a compressor or by cartridge [Daerden and Lefeber, 2000]. Furthermore, these robots are heavier and had fixed morphologies.

In mid 90's, Martin Buehler and his team constructed numerous dynamic legged robots [Buehler et al., 2000], namely monopod ARL I, ARL II, SCOUT quadruped I, II and six-legged Rhex. Except the six-legged Rhex that uses C-shaped compliant legs, the single and four legged robots

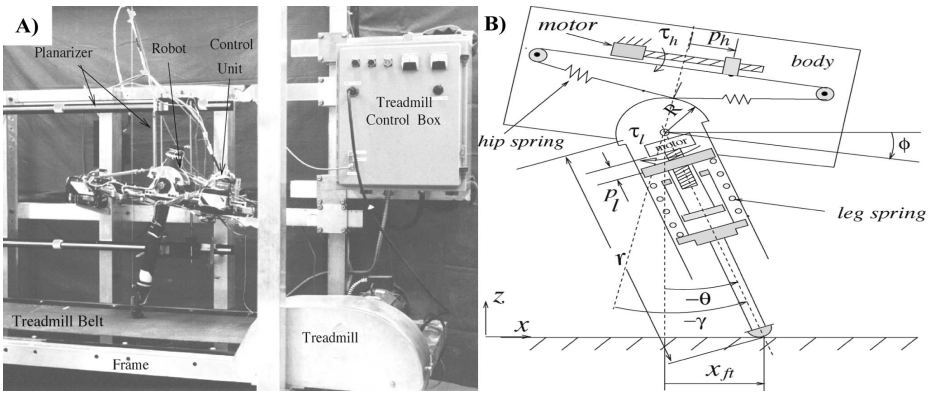

Figure 2.5: ARL monopod II (adapted from [Ahmadi and Buehler, 1997]). A) is the physical ARL monopod II running on treadmill and B) indicates the schematic of ARL II.

were mainly inspired by the design approach of [Raibert, 1986a]. They kept the design of a robotic leg similar to Raibert's, i.e., telescopic, and replaced the powerful actuators (hydraulic and pneumatic) by the low-cost conventionally DC brushed motors in series with a mechanical spring. This allows them to realize an autonomous robotic platform for both indoor and outdoor environments. The ARL monopod II was an electrically actuated 2D hopper [Ahmadi and Buehler, 1997] that uses two active joints: rotary and prismatic (see Fig. 2.6). The rotary joint was attached to the body unit that actuates the telescopic leg in fore and aft direction with the help of a timing-belt and a pulley-string mechanism, while the prismatic joint was realized by a ball-screw mechanism that works in series with the passive mechanical spring (steel coiled spring), as a series elastic actuator [Robinson et al., 1999]. Due to this particular leg design, the leg inertia was increased, which increases the resistance in an oscillatory motion of the telescopic leg. Despite the increase in inertia of the robotic leg, a model-driven closed-loop control approach was implemented successfully to control the passive dynamic running of the ARL II on a treadmill [Ahmadi and Buehler, 2006].

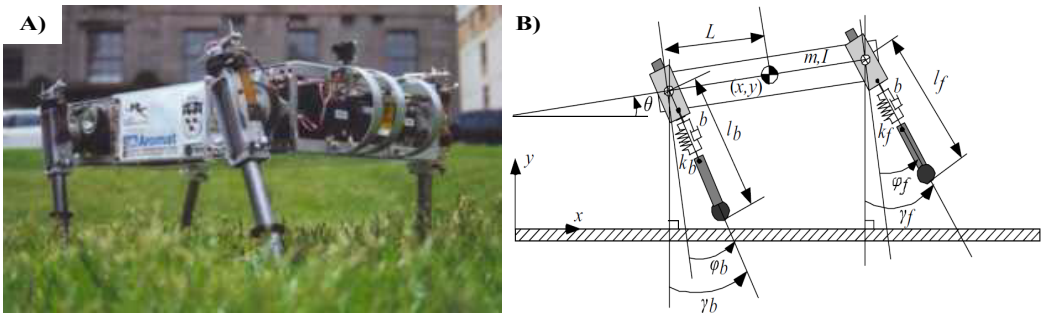

Figure 2.6: SCOUT II the four-legged quadruped robot (adapted from [Papadopoulos and Buehler, 2000]). A) is the real four-legged robot (Scout) and B) is the mechanical representation of the SCOUT robot on a 2D plane.

SCOUT II is a four-legged quadruped robot that can run with a bounding gait using its compliant leg [Papadopoulos and Buehler, 2000; Poulakakis et al., 2004]. The design of the SCOUT II leg was similar to the design of ARL II, i.e., telescopic leg, but instead of using two actuators

per leg, as in the ARL II monopod, only one active (motor) joint per leg was employed that oscillates the compliant telescopic leg in fore and aft direction (see Fig. 2.6). In total, four active joints or DC brushed motors were used in the SCOUT II robot, which considerably reduces the overall weight and makes the four legged system energy-efficient. However, it cannot change its leg length online as is one of our synthetic design requirement to deal with a certain degree of rough terrain.

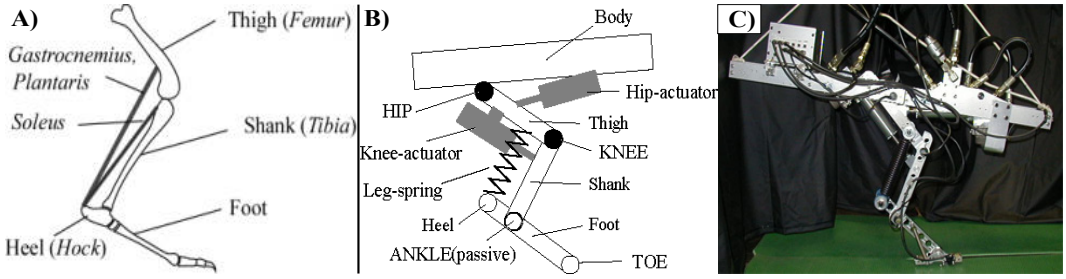

Figure 2.7: Kenken robot (adapted from [Hyon and Mita, 2002]). A) shows the anatomical structure of a dog's hind leg. B) indicates the schematic of the kenken robot that is inspired by figure A). C) is the real picture of the single-legged kenken robot.

The anatomical structure of animal and human leg usually consists of more than one segment, many muscles and tendons that are somehow useful for fast and energy-efficient legged locomotion. Inspired by this fact, a single-legged hopping robot called "Kenken" was developed [Hyon and Mita, 2002]. As can be seen in Fig. 2.7, its mechanical design was mimicking the entire structure of a dog's hind leg including the placement of a tendon called "Gastrocnemius plantaris". This tendon was mechanically realized by placing a big passive spring that connects the rotary motion of the lower-segment foot to the thigh segments via a heel. This robot uses two hydraulic actuators: one to power the swing motion of the robotic leg and the other to retract the leg for higher ground clearance. Similarly, forward hopping of this robot was controlled to achieve a hopping speed of 1.0 m/s. However, it was slightly too complex to be useful as a low-cost legged robot research platform.

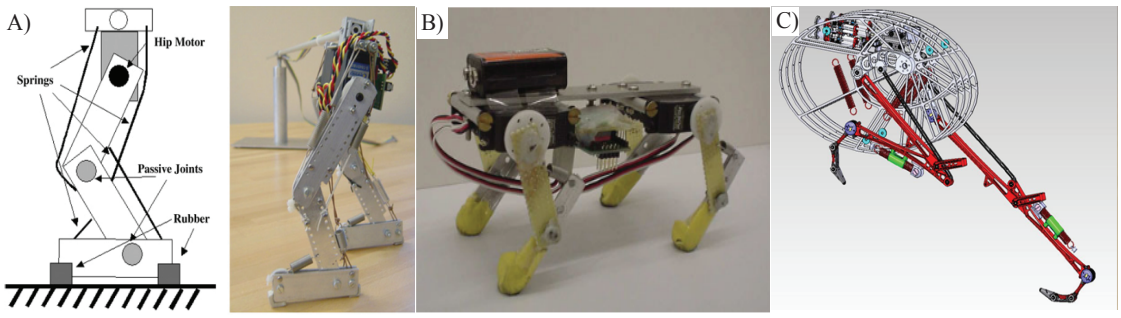

Figure 2.8: Under-actuated legged robots. A) the JenaWalker that mimics the tendon distribution of the human leg by the mechanical springs (adapted from [Iida et al., 2009]). B) the four-legged under-actuated robot (Puppy) [Iida et al., 2005]). C) the bipedal robot (FastRunner). It is taken from [Cotton et al., 2012]).

As we have seen until now, the function of mechanical spring in a robotic leg seems very important as it works very similar to the biological tendons, which is to store elastic strain energy during compression [Alexander, 1990]. By exploiting the role of the mechanical spring in a robotic leg, a multi-segmented compliant bipedal robot was built by Iida et al. [Iida et al., 2009]. This robot was comprised of a number of mechanical springs that are distributed along the segments of the robotic leg. This distribution of mechanical springs was inspired by the distribution of tendons in a human leg (see Fig. 2.8A). This particular leg was under-actuated as it only uses two degrees of freedom to control the oscillation of the two multi-segmented legs side by side. In other words, the function of the knee joint was simply tethered to the passive spring. By applying an open-loop control a limited functionality of human-like bipedal walking was demonstrated. Extending this design approach, a quadruped robot [Iida et al., 2005] named "puppy" was later built. This robot had four compliant multi-segmented legs (see Fig. 2.8B). Each leg consisted of one actuator located at the hip and a mechanical spring about the knee joint. By applying the open-loop control, the forward speed of the robot on a bounding gait was optimized on a treadmill. However, very limited parameter space was explored and only the bounding gait was studied. Following a similar approach a highly compliant and energy-efficient bipedal runner was constructed, named "FastRunner" [Cotton et al., 2012]. The mechanical design of the FastRunner is inspired by the morphology of a bird Ostrich. The planar simulation of this robot shows that it can run fast, up to the speed of 9.8 m/s in open-loop control. However, the real world demonstration of such speed has not yet been shown.

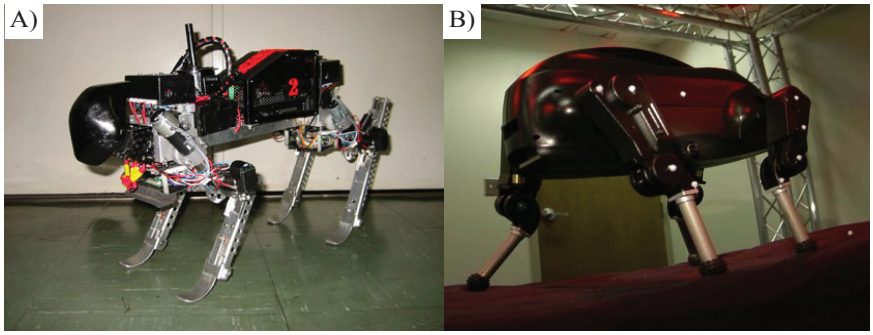

Figure 2.9: Fully-actuated robots with no hardware compliance. A) the four-legged robot "Tekken" (adapted from [KITRoboticsLab, 2003]). B) the Little dog that was built by "Boston Dynamics" and it is taken from [Pongas et al., 2007].

Unlike the under-actuated legged robots [Iida et al., 2005; Iida et al., 2009; Poulakakis et al., 2004], the fully-actuated electric motor driven quadruped robot called the Tekken [Kimura and Fukuoka, 2004] and the Little dog [Pongas et al., 2007; Vernaza et al., 2009] were later built. The leg design of these robots uses three active DoFs per leg, i.e, no passive spring. Instead of adding a mechanical spring (hardware compliance) to save energy, they implemented software controlled compliance per leg using a force/torque control approach. By actuating all three active joints per leg, these robots are potentially more capable of handling a certain degree of rough terrain than the under-actuated robots [Iida et al., 2005; Iida et al., 2009; Poulakakis et al., 2004]. However, the six legged robot (Rhex) [Saranli et al., 2001] is an exception as it can rotate its C-shaped compliant leg to full 360 deg, which is identical to the motion of wheel. The main motivations behind fully actuated robots were to advance the locomotion control of the quadruped robot on rough terrain, provided that an exact model of the terrain is available [Pongas et al., 2007; Vernaza et al., 2009]. However, with the accumulated number of electric motors the weight of these robots increased.

As a result, dynamic fast gaits become difficult to achieve.

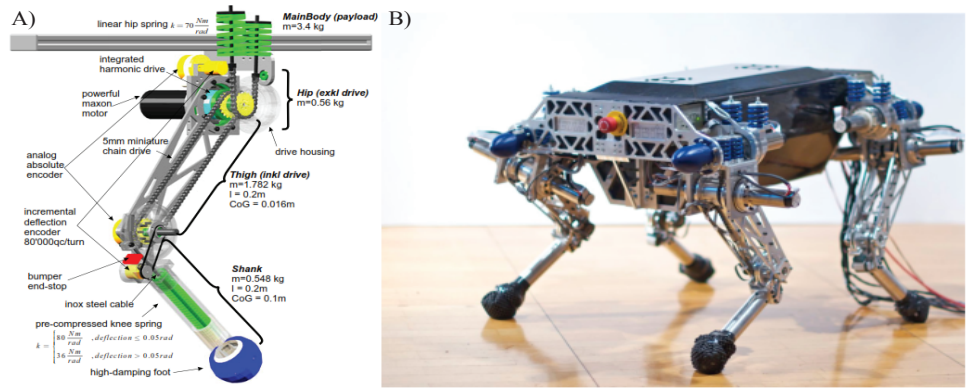

Figure 2.10: Single-legged and four-legged compliant legged robots developed by the team of ETH, Zurich. A) is the mechanical design of the single-legged compliant robot, which is called ScarlETH (adapted from [Hutter et al., 2013]). B) is the four-legged compliant robot, which is called STARLETH (adapted from [Hutter et al., 2012]). These two legged robots were built based on the principle of SEA (Series Elastic Actuator).

Contrary to the completely stiff fully-actuated design of the little dog robot, a single-legged compliant legged robot named "ScarlETH (Series Compliant Articulated Robotic Leg)" was recently built by ETH [Hutter et al., 2013]. It is designed based on the principle of series elastic actuators (SEA) [Robinson et al., 1999]. As can be seen in Fig. 2.10, the mechanical design of ScarlETH consists of two segments that are equal in length. These two segments bend about the knee joint to change the distance of between hip to toe of the robot. Moreover, the bending of the lower leg segment was powered by the motor located at the hip joint by using a mechanical chain, which considerably reduces the leg inertia. However, the forward locomotion speed of ScarlETH turned out slower (0.6 m/s [Hutter et al., 2013]) compared to the running speed of ARL-II [Ahmadi and Buehler, 1997] and our single-legged robot RLLH [Sheikh, 2013]. By utilizing similar leg design of the ScarlETH, a four-legged StarlETH (Springy Tetrapod with Articulated Robotic Legs) [Hutter et al., 2012] was developed. It is built for fast, efficient and versatile locomotion. This robot is potentially capable to produce different gaits, however currently the stable slow-trot gait has been tested by utilizing a high bandwidth closed-loop force/torque control.

Increasing research in the field of legged robots requires an affordable research platform. Towards this goal, the compliant quadruped robot a "Cheetah-cub" was built [Spröwitz et al., 2013]. The robotic leg of the cheetah-cub is based on a multi-segmented pantograph mechanical design, which is inspired by the leg segmentation of a cat's leg. It uses a mechanical spring in between the upper segment (l_1) and the lowest (l_3). l_1 and l_3 are parallel to each other (see Fig. 2.11 A)). The cheetah-cub uses eight RC-servo motors. Four motors are connected to the hip joints and the other four motors are attached to the four knee joints by a cable mechanism (see Fig. 2.11 B)). By operating the cheetah-cub in open-loop CPG, a dynamic trot gait was obtained with a highest froude number of 1.30 at speed of 1.42 m/s [Spröwitz et al., 2013]. The froude number is defined as $(\text{speed})^2/(\text{Gravity constant x Hip height})$ [Alexander, 2003]. Moreover, the two leg configurations that are different in segments (SLP (three segments) and ASLP (four segments)), were experimented. Interestingly, both leg configurations resulted the similar speed of locomotion. However, the ASLP leg was slightly more robust against ground slippage than the SLP. Following similar design approach, a reservoir quadruped robot was built that mimics the leg

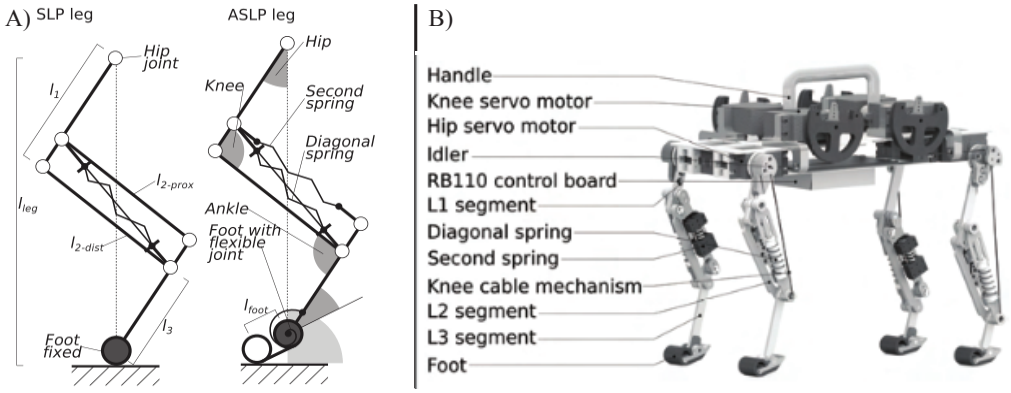

Figure 2.11: The Cheetah-cub robot developed by the team of EPFL. A) shows the schematic of the two pantograph robotic legs: SLP (spring-loaded pantograph) and Advanced-SLP (adapted from [Hutter et al., 2013]). B) depicts the mechanical design of the low cost cheetah-cub robot.

segmentation of a dog's legs [Wyffels et al., 2010]. This robot walked stably in open-loop control. According to these studies [Wyffels et al., 2010; Spröwitz et al., 2013], we can see that the leg segmentation might have certain advantages over telescopic leg. We were interested in such problem in the Locomorph project and based on this, we systematically investigated the role of a single-segmented foot and a two-segmented foot in this thesis (see chapter 6).

Recent research shows that the fast legged locomotion can be achieved by using powerful actuators, i.e., hydraulic and high-power to weight ratio electric actuators [BostonDynamics, 2013a; BostonDynamics, 2013b; MITBiomimeticLab, 2013]. Nevertheless, these four-legged robots are highly expensive and might be less energy-efficient compared to a four-legged robot of the same size that use mechanical springs. Among many electrically actuated robots, the MIT cheetah robot [MITBiomimeticLab, 2013] is an exception in terms of energy efficiency as it can recover some of the supplied energy from the electric motor during each stride [Seok et al., 2013]. This idea to recover supplied energy is based on the principle of regenerative breaking in an electric motor, which is very commonly used in hybrid vehicles to enhance energy efficiency. It has been implemented for the first time in a legged robot (MIT cheetah) that runs fast on a treadmill. Furthermore, the most notable feature of the MIT cheetah [MITBiomimeticLab, 2013] and the Wild-Cat [BostonDynamics, 2013b], is the use of an actuated spine that allows these two robots to run fast by actively bending the spine during each stride. As it is known from bio-mechanics, the cheetah increases its stride length with the help of spine motion [Hildebrand, 1959]. However, the stride length can also be increased to some extent by voluntary morphing of length of the robotic leg. In contrast to the actuated spine, which is indeed very useful, we built our four-legged system DTAR (Differential Terrain Adaptive Robot) using the reconfigurable leg length modules that can change the height of the robotic leg in real-time to increase stride length (see chapter 9). As we have seen, recently developed legged robots are not employing mechanical springs, which is mainly because the spring-loaded joints are difficult to control for precise motion. However, the research is underway to develop better strategies to precisely control compliant joints of robots. Perhaps, our research framework contributes to resolve this issue to some extent (see next section 2.3). Instead of these expensive legged robots [BostonDynamics, 2013a; MITBiomimeticLab, 2013] that are less modular, we were interested to build a compliant legged robot that does not use a conventional fixed joint approach to exploit the passive dynamic of the robot body. Furthermore, our long term goal is to build an affordable legged robot research platform for teaching principles of legged robot locomotion, which is very different from the previously developed

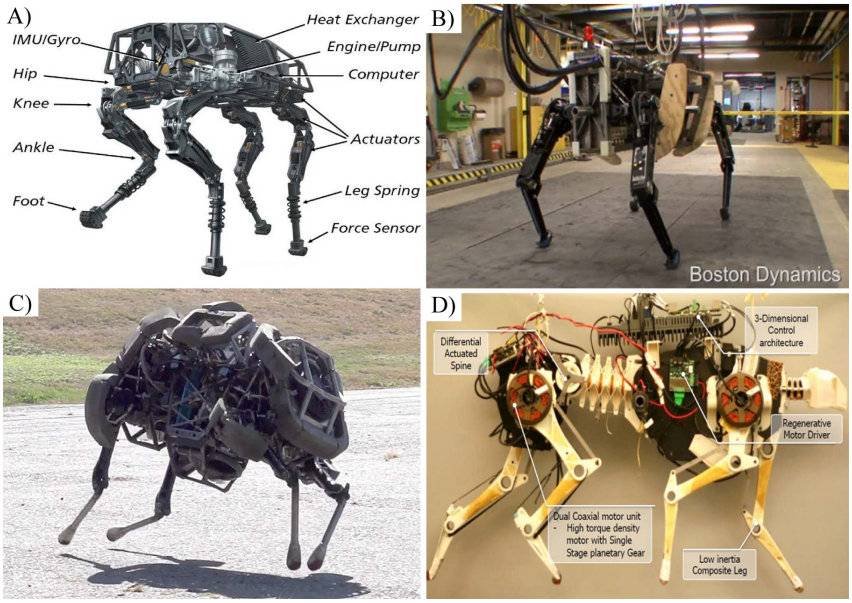

Figure 2.12: Highly advanced legged robots (adapted from [Raibert, 2008; BostonDynamics, 2013a; BostonDynamics, 2013b; MITBiomimeticLab, 2013]). A) the Big-dog that can traverse on rough terrain. B) the Alpha-dog that can carry heavy loads. C) the latest Wild-cat that runs fast by actuating spine. D) MIT-Cheetah robot that also designed to run fast on galloping gait by advancing electric motor technology.

legged robots.

Fig 2.13 illustrates our research framework. As can be seen in Fig 2.13 A), the global research can be divided into three components: control, morphology and environment. Each is indicated by a circle of different colors. Although, it is hard to state, what shape of each of these components should have and how much they should overlap. If we assume that each component is in the form of a circle and they overlapped with each other as indicated in Fig 2.13 A), then this results in eight different parts. Each part is indicated by the numeric labels (1) – (7) and their examples are shown in the lower left corner of Fig 2.13 A). From the author's perspective, each part is important, but the part indicated by the label (7) is more important than the others as it combines the effect of three components. This is defined as the "Embodiment Framework" [Pfeifer et al., 2007] within which this work is performed. The research conducted in this thesis is actually a small subset of the embodiment framework. Fig 2.13 B), illustrates that the legged robot research can be categorized into the two types of legged robots: under-actuated and fully-actuated. The under-actuated legged robots use more passive joints and less active joints. They produce a particular behavior in which the role of morphology dominates. Therefore, the dynamics of such robots are difficult to comprehend because some part of the control is outsourced to the passive compliance of the body. On the other hand, the fully-actuated legged robots use only active joints. These robots can walk over rough terrain by precisely positioning the foot to certain foot-hold, e.g., Litte dog. They require a complex closed-loop approach in which the environment needs to be sensed continuously. Therefore, the fully-actuated legged robots are closer to the control dominant region. In terms of design and control, our robots are situated in between these two existing approaches (see the red-box in Fig 2.13 B). In addition, our research is more focused on exploring the role of robot morphology. *First, our series of legged robots uses springs to aim for energy-efficient locomotion. Second, we add another joint in series with the spring, which is variable and not fixed compared to the*

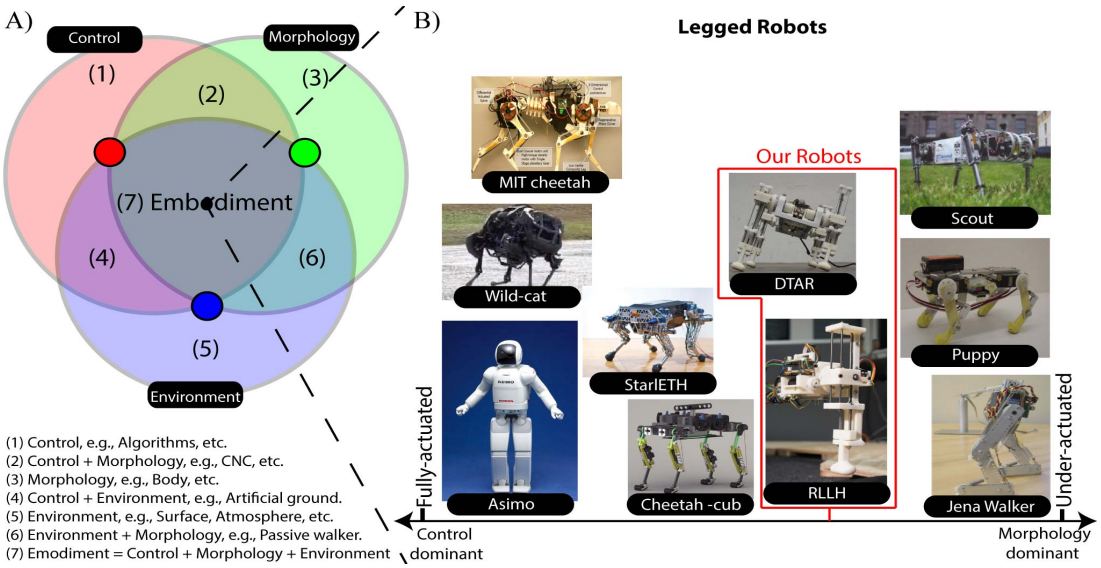

Figure 2.13: Research framework. A) shows the three parts of the global research framework. B) depicts the subset of the embodiment framework in a context of legged robots. The subset is indicated by the dotted lines from the label (7). In A), the dark-red circle at the intersection of control, morphology, and environment is the point, where the control dominates. Similarly, the dark-green circle represents the point, where the morphology dominates and the dark-blue circle indicates the point, where the environment dominates.

existing legged robots. Third, we wanted to advance the open-loop control instead of using the closed-loop because the open-loop exploration can become a strong foundation of a robust closed-loop control for the compliant robots (see chapter 5). Fourth, we kept the design of our legged robots to some extent modular, which was needed to investigate the role of different morphologies and their influence on the control (see chapter 6). Finally, the ultimate purpose of our series of legged robots is to understand the characteristics of legged locomotion such as energy-efficient, adaptive, fast, maneuverability, gait versatility, etc.

2.3 Research Methodology

As described previously, our research methodology is based on the embodiment framework [Pfeifer et al., 2007]. According to the concept of embodiment, it is essential to explore the dynamic coupling of the control and morphology in an ecological niche, i.e., to understand the overall dynamics of a robotic system. In addition, this framework allows us to study self-organized and emergent behaviors that are usually occurred by the interaction of a physical system with the real environment. The research conducted in a real-world environment has a number of advantages. First, it allows us to identify the limitations of the robot's control and body to achieve a particular task. Second, the recorded sensory data can help to explain the particular behavior in greater detail. Third, the results obtained by this approach are directly applicable to the development of a better physical model of legged robot locomotion. Fourth, these results can also be useful to understand the biological system. For example, the function of a mechanical spring is analogous to that of biological tendons [Alexander, 1990] in the context of legged locomotion, so incorporating more mechanical springs in a robotic leg may be useful to understand the role of different groups of tendons in natural systems. Finally, the artificial system requires a control to produce a

particular behavior by the interaction with its environment, i.e., the control approach developed and tested on an artificial system can also be helpful to understand the control working in an natural system. Inspired by these advantages, we anchored this work in real-physical environments instead of simulating robots in a virtual environment. However, the simulations are also very useful to develop a better understanding of a robotic system.

This work was funded by the EU project "Locomorph FP7-231688". The main objective of this project was to explore the role of various morphologies in dynamic legged robot locomotion. According to this project, we conducted our research in two phases. The research done in the initial phase was based on exploring the effects of different morphologies passively, i.e., we changed the morphology of our quadruped robot manually and ran it by using open-loop control in the real-physical environment. For example, we experimented with leg segmentation, increasing the number of active joints, increasing number of passive joints, passive spine, and active spine. We found that it is extremely difficult to explore large number of morphologies in real-physical environments. By realizing this, we later designed a legged robot that can actively change one aspect of the robot morphology and explore its function to understand legged locomotion. Focusing on this, we introduced the idea of having a reconfigurable leg length segment that potentially allows us to produce a robotic leg of various lengths (see chapter 3). In other words, instead of exploring the role of different morphologies, we focused on exploring the role of changeable leg length.

2.3.1 Initial Phase

In the initial phase of our research, we designed and built two types of four-legged robots: UZH-0 and mini-quad modular (Fig. 2.14). The UZH-0 robot was the first quadrupedal robotic platform built in June 2009, as shown in Fig 2.14A. It was built as a learning tool to obtain the domain specific knowledge. It was designed based on an existing robot's morphology, Puppy [Iida et al., 2005]. It had four actuated hip joints and four passive compliant knee joints. The only difference was that its hind legs were rotated 180 deg compared to the hind legs of the Puppy robot. This robot successfully exhibited trot, bound and pace gaits (Fig 2.14A right). However, we could not explore the effect of different morphologies due to its fixed design. Therefore, by exploring other morphologies and their interaction with a real environment, we built another robot called modular "mini-quad" in 2010 (Fig 2.14B). It was built of easily constructable active and passive compliant modules that enable us to experiment with different morphological factors, i.e., passive and active spine, single segment or multi-segmented leg with passive and active joints, passive and active tail, etc (Fig 2.14B right). Each morphological factor was physically embedded and tested in a complete quadruped robot and their performance evaluated based on the criteria of gait versatility (walk, trot, bound, pace), self-stability and energy efficiency.

2.3.2 Final Phase

By gaining practical experience from the initial phase, we extracted three synthetic design requirements (see Chapter 1) for our next robots that can also be used to study a wide range of problems pertaining to legged locomotion in general. Now, in the final phase our research is entirely based on the idea of exploring the role of individual changes in morphology, i.e, changeable leg length. This feature is implemented in a novel compliant robotic leg by using a reconfigurable joint (see chapter 3). By physically embedding this feature in a robot, we constructed two types of research platforms: one is called the single-legged reconfigurable leg length hopper (RLLH) that has two active joints and a single passive joint, and second is called the four-legged differential terrain adaptive robot (DTAR) that consists of eight active joints and four passive joints. Both legged robots used custom designed electronics, software and mechanics to achieve robust locomotion (see Fig. 2.15).

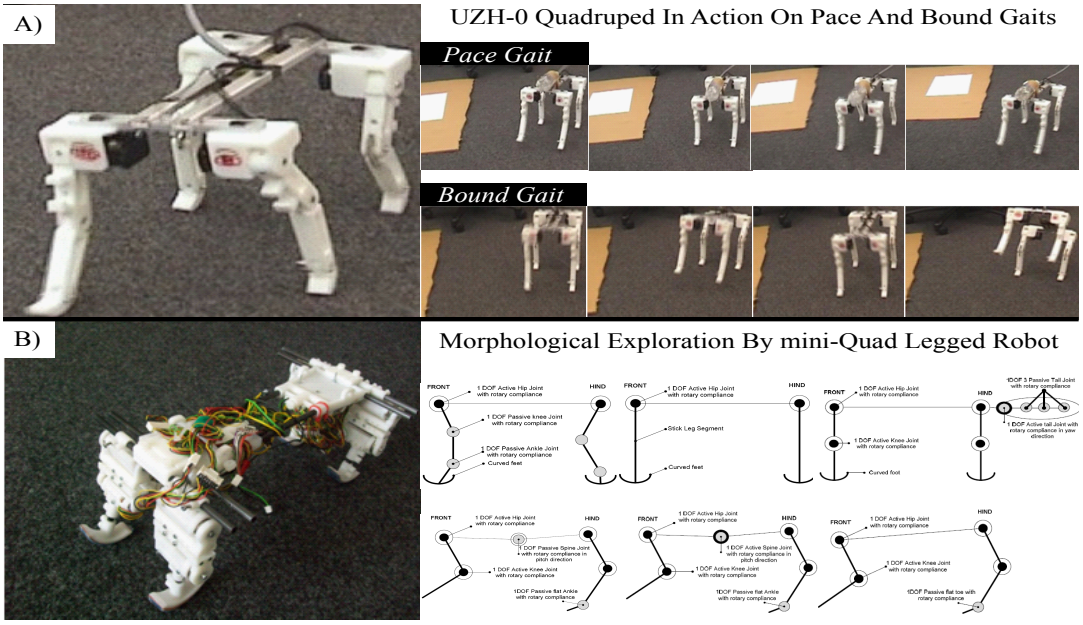

Figure 2.14: Preliminary phase of embodied legged robot locomotion. A) is the UZH-0 quadruped robot built in this thesis. This robot was under-actuated and it uses only four motors to oscillate the four legs. On the right of A) the qualitative results of two gaits (pacing and bounding) are shown. B) is the second quadruped robot named "mini-quad". Using this robot different morphologies were experimented as shown in B).

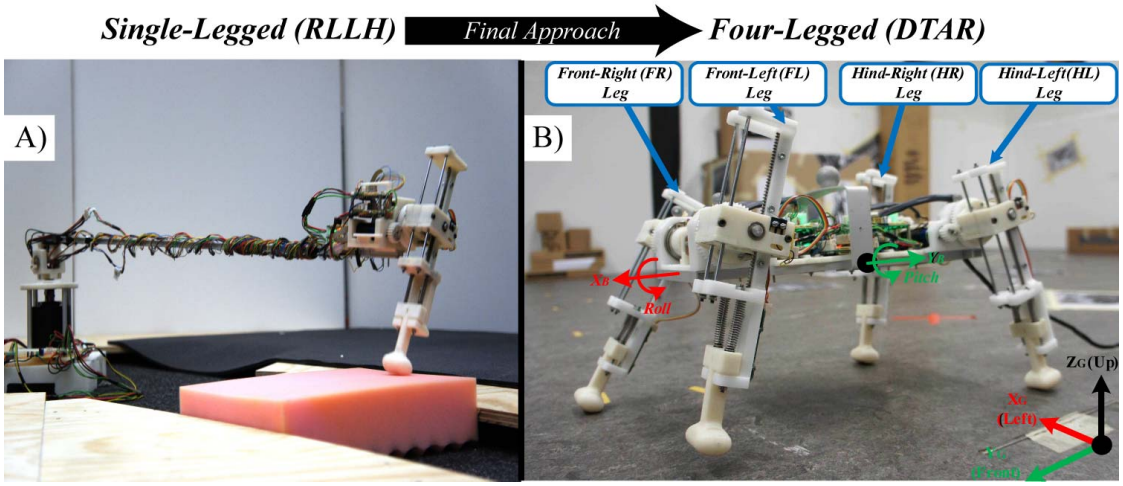

Figure 2.15: Reconfigurable leg length robots. A) the single-legged reconfigurable leg length hopper (RLLH) running on ground surface of different stiffness. B) the four-legged differential terrain adaptive robot (DTAR) that can adapt to terrain geometry through leg reconfiguration (adapted from our publication [Sheikh and Shams-Ul-Haq, 2013]). Arrow on the top shows the direction of our approach that starts from low dimensional to high dimensional systems.

In this phase of our research, we began to study the role of a reconfigurable mechanism using a single-legged system first, and then we explored the feasibility of our single-legged robot (RLLH) to investigate principles of legged locomotion. By realizing the practical limitation of the single-legged robot in producing versatile gaits, we scaled-up the single-legged robot design into a more complicated four-legged system (DTAR) to study maneuverability and gait versatility problems. Furthermore, we aimed at investigating the dynamic coupling of simple control and morphology based on the bio-mechanical approach.

Control

Throughout this thesis, we use a sinusoidal open-loop (feed-forward) control approach, i.e., without any external sensory feed-back. This control approach is simple, but it is also very sensitive to external perturbations, e.g., a little disturbance can easily make the system unstable. However, if the open-loop approach can stably drive the system over rough terrain without any feedback then it is the result of the intrinsic dynamical properties of the system, i.e., self-stabilization. We used open-loop approach as it is suited for rapid locomotion in which the system stability rely mostly on its internal dynamics. Another reason of using this control approach is to systematically explore control-body interaction with its environment such that end control can be extremely simple and robust. Moreover, the role of morphology becomes clear. Therefore, both of our robots (RLLH and DTAR) were controlled systematically in open-loop despite their level of complexity. Furthermore, the range of parameters that we choose to alter systematically was also bio-inspired to some extent. For example, human hopping in-place is the result of bending knee joint at a particular range of frequencies [Farley et al., 1991]. This allows us to start with the frequency and amplitude control parameters of the reconfigurable joint that result in in-place hopping behavior, which is very similar to the in-place hopping in humans (see chapter 3). The control function of the two active joints per robotic leg is described in equation 2.1, whose parameters are systematically altered.

$$\begin{bmatrix} \theta_R(t) \\ d_L(t) \end{bmatrix} = \begin{bmatrix} A_R + O_R + \Delta A_R \sin(\omega_R t + \phi_R) \\ d_0 + O_L + \Delta d_L \sin(\omega_L t + \phi_L) \end{bmatrix} \tag{2.1}$$

where

θ_R is the oscillatory positional command for the fixed rotary joint.

O_R is the offset in leg oscillation.

A_R is the angular reference position of the robotic leg.

ω_R is the angular frequency of oscillating leg.

ϕ_R is the phase shift of θ_R.

d_L is the oscillatory positional command for the reconfigurable linear joint.

d_0 is the initial effective leg length of the robotic leg at rest.

O_L is the offset in change in leg length.

Δd_L is the amplitude of change in leg length.

ω_L is the angular frequency of change in leg length.

ϕ_L is the phase shift of d_L.

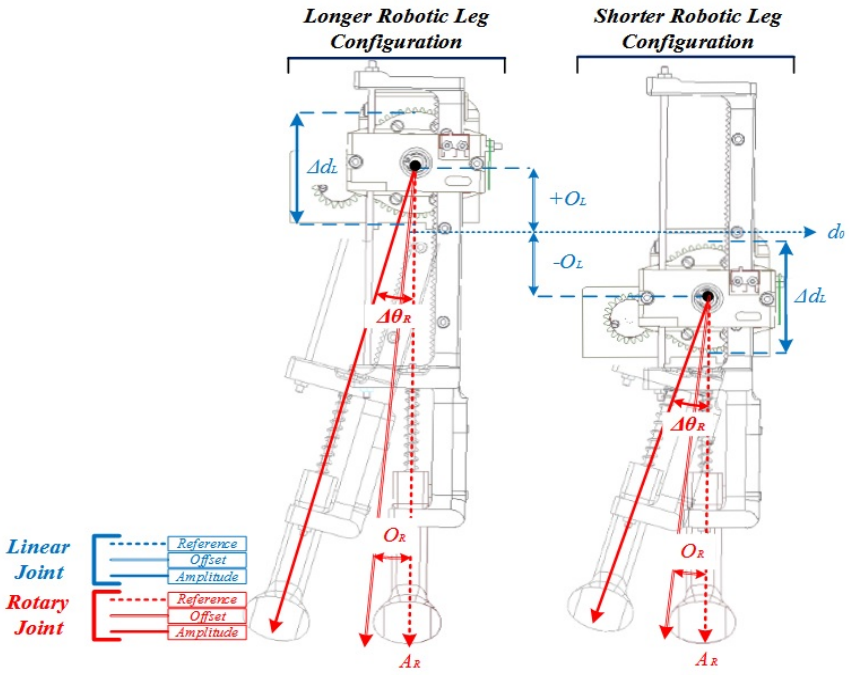

Figure 2.16: Pictorial representation of feed-forward control parameters. Left shows the longer robotic leg configuration and right shows the shorter robotic leg configuration.

Sensory Measurements

Sensory information plays an important role to understand the dynamic coupling between control and morphology, and their interaction with the environment. For example, legged robots tend to exhibit a chaotic behavior all of a sudden on certain control parameters, but why this behavior emerge? Perhaps, this can be studied by looking at the internal and external sensory information together. We equipped both legged research platforms with some internal sensors to . These sensors measures the linear deflection of the spring, leg reconfiguration, motor current, system voltage and leg oscillation. In addition to the internal sensors, we also include the external sensors, e.g., force plate, motion capture, inertial measurement unit (3D gyro and 3D accelerometer).

In most of our studies, we focused on two types of measurements (electrical power and speed) because both can be used to compute the dimensionless parameter called specific resistance or cost of transport (CoT) [Ahmadi and Buehler, 1999]. It allows us to compare the performance of our robots with other legged robots. Furthermore, it is also very useful to see, how these two parameters are affected with respect to the control parameters and the change in morphology. The electrical power consumption of each actuator can explain, which actuator is contributing most to the particular behavior and how much energy is being utilized by the actuator to achieve a particular speed in a specific environment. These three sensory measurements electrical power, speed and specific resistance can be computed by equations 2.2, 2.3 and 2.4. We used this sensory information to identify energy-efficient regions for fast legged locomotion.

Electrical Input Power of the DC Motor:

$$P_{m_i} = V_{m_i} I_{m_i} \tag{2.2}$$

where

i is the index of active joint.

P_m is the electrical power consumption of the electric motor.

V_m is the operating voltage of the electric motor.

I_m is the operating current of the electric motor.

Running Speed of the Legged Robots [Alexander, 2003]:

$$v_x = \Delta x_s f_s \tag{2.3}$$

where

v_x is the running speed.

Δx_s is the step-length or distance covered during a single step.

f_s is the stride frequency or number of steps in a second.

Specific Resistance or Cost of Transport [Ahmadi and Buehler, 1999]:
It is a non-dimensional quantity, which is simply the ratio between the tractive force or thrust force $F_x = P_T/v_x$ and the robot total weight or vertical force $Fy = mg$ [Gabrielli and Kàrmàn, 1950].

$$\epsilon = \frac{P_T}{m_T g v_x} \tag{2.4}$$

where

ϵ is the specific resistance or energy efficiency.

m_T is the total mass of the robot.

g is the gravitational constant.

P_T is the total electrical power consumed by the robot.

v_x is the running speed of robot.

Experimental Platforms

Experimenting in the real-world always requires a good experimental setup. In this thesis, we have employed several experimental platforms, few of them we built by ourselves to study legged locomotion (see Fig. 2.17). Each generation of our experimental setup has evolved based on the complexity of the task that we aimed to investigate using a particular research platform. For example, experimental setup 1 was built to investigate the vertical in-place hopping gait, experimental setup 2 was constructed to understand the role of in-place hopping and forward hopping for fast and adaptive locomotion, and experimental platform setup 3 was used to explore different gaits of the four-legged system. By systematically exploring the body dynamics of single-legged (RLLH) and four-legged (DTAR) robots using open-loop control strategy, we demonstrate that the reconfigurable leg length robots are very useful research tools to investigate principles of legged

locomotion. Although, the systematic approach is highly time intensive as requires large number of experiments, it is an important step towards our long term goal of constructing a better model of legged robot locomotion. According to [Webb, 2001], the physical robot can be a useful model to study a particular behavior of a biological system as it faces real problems that a real biological system encounters in real environments. Following this approach, we can understand the intrinsic dynamics of various types of compliant legged systems in greater detail, which can be useful to build a robust control and better legged robots. In addition, we demonstrate that this approach is highly effective to control the four-legged system (DTAR) based on the knowledge of the single-legged system (RLLH).

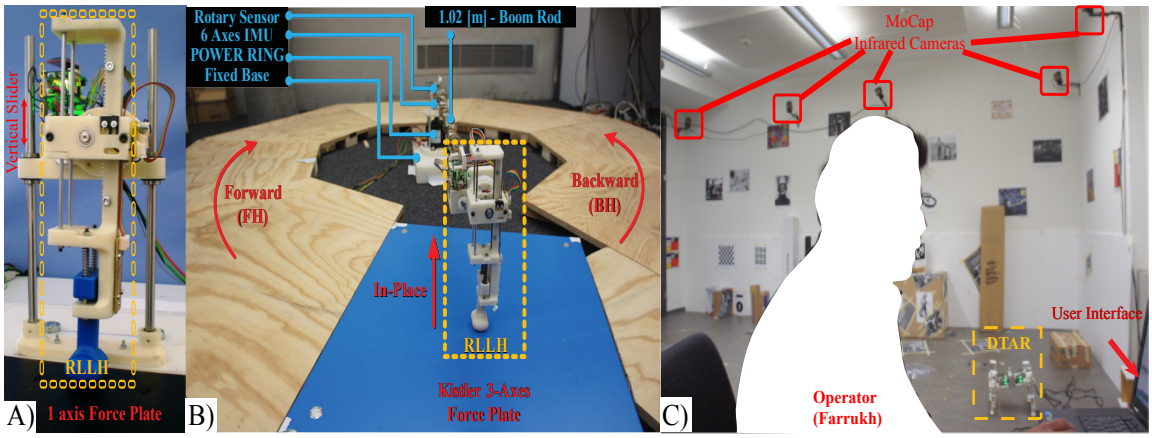

Figure 2.17: Series of experimental setups. A) the experimental setup 1. B) the experimental setup 2. C) the experimental setup 3. Setup A) and B) were utilized for 1D and 2D hopping of the single legged robot. Setup C was used for 3D four-legged walking and running.

Chapter 3

Bio-inspired Reconfigurable Leg Length Hopper

In this chapter, we first provide additional details about the key features of our robotic leg design. Second, we discuss the results that were published in [Sheikh et al., 2011], which can also be found in Appendix A.

Abstract: *We present a novel robotic leg design with reconfigurable length. The design combines key features from bio-mechanical principles into a novel robotic leg with only two actuated degrees of freedom (DOF). The leg configuration with one rotary hip joint and one prismatic knee joint makes it compatible to the Spring Loaded Inverted Pendulum (SLIP) model and will therefore potentially allow direct transfer of suitable control parameters obtained by the simulation of the SLIP model. We have implemented the first prototype and conducted preliminary hopping experiments based on energy-efficient hopping at optimal frequency in human experiment. We measured the ground reaction force and electrical power consumption of the module over a range of hopping frequencies. Our results suggest that the leg driven at its optimal frequency is more dynamic and energy efficient. The externally measured ground reaction forces are very consistent with the results obtained in [Farley et al., 1991].*

In this work [Sheikh et al., 2011], we introduce a robotic leg that does not mimic the kinematic configuration of the animal's leg, but rather matches the underlying dynamic (ground reaction force pattern) through leg reconfiguration. It uses only two active joints and one pair of passive springs. Among these two active joints: a rotary and linear one. The rotary joint controls the fore-aft motion of the leg and the linear joint controls the leg reconfiguration, i.e., the change in nominal leg length. Compared to the existing legged robot designs, this particular way of implementing the leg reconfiguration is novel.

3.1 Key Design Features

The key features of the robotic leg that were initially considered, are as follows:

- Regulating Ground Reaction Forces (GRF)
- Enhancing Structural Endurance
- Obstacle Avoidance
- Voluntary Morphing of the Effective Leg Length

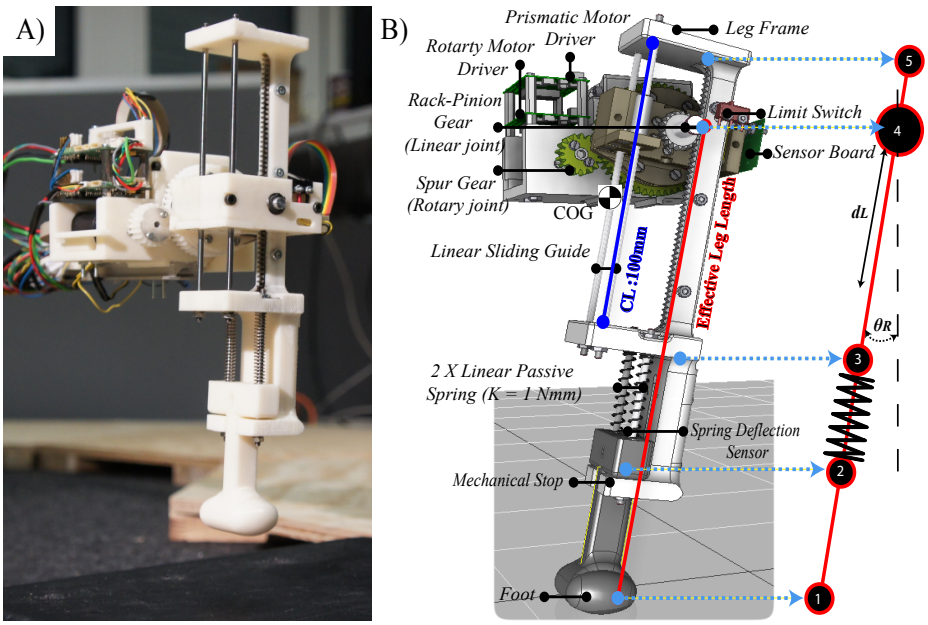

Figure 3.1: Reconfigurable Leg Length Hopper (RLLH). A) shows the airborne phase of the physical reconfigurable leg length hopper, which is hopping on a force plate. B) indicates the CAD model that shows various components of the hopper (adapted from [Sheikh, 2013]). In B) the right side describes the simplified stick diagram of the RLLH.

3.1.1 Regulating Ground Reaction Forces (GRF)

In general, any physical system dissipates some of the supplied energy into air usually in the form of heat. This means that the output energy is never be equal to the input energy, i.e., system efficiency η will always be less than 100% ($\eta < 100\%$). Therefore, it is very essential to regulate the total energy of the system by doing external work. As in our robotic leg, the trunk mass is 3.5 times heavier than the leg mass. Therefore, by moving the trunk mass along the leg axis does the positive and negative mechanical work at the mechanical spring. As a result of this motion, the mechanical spring can be excited in such a way that a required force can be exerted to the ground. Hence, this feature allows us to regulate the SLIP-like ground reaction force pattern.

3.1.2 Enhancing Structural Endurance

The legged robot jumps up and falls down in a periodic fashion. This behavior is called hopping. While hopping In-place and running forward, the foot always strikes the ground that transmits impact forces back to the actuator at every touch-down. Normally, such forces can reduce the life of any legged robot system. In this leg design, we carefully consider this aspect by placing the linear joint (reconfigurable) in series with the mechanical spring. As it is well known, the spring can act like a shock absorber. Thus, placing a mechanical spring in series with the actuator reduces the effect of impact forces up to certain extent. By adding this reconfigurable linear joint, we can control the leg length during touch down to reduce the impact forces further, which can potentially increase the structural endurance of the legged system.

3.1.3 Handling obstacles and rough terrain

Legged robots move in discrete steps, which distinguishes them from their counterpart, the wheeled robots. Based on this feature, legged robots are effectively capable to avoid obstacles and deal with uneven surface. There are two ways by which legged robots can jump high to avoid obstacles and handle rough terrain: one way is to exert higher forces to the ground and second is to retract the leg in air. Humans and animals use both ways of dealing with obstacles and rough terrain. By considering the importance of these two ways of handling rough terrain, we use the reconfigurable linear joint in series with the mechanical spring.

3.1.4 Voluntary Morphing the Effective Leg Length

Animals and humans can run fast by either altering their step-length or step-frequency. Both techniques are very useful. In contrast to the existing legged robots, we introduce the idea of a variable joint. Our robots use a variable linear joint that can be reconfigured to various leg lengths. This allows us to produces a robotic leg of various heights. This feature is defined as voluntary morphosis (see Fig. 3.2). As a result of this feature, our robotic leg is capable to adapt to the current task and its environment using a minimalistic control approach (see chapter 4).

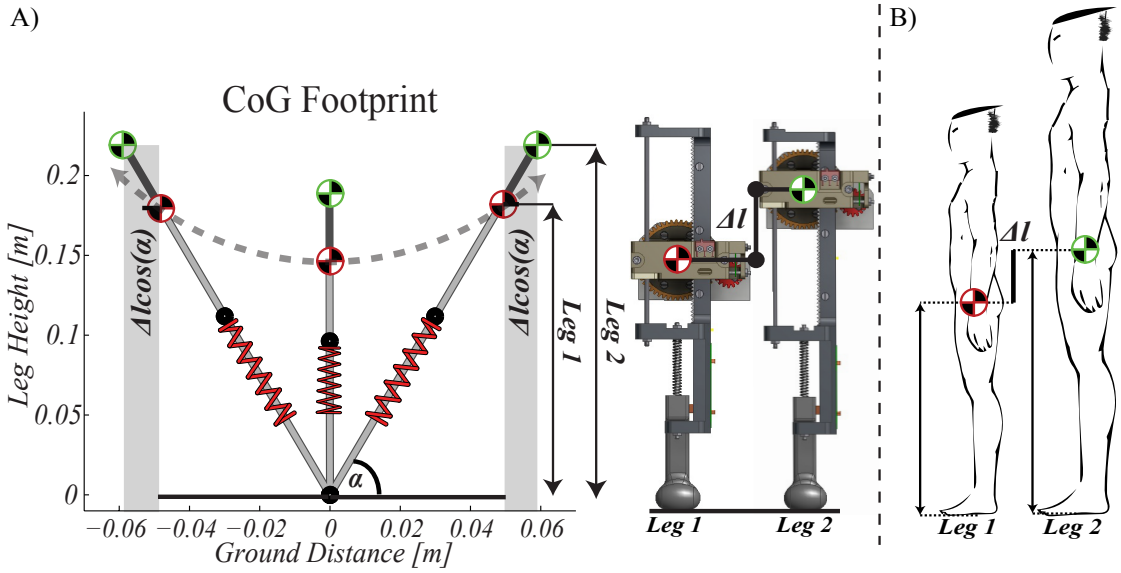

Figure 3.2: Voluntary morphing the effective leg length. A) shows the increase and decrease in effective leg length that influences to the distance covered by the robot body, i.e., stride-length. As it is shown in A), the longer leg configuration (Leg 2) can increase the excursion of body (CoG), i.e., it increase the step-length, whereas the shorter leg configuration (leg 1) can reduce the step-length. B) indicates this feature in the context of human locomotion of different leg heights.

Intuitively, when two humans of different leg heights walk at a constant stride frequency fs then the one who has longer legs will certainly cover more ground distance than the other. Similarly our single-legged robot can increase and decrease the speed of locomotion up to certain extent by altering its leg length to different heights. It is important to note that the effective leg length means the height of the robotic leg before starting locomotion. Furthermore, this feature

in a four-legged system is useful to achieve various tasks, such as maneuverability, stability and dynamic gait versatility. This same property allows the robotic leg to adapt to various ground conditions, stiffness, damping and friction (see chapter 4). For example, shorter legs can deal better with high-frictional ground than the longer legs.

3.2 Results

By reviewing research from the field of bio-mechanics and robotics, we successfully developed a novel robotic leg that can reconfigure its leg height online. By utilizing this feature, we explore wide range of characteristics of legged locomotion using a single and four legged robotic systems.

As we described in section 1, the SLIP (spring loaded inverted pendulum) is a conservative model that describes running behavior of a large number of animals. According to this model, it produces a ground reaction force pattern that is qualitatively similar to the ground reaction force pattern as observed in human and animal locomotion. Similarly a legged robot that produces similar ground reaction force pattern as observed in human experiments, can directly be used as a practical research platform, to understand animals and humans locomotion in greater detail. Considering this fact, we experimented with our first robotic leg design based on the concept of human hopping in-place at various stride frequencies [Farley et al., 1991]. We showed that this robotic research platform is capable to produce qualitatively similar underlying dynamics of human hopping in-place, i.e., the pattern of ground reaction force. Fig. 3.3 shows a qualitative comparison between the ground reaction force pattern of the robotic leg and human during in-place hopping.

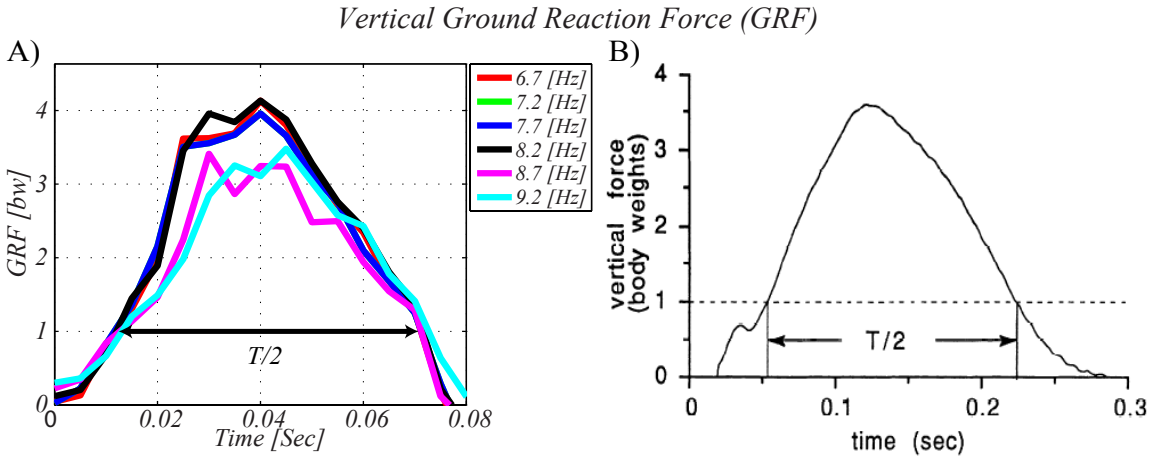

Figure 3.3: Vertical ground reaction force. A) shows the pattern of vertical ground reaction force of our robotic leg hopping in-place at various frequencies; B) is the vertical ground reaction force pattern of human hopping in-place. Note that the plot shown in B) is taken from this [Farley et al., 1991].

3.3 Contributions

The main contributions of this work are as follow:

- Development of Research Platform: This robotic leg is called "Reconfigurable leg length hopper (RLLH)" that we designed to meet the three synthetic design requirements (see chapter 1). In this particular design, we introduced an online reconfigurable joint that alters the length of the robotic leg.
- Testing the Research Platform: Contrast to the existing legged robots approach, we tested this robotic leg based on the experimental approach of bio-mechanics. By comparing our results with the biological data, we showed the relevance of this design as a research platform to understand various characteristics of legged locomotion, e.g., energy efficiency, adaptivity, maneuverability, etc. These characteristics of legged locomotion are explored further in the subsequent chapters of this thesis.
- Humans can move with a wide range of gaits. Among the many gaits, the fundamental gait is 1D in-place hopping. By experimenting with our robotic leg on different frequencies during in-place hopping, we successfully demonstrated that this robotic leg can produce the SLIP-model like ground reaction force patterns. Therefore, it is to some extent SLIP model compatible. In addition, this particular design of the robotic leg can exert the peak of vertical ground reaction force of about ≈ 4 body weights, which is identical in magnitude and pattern of the vertical ground reaction force observed in human hopping in-place. It is important to note that the unit of vertical ground reaction is in body weight, which is simply the vertical component of the ground reaction force divide by the total weight of the body.

Chapter 4

Adaptive Locomotion on Varying Ground Surfaces

This chapter provides a summary of our publication [Sheikh and Pfeifer, 2012], which can also be found in Appendix B.

Abstract: *In this paper, we present the concept of adapting to changes in ground conditions like stiffness, damping and friction, using a novel two degree of freedom reconfigurable leg length hopping robot with a fixed passive compliance. In such a robot, the change in the dynamics of the single legged hopper can be induced by the change in coupled stiffness and damping of the system, i.e., stiffness and damping of the ground coupled with the stiffness and damping of the robotic leg. It is experimentally shown by in-place hopping of a robotic leg on various grounds (stiff, less stiff and soft) that the leg can effectively adapt to changes in coupled stiffness and damping by the rate and the amplitude at which the leg length changes. This is true, while the leg hops in-place as the role of ground friction is negligible. However, in forward motion where the ground friction dominates, a change in initial effective leg length, i.e., shortening or lengthening can provide an additional support to the hip motor in overcoming even large variations in ground friction. This is demonstrated through a planar locomotion experiment on different ground surfaces. The overall results provide strong support for this concept.*

4.1 Results

Research in bio-mechanics suggests that humans change their leg-stiffness to compensate for the change in ground stiffness [Ferris and Farley, 1997; Ferris et al., 1998]. However, we believe that a robust legged locomotion should be capable to adapt to the change in all three properties of a ground surface, namely stiffness, damping and friction. Inspired from the non-linear interaction of a robotic leg with the ground, we conduct experiments with the reconfigurable leg length hopper on various ground conditions. The main purpose of this study is to identify a concept to adapt to the change in ground properties (stiffness, damping and friction) through leg reconfiguration, i.e, without changing the stiffness of the passive mechanical spring. It is important to note that for this particular work, we did not change the mechanical spring of our robot, i.e., the compliance of the robotic leg remained unchanged.

4.1.1 Adaptation to the Change in Ground Stiffness and Damping

The reconfigurable leg length hopper is capable to robustly adapt to the change in ground stiffness and damping using a simple sinusoidal open-loop control. We conducted in-place hopping experiments on three different real grounds, namely highly-stiff (force plate), moderately-stiff (gym

training mat) and less-stiff (foam). We found that change in ground stiffness actually changes the coupled stiffness, which is the resultant stiffness. It can be represented as,

$$k_c = \frac{k_l k_g}{(k_l + k_g)} \tag{4.1}$$

where

k_c is the coupled stiffness.

k_l is the leg stiffness.

k_g is the ground stiffness.

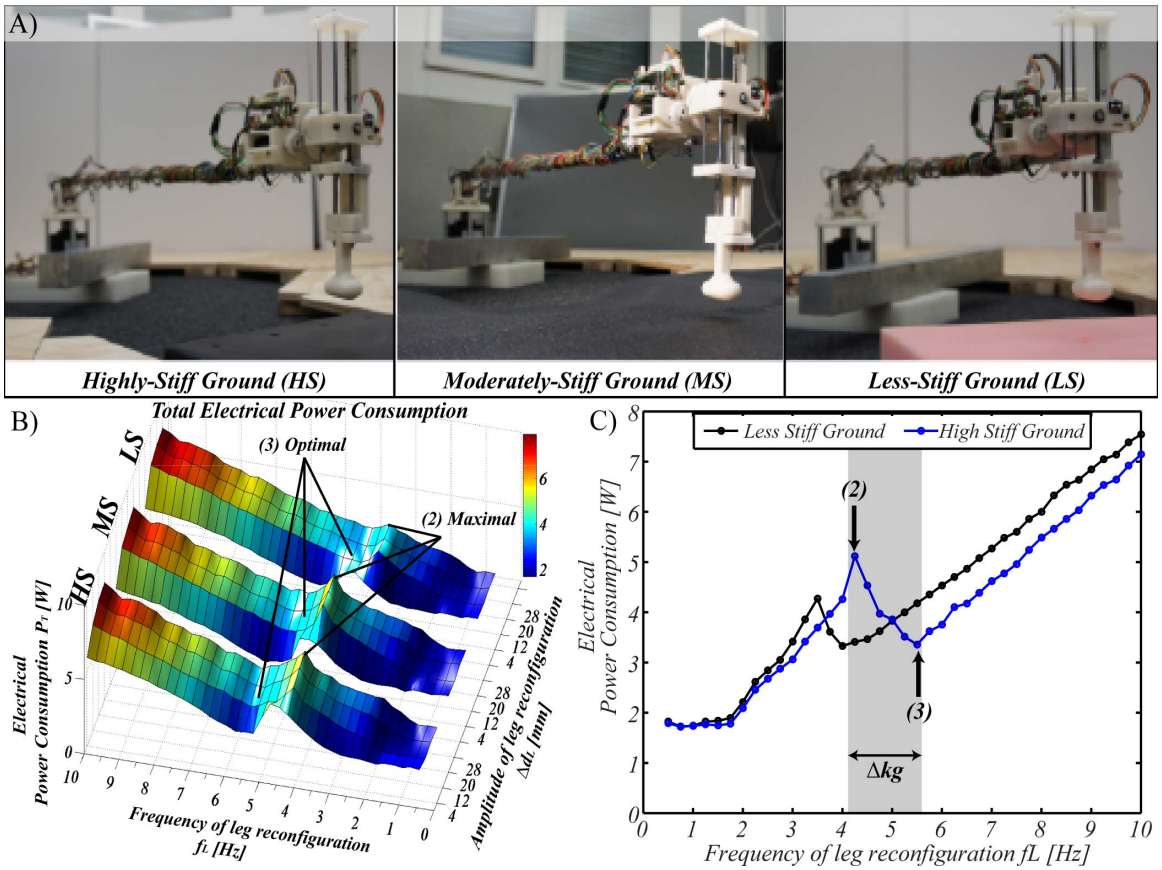

Figure 4.1: Adapting to the change in ground stiffness k_g. A) shows the hopping of the reconfigurable leg length hopper on three different grounds: highly-stiff ($k_g >> k_l$), moderately-stiff ($k_g < k_l$) and less-stiff $k_g << k_l$. B) indicates the result w.r.t the control parameters f_L and ΔL. Label (2) is the maximum point at which the leg's hopping is energy-inefficient and (3) is the optimal frequency point at which leg's hopping is energy-efficient. C) depicts that the change in ground stiffness Δk_g can be compensated by adjusting the operating frequency f_L.

Equation 4.1 shows, the coupled stiffness k_c can be influenced either by the leg stiffness k_l or by the ground stiffness k_g. As the leg stiffness is not being altered (constant), only the ground

stiffness is being changed during experiment. Thus, the coupled stiffness k_c only depends on the variable k_g. This change in coupled stiffness changes the resonance frequency at which compliant robotic leg exhibit an energy-efficient hopping (see Fig. 4.1). This indicates that the change in coupled stiffness can be compensated by adjusting the rate at which the robotic leg reconfigures its length f_L. Similarly, the change in ground damping causes increases or decreases in coupled damping, which means increase and decrease of total energy during each step of hopping and running. As our robotic leg uses the reconfigurable joint in series with the passive mechanical spring. This means that by increasing the amplitude of leg reconfiguration Δd_L, we can increase the external work to compensate the effect of change in ground damping.

4.1.2 Adaptation to the Change in Ground Friction

As we described earlier in the previous chapter that the reconfigurable leg length hopper is able to adjust its leg length to various heights, which is called voluntary morphosis. This feature is essentially useful to enhance the fore and aft motion of the leg such that change in ground friction can be compensated (see Fig. 4.2). As we can see in Fig. 4.2B), the shorter leg can overcome the static ground friction better than the medium and long legs. However, once the leg starts hopping then the effect of kinetic friction is negligible because kinetic friction is always less than the static friction.

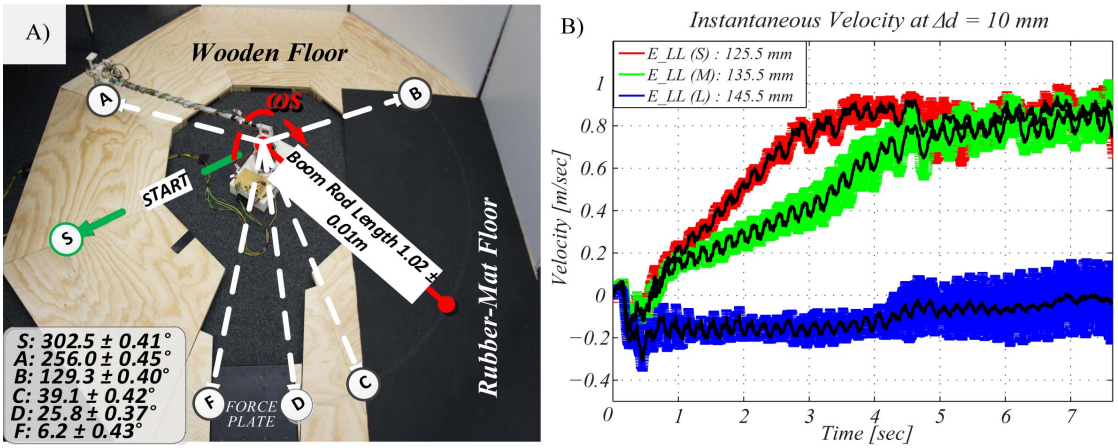

Figure 4.2: Adapting to the change in ground friction. A) shows the top layout of our experimental setup including two different grounds. In A) the two grounds are wooden floor (less-friction) and rubber-mat floor (high-friction.B) describes the effect of effective change in leg length on different grounds. In B), we measured the speed of three leg settings, namely short (125.5 mm), medium (135.5 mm) and large (145.5 mm).

4.2 Contributions

The main contribution of this work is to demonstrate the capability of the reconfigurable leg length hopper to adapt to the change in ground properties (stiffness, damping and friction). This adaptation to different grounds is achieved by exploiting the dynamic coupling of the robot's body with its controls and the physical environment. This exploration leads us to identify the

concept of adapting to the different ground conditions using a simple control. They are summarized as follows.

- Change in ground stiffness can be compensated by adjusting the frequency (f_L) of the leg reconfiguration control (see Fig. 4.1).
- Change in ground friction can be compensated by adjusting the effective leg length Δd_0 (see Fig. 4.2).
- The in-place hopping experiments show two frequency points (see label (2) and (3) in Fig. 4.1C). The point which is shown as label (2) in Fig. 4.1, is the point at which the robotic leg exhibits higher ground clearance than the label (3). However, by operating the robotic leg at this frequency (label (2) point) consumes more electrical power than the label (3) point.
- The label (3) point in Fig. 4.1 is the natural frequency of our robotic system, where the robotic leg is energy-efficient with moderate ground clearance.

Chapter 5

Open-loop Speed and Direction Control for Fast Running

This chapter provides a summary of our publication [Sheikh, 2013], which can also be found in Appendix C.

Abstract: *Traditional 2D single-legged hoppers were able to demonstrate stable bi-directional running in a closed-loop approach. In contrast, we employ an open-loop control to achieve high-speed (≈0.8 m/sec or 1.78 mph) bi-directional dynamic running of the reconfigurable leg length hopper (RLLH). Our hopper has variable linear joint in series with a passive spring that allows changing its effective leg length in real-time. Furthermore by instantaneously changing the leg length at a particular amplitude and frequency, the required "thrust-forces" can be produced. We hypothesize that the direction and the speed of our hopper can be smoothly controlled by only changing the phase of the thrust-forces being applied to the ground, i.e., the change in phase between the leg-reconfiguration and the leg-oscillation. This is experimentally evaluated by varying the phase of leg-reconfiguration up-to the range of 0-2π rad (0-360 deg). Our results show a large region of a symmetric running. Moreover, a novel gait called "in-place running*[1]*" is found, where the speed of running is zero. We demonstrate that by only altering the phase of applying thrust-forces together with a constant leg oscillation can robustly control the speed and transition in the direction of locomotion.*

5.1 Results

The result of this work is divided into two parts. The first part explores the effect of change in thrust-force by altering the phase of leg reconfiguration ϕ_L. The second part is to show the significance of the ϕ_L parameter as a control to alter the speed and direction of single-legged running. In the second part, we demonstrate, how the online speed and direction of the reconfigurable leg length hopper can be successfully controlled during fast running at speed of ≈ 0.8 m/s.

5.1.1 Effect of the Phase of Leg Reconfiguration ϕ_L

We experimentally explored the effect of the phase of leg reconfiguration ϕ_L up to the range of 0-2π rad (0-360 deg). The result of this exploration can be seen in Fig 5.1. It shows symmetry in speed of running, which is grouped into three regions: forward hopping (FH), phase transition (PT) and backward hopping (BH). In the forward hopping region, the single-legged hopper runs at a constant speed of ≈ 0.8 m/s in a clockwise direction about the boom. Similarly, the single-legged hopper runs at a constant speed of ≈ -0.8 m/s in an anticlockwise direction about the

[1] In-place running is like an in-place jogging, in which the motion of the body is mainly restricted in-place by the continuous movement of each joint of the leg.

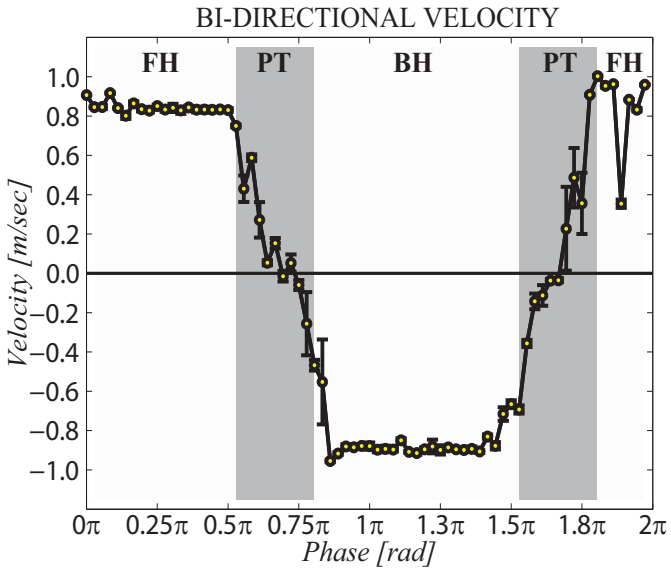

Figure 5.1: Symmetry in speed of running (adapted from [Sheikh, 2013]). It comprises of three separate regions: forward hopping (FH), phase transition (PT) and backward hopping (BH). The forward hopping region is the set of control parameters, where the speed of running is positive and constant. While the backward hopping region is the set of control parameters, where the speed of running is negative and constant; the phase transition region is the set of control parameters, where the speed starts changing from positive direction to negative direction.

boom, which is indicated by the negative sign of the speed. However, the set of control parameters that causes a change in speed of locomotion, is defined as the phase transition region (PT). As can be seen in Fig 5.1, the control parameters of the phase transition (PT) region allow us to smoothly alter the direction of locomotion (see section 5.1.3), while changing the speed of locomotion at high speed running. In addition, we report that within this phase transition region, there is a control parameter at which the speed of running is zero. This control parameter is defined as the phase ϕ_L of novel gait called *in-place running* [Sheikh, 2013].

5.1.2 Difference Between In-Place Hopping and In-Place Running

It has been known for long time that the in-place hopping is simple jumping vertically in-place [Blickhan, 1989; Farley et al., 1991]. However, by exploring the effect of the phase of leg reconfiguration ϕ_L, we found a novel gait called in-place running, which is very similar to the in-place jogging of a human. This particular gait is the result of limiting the motion of robot's body in-place by the particular phase difference of the continuous motion of each robotic leg joint. In this way, we can characterize the in-place hopping gait further into the vertical in-place hopping and the oscillatory in-place running (see Fig 5.2).

5.1.3 Online Speed and Direction Control

Fig. 5.3 indicates the experimental evidence of controlling the speed and direction of fast single-legged running in open-loop control. This is implemented only by varying the single control parameter, which is the phase of leg reconfiguration ϕ_L.

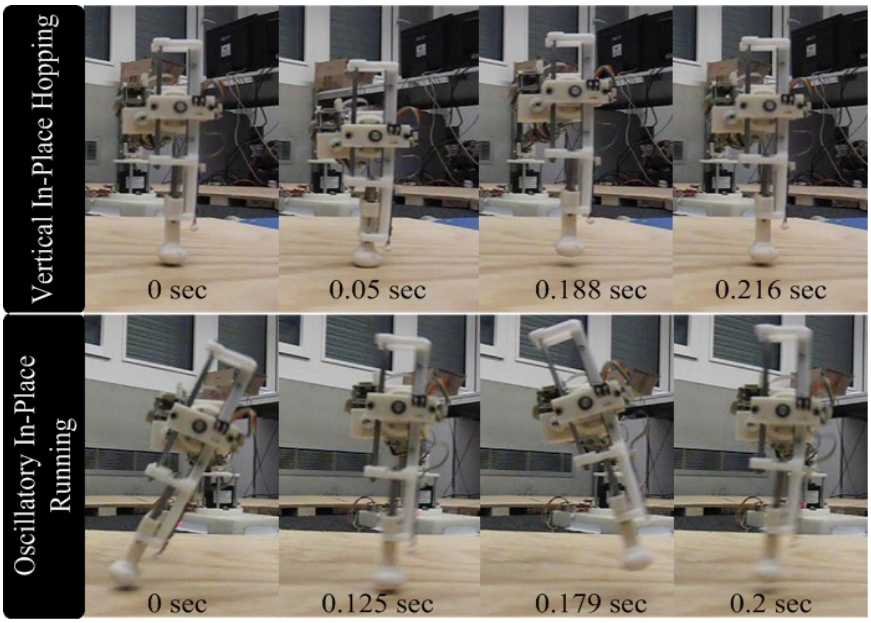

Figure 5.2: Two types of in-place hopping(adapted from [Sheikh, 2013]). Top the vertical in-place hopping. Bottom the oscillatory in-place running.

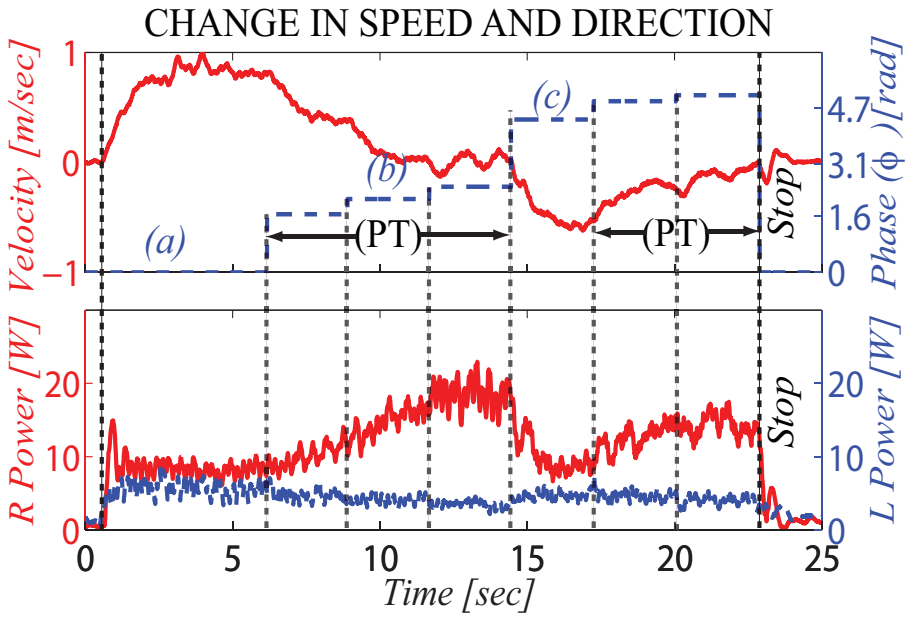

Figure 5.3: Online speed control of bi-directional running (adapted from [Sheikh, 2013]). The first plot shows the effect of different phase values to control the speed and the direction with respect to time. The second indicates the progression of the change in electrical power of each active joint with respect to time. Phase values used in this process: Phase (a) $\phi_L = 0$ rad shows forward running, (b) $\phi_L = 0.53\pi$ rad indicates in-place running, and (c) $\phi_L = 1.38\pi$ rad shows backward running. PT defines the phase transition region.

5.2 Contributions

This work contributes the following results.

- Simple control for controlling the speed and direction of a single-legged hopper can be obtained by exploiting body dynamics. We successfully demonstrate that the speed and direction (forward and backward) of the single-legged robot locomotion can be controlled by only varying a single control parameter, which is the phase of leg reconfiguration ϕ_L. It is achieved by exploiting the body-dynamics of the robot.
- In-place hopping can now be further characterized into vertical in-place hopping and oscillatory in-place running.
- We demonstrate the use of simple open-loop control to alter the speed and direction (forward and backward) of a single-legged hopper during fast running (0.8 m/s).

Chapter 6

Significance of Foot Compliance for Fast and Energy-Efficient Locomotion

This chapter provides a summary of our publication [Sheikh et al., 2014], which can also be found in Appendix D.

Abstract: *This paper addresses the significance of foot compliance. We experimented with two robotic legs. Each has a different foot. A stiff foot robotic leg is called the "S-RLLH" and a compliant foot robotic leg named the "C-RLLH". The length and mass properties of the two robotic legs are the same, but they differ in number of segments, shape and compliance because of different foot. First, we explored the maximal speed of the S-RLLH robot in open-loop by systematically altering two control parameters: stride frequency f_s and amplitude of leg oscillation ΔA_R. Latter, we investigated the C-RLLH by applying the control parameters of the S-RLLH robot. By comparing their speed and electrical power consumption, we observed that the S-RLLH robot can run up to ≈ 1.22 m/s at a stride frequency of 7.0 Hz, whereas the C-RLLH robot exhibits a similar speed of ≈ 1.23 m/s at a stride frequency of 4.8 Hz. Moreover, the total electrical power consumption of the C-RLLH foot is less than the S-RLLH. Overall results suggest that the foot compliance is important to increase the leg compliance, thereby it reduces the electrical power consumption and shifts the maximal speed of legged locomotion to the lower stride frequency.*

6.1 Results

In this work, we focused on exploring the significance of foot compliance (morphology) to enhance speed and energy efficiency of our single-legged reconfigurable leg length hopper. Two foot morphologies are identical in mass and length, but they differ in number of segments, compliance and shape (see Fig. 6.1). Based on their differences, we called the single-segmented rigid foot the *stiff foot*, and the two-segmented foot that uses a compliant element (spring) between the two segments, is the *compliant foot*.

In order to compare both foot configurations, we first explore the forward speed of the stiff foot robotic leg (S-RLLH) in open-loop control, and then we evaluate the compliant foot robotic leg (C-RLLH) based on the 2D control parameter space of the stiff foot robotic leg. As it is well known, the speed of a legged animal is the product of step-length (distance covered by the body in a single cycle of locomotion) and stride frequency (the cycle of locomotion repeated in 1 sec) [Alexander, 2003]. Considering this fact, we chose to alter three control parameters: frequency of leg oscillation f_R, frequency of leg reconfiguration f_L and amplitude of leg oscillation ΔA_R. Two control parameters (f_R and f_L), were altered together as a single parameter (stride-frequency f_s) from 4.8 Hz to 7.0 Hz in steps of 0.2 Hz, while the amplitude of leg oscillation that normally affects the step-length, was altered from 0.044π to 0.07π in steps of 0.011π. At each of these control parameters, we performed 5 trials with both foot configurations. Fig. 6.2 shows the comparative results

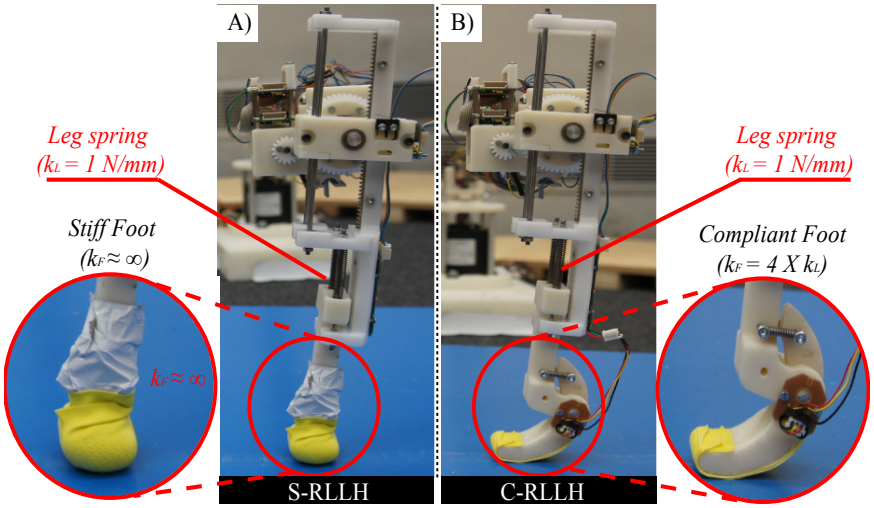

Figure 6.1: Two different foot morphologies in RLLH. A) the stiff foot reconfigurable leg length hopper (S-RLLH). B) the compliant foot reconfigurable leg length hopper (C-RLLH).

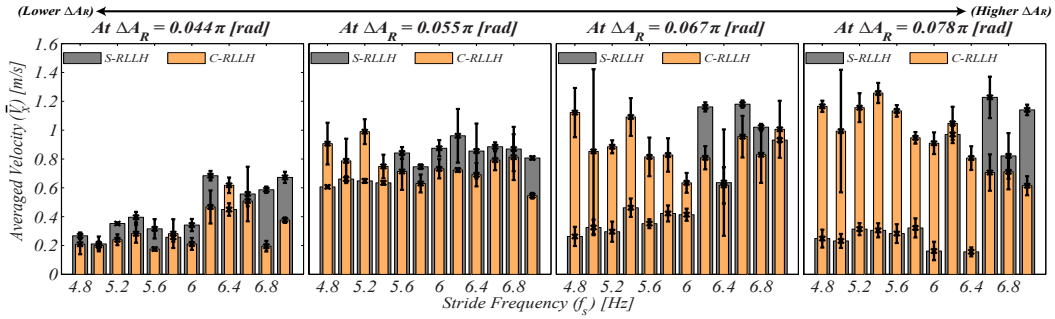

(a) Averaged speed comparison.

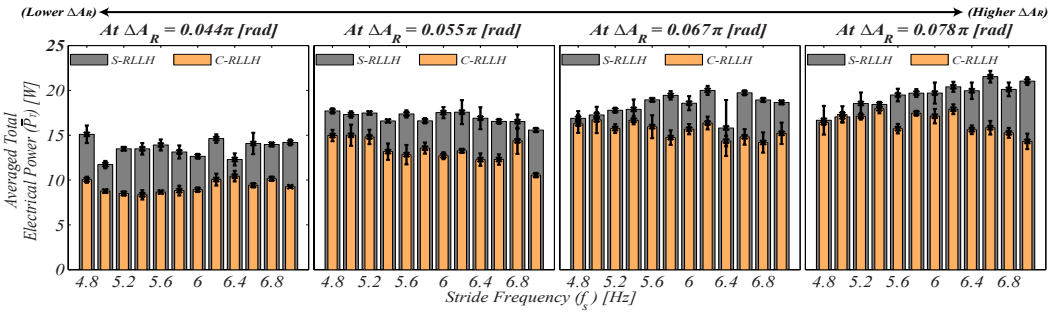

(b) Averaged electrical power consumption comparison.

Figure 6.2: Comparison between the stiff foot robotic leg (S-RLLH) and the compliant foot robotic leg (C-RLLH). a) shows the comparison between an averaged speed of the S-RLLH and C-RLLH. b) depicts the comparison of an averaged total electrical power consumption between the S-RLLH and C-RLLH. In a) left most figure shows the comparison between the S-RLLH and C-RLLH at the lowest amplitude of leg oscillation ΔA_R. Right most indicates the result at the highest amplitude of leg oscillation ΔA_R. The grey bar represents the result of S-RLLH, while the light-brown bar indicates the result of C-RLLH.

of the experiments of the S-RLLH and C-RLLH. As can be seen in Fig. 6.2a, by comparing the averaged speed of locomotion with respect to the 2D control space, we can see that the stiff foot robotic leg (S-RLLH) can result in an average speed of 1.2 m/s (2.72 mph) at a stride frequency of 7.0 Hz, whereas the compliant foot robotic leg (C-RLLH) can result in an approximately similar average speed 1.23 m/s (2.75 mph) at a stride frequency of 4.8 Hz. This indicates that the foot compliance affects the stride frequency at which a maximal speed of locomotion can be realized. However, when we observed the total electrical power consumption with respect to the control parameter space, as shown in Fig. 6.2b, C-RLLH consumes less power than S-RLLH.

6.2 Contributions

We introduce a systematic experimental approach to investigate and compare two different foot morphologies in a single legged robot. This study provides the role of foot morphology for building fast and energy-efficient locomotion. The main contributions of this work are summarized as follows.

- Establishing a systematic experimental approach of comparing two foot morphologies that are equal in mass and length, but differ in number of segments, compliance and shape.
- By increasing the foot compliance, we can significantly reduce the electrical power consumption, i.e., enhancing actuator efficiency.
- The compliant foot robotic leg (C-RLLH) shows the significance decrease in operating frequency to achieve maximal speed 1.23 m/s (2.75 mph) than the stiff foot robotic leg (S-RLLH). In other words, compliant leg can potentially run fast at lower operating frequency than the stiff leg.
- Overall experimental results suggest that the variable compliant mechanism (active compliance) may be more effective, when it is placed at the foot joint as the foot compliance can play a major role in increasing energy efficiency for fast legged locomotion.

Chapter 7

Dynamic Maneuverability Through Voluntary Morphosis

This chapter provides a summary of our publication [Sheikh and Shams-Ul-Haq, 2013], which can also be found in Appendix E.

Abstract: *Dynamic maneuverability is an inherent skill of any legged animal locomotion. Thus it is useful and challenging for a physical four-legged robot that runs in open-loop control. This paper presents a concept of dynamic maneuverability in a four-legged system that can alter its morphology through leg reconfiguration, i.e., voluntary morphosis*[1]*. By exploiting this unique feature of the robot body, we designed a dynamic maneuverability control in open-loop that changes the leg length of the ipsilateral pairs of legs to smoothly control the turning of the robot on a particular gait. We verified our control approach on trot gait locomotion. Our results demonstrate that the maneuverability in a four-legged robot is mainly the result of an active change in robot morphology.*

7.1 Results

In previous chapters, we were exploring the morphology and control of a single-legged reconfigurable leg length hopper (RLLH) to illustrate energy-efficient, adaptive, fast and robust locomotion. Now the following studies demonstrate the morphological advantages of a reconfigurable leg length mechanism in a four-legged system (DTAR), which in contrast to the single-legged system is more complex and high-dimensional. As we described in chapter 3, the reconfigurable leg length mechanism allows us to produce a robotic leg of various heights, which we described as voluntary morphosis. This feature in a four legged system that has a total of eight degrees of freedom, can simplify the control of turning in a four legged system. Based on this feature, we designed and implemented a dynamic maneuverability control that allows us to turn the robot on potentially different gaits. However, due to the limited area of an experimental room, we only verified the turning through voluntary morphosis on a stable trot gait.

As can be seen in Fig. 7.1 B), by introducing a change ΔD (Differential change) in ipsilateral pairs of legs, i.e., increasing the leg length of the right side pair of legs by a factor ΔD and decreasing the leg length of the right side pair of legs by a factor ΔD, we can turn the robot either to its left or right side (see further detail in [Sheikh and Shams-Ul-Haq, 2013]). In order to smoothly turn the direction of robot during a stable gait, we embedded this maneuverability control on top of the simple sinusoidal open-loop control to generalize the control for a wide range of gaits. Using this layered control architecture, we successfully showed maneuverability on a stable trot gait. Fig. 7.2 shows the experimental results.

[1]Voluntary morphosis is an inherent ability of a robot to self-adjust its own morphology to adapt to the current tasks

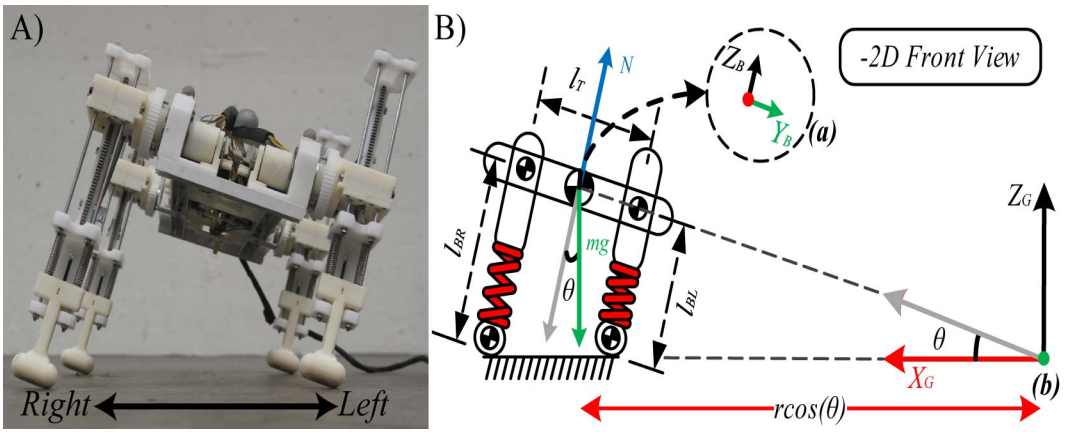

Figure 7.1: Maneuverability through voluntary morphosis. A) shows a configuration of a four-legged reconfigurable leg length robot (DTAR) that turns the robot to its left side. B) is taken from [Sheikh and Shams-Ul-Haq, 2013], which describes the turning model of our four-legged system. In B), (a) is the robot body frame and (b) is the ground frame.

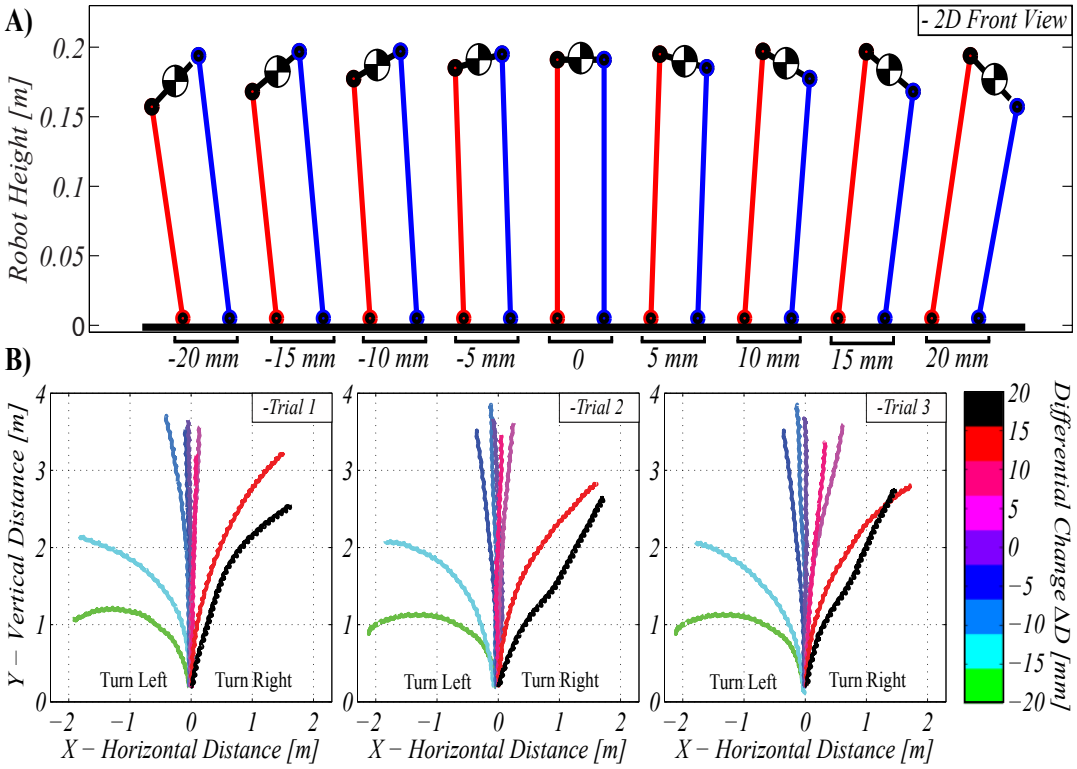

Figure 7.2: Maneuverability test on trot gait. A) shows the effect of increasing and decreasing the differential change factor ΔD on the four-legged reconfigurable leg length robot (DTAR). B) shows three trials of a robot turning with respect to the differential change in robot morphology in open-loop control [Sheikh and Shams-Ul-Haq, 2013].

Fig. 7.2 shows that the differential change factor ΔD plays an important role in the turning of the four-legged system. By varying this single parameter ΔD in a layered open-loop control approach, we can smoothly control the turning of the four-legged system either to the left or right.

7.2 Contributions

The main contributions of this work are as follows.

1. We introduced a principle of dynamic maneuverability through voluntary morphosis (leg reconfiguration to various heights) in a four-legged system that takes into account shape of the robot structure to predict the direction of motion.
2. We formulate the maneuverability control as a single control variable (differential change ΔD) that can potentially be used to control the turning on wide range of gaits. However, we only validated this principle on trot gait.
3. We situate this maneuverability control on top of the existing open-loop control such that the turning can be smoothly achieved during slow and fast locomotion.
4. Overall experimental results on trot gait suggest that the sharp turning is possible by increasing the differential change in ipsilateral pairs of legs.

and environments.

Chapter 8

Summary and Conclusions

In this chapter, we first summarize and then discuss the main results of our published work presented in chapters 3-6. Second, we draw general conclusions. Finally, we discuss the future directions of this work.

8.1 Summary

In this thesis, we tried to address our research questions by building two types of physical legged robots (single-legged RLLH and four-legged DTAR). Both legged robots were utilized to understand the following characteristics of legged locomotion: energy efficiency, adaptivity, speed, maneuverability and gait versatility..

In chapter 2, we reviewed the work of two research fields, namely bio-mechanics and legged robots. By combining the strengths of both, we derived three synthetic design requirements that can be considered useful in building a legged robot. These three requirements were as follows: SLIP-like GRF, voluntary morphosis and gait versatility (see chapter 1). We built our robots aiming to fulfill these requirements. Unlike the traditional legged robots research that usually focused more on the control, our research takes all three aspects of embodiment (control, morphology and environment) into account. Following the embodiment framework, we designed our research methodology that utilizes experimental ways of the bio-mechanical approach. In bio-mechanics, researchers study human and animal locomotion with the help of external sensors, e.g., 3D force plates, and high speed cameras. These external sensors accurately measure the dynamics of animal locomotion from an observer's perspective, to understand the complete "physiology" of a system also need to be considered internal sensory information, e.g., activation of different muscle groups, sensory feedback pattern, etc. Having the flexibility to use both internal and external sensors in the field of robotics, we custom developed a single-legged experimental setup that allows us to evaluate the performance of our legged robot.

By focusing on the design requirements, we introduced the idea of real-time changeable leg length to achieve voluntary morphosis in chapter 3. We successfully demonstrate that this particular design can produce SLIP model like ground reaction force pattern. In addition, we showed that our robotic leg can generate peak vertical ground reaction force of about 4 body weights, which is similar to human hopping in-place [Farley et al., 1991]. By achieving this, we indicate that such robotic leg design can be useful to explore the characteristics of legged locomotion.

The dynamics of a running legged robot is very sensitive to the change in various ground conditions: stiffness, damping and friction. Each is very important to compensate in the context of adaptive locomotion. Our reconfigurable leg length mechanism is capable of adapting to the change in aforementioned ground conditions. This was practically demonstrated on three different grounds: stiff (force-plate), moderately stiff (gym training mat) and soft (foam). The

overall results suggest that there is no need to change the stiffness of the passive spring to adapt to the change in ground stiffness, but such change can be compensated by adjusting the operating frequency of the variable linear joint (reconfigurable joint) variable joint. Similarly, the change in ground damping which affects the total system energy, can be overcome by increasing the external work (oscillation trunk) through leg reconfiguration. Finally, our robotic leg design can change its effective height, i.e., initial leg length can be set to various heights. This has been previously defined as "voluntary morphosis". It allows us to deal with the change in ground frictions, e.g., shorter leg configuration can better negotiate the high frictional ground compared to the longer leg.

Speed and transition in a particular direction of a legged robot system are often controlled in carefully designed closed-loop control that relies on global sensory feedback. We showed that the speed and direction of our single-legged hopper can be controlled in simple open-loop control, i.e., without external sensory feedback (see chapter 5). We demonstrate this by exploring the change in the phase of applied thrust-forces in open-loop control. The exploration shows that there is a region, where high speed locomotion (0.8 m/s) can be smoothly controlled and easily be changed from one direction to another. Furthermore, we report a new gait called "in-place running" (in-place jogging), which is different from vertical in-place hopping in terms of the motion of the robot center of mass (COM). For instance, ideally in the vertical in-place hopping the robot CoG (center of gravity) moves in single axis (1D motion), whereas in the in-place running, it moves in a plane (2D motion).

Control is important to increase the speed and energy efficiency of legged robot locomotion, however the morphology can further facilitate the control to enhance speed and energy efficiency of legged robot locomotion, as studied in chapter 5. We experimented with two different foot morphologies to enhance speed and energy efficiency of our existing legged robot. Both foot morphologies were equal in weight and length, but they were different in shape and compliance. The experimental results show that foot compliance plays an important role in two aspects of legged locomotion: Firstly, it shifts the region of maximal speed of locomotion to the lower operating frequency and secondly, it reduces the electrical power consumption (increased actuator performance).

Up to this point, our work was based on single-legged **"Reconfigurable leg length hopper (RLLH)"** robot locomotion that resolves certain aspects of legged robot locomotion. However, the feasibility of this mechanism in a more complex system such as a four-legged system remained unexplored. In chapter 6, we constructed a four-legged system the **"Differential Terrain Adaptive Robot (DTAR)"**. This robot has been developed to advance our understanding about maneuverability and dynamic gait versatility. We implemented these features without relying on global sensor feedback, i.e., in simple open-loop control. Following this, we designed a dynamic maneuverability control of the four-legged (DTAR) system that takes the robot morphology into account to achieve stable turning on potentially wide range of gaits. Our model for maneuverability suggests that by actively changing the robot morphology, we can guide the robot motion in its left or right direction online. The same approach is also applicable to correct the direction of locomotion, if the robot starts heading in a wrong direction on unstable gait pattern. Furthermore, the experiments with maneuverability control indicate that direction of legged robot locomotion is very sensitive to the change in robot morphology, i.e., a slight asymmetry in the robot morphology can affect the turning behavior of the robot. We validated this concept of maneuverability on a trotting gait. The same approach can also be applied to other types of gaits (pronk and bound).

Compared to a single-legged robot, a four-legged robot can potentially exhibit a wide range of gaits starting from slow walking (trot) to fast running (pronk, pace, bound and gallop). In order to understand gait versatility, we tested the capability of our four-legged system to produce different gaits (trot, pronk and bound) in open-loop control. Preliminary results suggest (see in Appendix F) that pronk and bound can be designed based on the knowledge of a single-legged

open-loop control, i.e., some optimal parameters (stride frequency and amplitude of leg oscillation) can be directly used.

8.2 Discussion

As described in chapter 2, we conducted this research in two phases. In the initial phase, we explored the effects of different morphologies (leg segmentation, increasing the number of active joints, increasing number of passive joints, passive spine, and active spine) in a four-legged robot locomotion. During this phase, we observed that different morphologies are good for different gaits, but none of the morphologies showed superior performance on all gaits. It becomes a real challenge both from the engineering and a scientific perspective, how to achieve all these functions by using a single robotic leg design. This work lead us to think about developing a novel robotic leg that uses a reconfigurable linear joint in series with a passive spring. Our custom developed reconfigurable leg length mechanism allows us to produce robotic leg of various heights. In the latter phase, we explore the use of this mechanism in legged robot locomotion.

The results presented in this thesis were obtained by experimenting with two important morphological factors: leg length and compliance. For example, first we explored the function of a changeable leg length joint in a passive compliant single-legged robot, second we aimed at improving the performance of our single-legged robot by experimenting with different foot morphologies, and finally we extended our studies to different gaits in a passive compliant four-legged system. However, there are many other morphological factors (spine, active compliance, leg segmentation, etc). Each is important in the context of legged locomotion. For example, very recent research on the use of an active compliant knee joint in a two-segmented robotic leg shows that the energy-efficient hopping can be achieved at various operating frequencies [Hung et al., 2013]. As our robotic leg only has a single passive compliant joint, it can only achieve energy-efficient hopping at a particular operating frequency as demonstrated in chapter 4). The role of a variable compliant actuator is certainly advantageous for legged robot locomotion. However, its practical application is currently limited because such actuators are not commercially available in different weights, sizes, speeds, and operating voltages. Due to this reason, we did not add an active compliant actuator in our robots, but we provided some practical insights about the placement of such actuators, e.g., a variable compliant foot (see chapter 6).

The primary focus of this thesis was to exploit the natural dynamics of the robot for fast and energy-efficient locomotion. This implies that the stability of our robot while running was not controlled but relied on the feed-forward control signal and the intrinsic dynamical properties of a system. However, the open-loop approach has serious limitation, when we aim to handle rough terrain. Traversing on rough terrain is another important area of legged robot research that certainly requires a closed-loop control (e.g., for balance). We believe that future legged robots can benefit from both open-loop and closed-loop control approaches, as one (open-loop) can drive the robot fast on level ground [Sheikh, 2013] and the other (closed-loop) can safely locomote the robot on rough terrain. Intuitively, these two control modes can interact with each other based on sensory information of the environment, e.g., ground roughness. Once the robot is able to know the roughness of the ground surface then it may be possible to design a switching scheme for the two control modes. However, the practical implementation of such transition method can be very difficult because it requires to actively sense the environment, e.g., by LIDAR (Light Detection and Ranging) or by an IMU (Inertial Measurement Unit).

With respect to dynamic legged locomotion, we studied legged locomotion behavior (gaits) by starting with a vertical in-place hopping gait (1D motion), and then forward running (2D motion). While exploring these two gaits, we discovered another interesting gait, which we named "in-place running (2D motion)" (see chapter 5.1.2). These gaits are only a subset of commonly

found gaits in four-legged systems, which can exhibit various gaits (crawl, walk, trot, pronk, bound, gallop). As we were interested to study more animal-like gaits, we built a four-legged system (DTAR). Our four legged robot is a direct successor of the single-legged system as it uses four legs of the same single-legged mechanical design. It is potentially capable of producing all aforementioned gaits. However, we were able to demonstrate walk, trot, pronk and bound. According to our experience, it was challenging to generate different gaits because of the following reasons: First, it had rich dynamical interactions with its environment as it can freely move in three dimensions; Second, it had eight active joints that should be actuated simultaneously for a desired gait pattern; and finally, it generates huge sensory data that must be carefully recorded and analyzed to understand a particular behavior. Due to these reasons, our research with four-legged system about different gaits is currently limited. However, our preliminary results indicate that we can successfully design pronk and bound gaits of our four-legged system based on the knowledge of the single-legged system RLLH.

8.3 Conclusions

The main objective of this thesis has been developing a practical framework that can be readily used to explore, study, and understand the role of robot morphology and its control in real environments. The primary application was focused on legged robots that can actively change one aspect of their morphology, i.e., leg length. By exploiting this feature in a passive compliant legged robots (single-legged RLLH and four-legged DTAR), we have successfully demonstrated fast, energy-efficient, adaptive, and versatile locomotion.
The important meessages from this thesis are:

- An active change in robot morphology is important as it can help us to simplify the control of a particular task. In addition, it can increase stability and adaptivity. For example, as demonstrated in chapter 4, the single-legged reconfigurable leg length robot is able to adapt to various ground surfaces. Similarly, this feature can simplify the turning control (see chapter 7) and enhance the stability of our four-legged system over an inclined surface (see Fig. F.3 in Appendix F).
- Controlling rapid legged locomotion in open-loop control is an extremely challenging task because the stability of a running machine at high speed is more vulnerable to slight changes in control compared to a walking machine. Using our approach, we demonstrated that it can be accomplished by exploiting the natural dynamics of a legged robot system.
- Behaviors of a real robot can be understood by observing and analyzing sensory data. It can be also helpful for optimizing the control and morphology for a required task.
- Exploring basic dynamics of a single-legged robot, such as hopping and running, can be useful in designing self-stable dynamic gaits of a multi-legged system.
- Foot compliance is important for increasing speed and energy efficiency of a legged robot locomotion.
- Building a fast legged robot requires us to either increase the step-length or the step-frequency. As presented in this thesis, the change in leg length increased the step-length and the step-frequency can be altered by adding a variable compliant-articulated foot. By incorporating both features in a future legged robot, we can enhance speed of a legged robot further.

Chapter 9

Future Directions

Legged robot research has a promising future. It has been strengthening our understanding of legged locomotion for long time. In addition, the amount of knowledge and experience that we gather by building and experimenting with physical legged robot, will eventually lead us to develop a new form of vehicle in the near future. The vehicle which could traverse any kind of terrain in a similar way as legged animals or humans. In this thesis, we attempt to develop an approach that uses robots as a research tool to explore various characteristics of legged locomotion, however still a lot more research is required to improve our understanding further about more complex problems such as handling rough terrain, jumping high, running fast, making sharp turns, climbing steep hills, gaits, etc. Most of these problems might seem simple, but resolving these problems by building a physical platform is enormously difficult and an extremely challenging task.

9.1 Handling Rough Terrain with Closed-loop Approach

Legged robots are potentially more capable of handling rough terrain compared to wheeled robots as described in chapter 1. In this thesis, we only explored the body dynamic of our robot in simple open-loop control on a level ground, i.e., we did not experiment with our four-legged robot on rough terrain yet. However, we would like to enhance the potential of our robot to deal with uneven surfaces in future. Based on the previous study [Vernaza et al., 2009; Pongas et al., 2007], we can assume that a solution of this task is definitely required a robust closed-loop approach. Such control is highly useful for actively balancing the robot body on rough terrain, i.e., it prevents the robot from tipping over. Currently, we do not have an active balance control in our robot because we were interested in exploiting the natural dynamics of the robot for fast and energy-efficient locomotion, but it can be implemented in future by combining the sensory information of the on-board IMU (inertial measurement unit) with the change in the robot's morphology.

9.2 Jumping High

Suppose we want to build a legged robot that jumps twice as high as its body height. Knowing the nature of the problem, one could easily suggest that we need an actuator in a leg that exerts a ground reaction force large enough to push the body up at least twice of its actual body height. However, when you start building a robot that achieves a similar task using a conventional actuator, e.g., DC motors, you realize that the power of available actuators is not sufficient to accomplish this in practice. Then this problem becomes a research problem to build a novel actuator that advances both the field of science and technology. Currently, the jumping/hopping

capability of our robot is limited up to 20 – 50 mm in height. However, we intend to advance the mechanism of our robot (morphology) that allows it to jump higher. An alternative approach could be to investigate the control first using an existing robot morphology. In future, we would like to take into account both approaches (control and morphology) to accomplish this task as both are important from the perspective of embodiment.

9.3 Running Fast

Current technology allows wheeled vehicles to move rapidly on artificial terrain (road). In contrast, today's legged robots are still very far to reach the pace of a wheeled vehicle on a level ground. Though nature has already provided us a good example in the shape of an animal "cheetah". Cheetah is the fastest land animal on this planet. It can reach roughly 47 m/s. It has been suggested in biology that cheetah uses its spine to increase stride length for fast locomotion [Hildebrand, 1959]. Although, our four-legged system uses a rigid trunk, we can increase the speed of our robot to some extent by reconfiguring its effective leg length (voluntary morphosis). For example, by reconfiguring the leg length of the front and hind pairs of legs online to different leg settings, we can achieve different stride lengths on a particular gait. Because of this feature (reconfigurable leg length), the bound gait of our robot seems remarkably similar to the bound gait of a four-legged animal (see Fig. 9.1). Furthermore, we would like to add an active spine to increase the speed of our robot further.

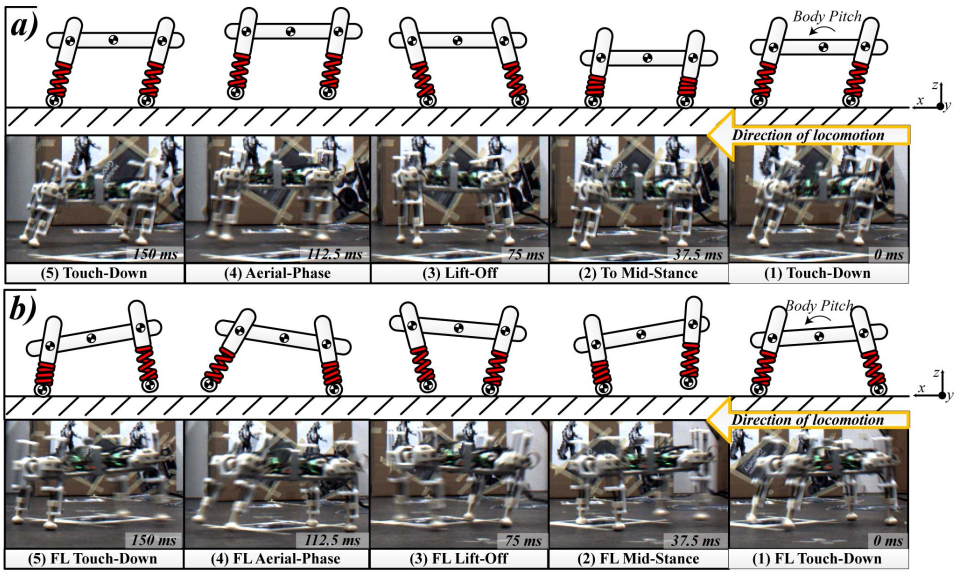

Figure 9.1: Gait versatility of the DTAR robot. a) shows the pronk gait and b) shows the bound gait. In a), we can see that when four legs touch and leave the ground simultaneously during a single cycle of locomotion, defines pronking. On the other hand, in bound gait b), the front pair of legs (FL) moves 180 deg out of phase than the hind pair of legs, i.e, when front pair of legs (FL) touch the ground then hind pair of leg leave the ground and vice-versa.

9.4 Turning Sharp

In this thesis, we implemented the turning control of our four legged system, but can our robot makes sharp turns during fast gait locomotion? This sharp turning is a very exciting problem. We intend to advance our control approach to achieve sharp turning on a level ground. Intuitively, it is highly likely that robot loses its stability while turning at speed of "1 m/s" in an open-loop control mode, but this reveals the limitation of the robot's body and control.

9.5 Galloping Gait

This is our ongoing research work. Currently, our four-legged system (DTAR) can dynamically pronk and bound at speed of " 1 m/s", but can we increase this speed further by implementing a gallop gait? The gallop gait is asymmetrical gait (see chapter 1). It is divided into two types according to their foot-fall pattern: transverse gallop and rotary gallop [Hildebrand, 1959]. The horse uses transverse gallop for fast running, whereas the cheetah uses rotary gallop [Bertram and Gutmann, 2010]. Achieving these two types of gallop gaits in a synthetic four-legged robotic system is extremely challenging. We intend to implement these two gaits for fast dynamic locomotion to extend our understanding about fast locomotion in general.

Bibliography

[Ahmadi and Buehler, 1997] Ahmadi, M. and Buehler, M. (1997). Stable control of a simulated one-legged running robot with hip and leg compliance. *IEEE Transactions on Robotics and Automation*, 13(1):96–104.

[Ahmadi and Buehler, 1999] Ahmadi, M. and Buehler, M. (1999). The ARL Monopod II Running Robot : Control and Energetics. *Proc. of the 1999 IEEE International Conference on Robotics and Automation*, 3(May):1689–1694.

[Ahmadi and Buehler, 2006] Ahmadi, M. and Buehler, M. (2006). Controlled Passive Dynamic Running Experiments With the ARL-Monopod II. *IEEE Transactions on Robotics and Automation*, 22:974–986.

[Alexander, 1990] Alexander, R. M. (1990). Three uses for springs in Legged locomotion. *The International Journal of Robotics Research*, 2:53–61.

[Alexander, 1992] Alexander, R. M. (1992). Simple models of walking and jumping. *Human Movement Science*, 11(1–2):3–9.

[Alexander, 2003] Alexander, R. M. (2003). *Principles of Animal Locomotion*. Princeton University Press.

[Ankarali and Saranli, 2010] Ankarali, M. M. and Saranli, U. (2010). Analysis and control of a dissipative spring-mass hopper with torque actuation. In Matsuoka, Y., Durrant-Whyte, H. F., and Neira, J., editors, *Proc. of the 2010 Robotics: Science and Systems VI*. The MIT Press.

[BBC, 2014] BBC (2014). Adapted to jumping. `http://www.bbc.co.uk/nature/adaptations/Jumping`. [Online; accessed MARCH-2014].

[Bertram and Gutmann, 2010] Bertram, J. E. and Gutmann, A. (2010). Motions of the running horse and cheetah revisited: fundamental mechanics of the transverse and rotary gallop. *Journal of The Royal Society Interface*.

[Blickhan, 1989] Blickhan, R. (1989). The spring-mass model for running and hopping. *Journal of Biomechanics*, 22(11-12):1217–1227.

[Blickhan et al., 2007] Blickhan, R., Seyfarth, A., Geyer, H., Grimmer, S., Wagner, H., and Günther, M. (2007). Intelligence by mechanics. *Philosophical Transactions of the Royal Society A*, 365(1850):199–220.

[Blum et al., 2009] Blum, Y., Lipfert, S. W., and Seyfarth, A. (2009). Effective leg stiffness in running. *Journal of biomechanics*, 42(14):2400–5.

[BostonDynamics, 2013a] BostonDynamics (2013a). Four Legged Robots, Big Dog and Alpha Dog. http://www.bostondynamics.com/. [Online; accessed JUNE-2013].

[BostonDynamics, 2013b] BostonDynamics (2013b). Whoa: Boston Dynamics Announces New WildCat Quadruped Robot. http://spectrum.ieee.org/automaton/robotics/military-robots/whoa-boston-dynamics-announces-new-wildcat-quadruped. [Online; accessed OCT-2013].

[Buehler et al., 2000] Buehler, M., Saranli, U., Papadopoulos, D., and Koditschek, D. (2000). Dynamic locomotion with four and six-legged robots. In *in Int. Symp. Adaptive Motion of Animals and Machines*.

[Cotton et al., 2012] Cotton, S., Olaru, I., Bellman, M., Ven, T., Godowski, J., and Pratt, J. (2012). Fastrunner: A fast, efficient and robust bipedal robot. concept and planar simulation. In *Proc. of the International Conference on Robotics and Automation*, pages 2358 – 2364, Saint Paul, MN, USA. IEEE.

[Daerden and Lefeber, 2000] Daerden, F. and Lefeber, D. (2000). Pneumatic artificial muscles: actuators for robotics and automation. *European journal of Mechanical and Environmental Engineering*, 47:10–21.

[Farley et al., 1991] Farley, C. T., Blickhan, R., Saito, J., and Taylor, C. R. (1991). Hopping frequency in humans: a test of how springs set stride frequency in bouncing gaits. *Journal of applied physiology (Bethesda, Md. : 1985)*, 71(6):2127–32.

[Ferris and Farley, 1997] Ferris, D. P. and Farley, C. T. (1997). Interaction of leg stiffness and surfaces stiffness during human hopping. *Journal of applied physiology (Bethesda, Md. : 1985)*, 82.

[Ferris et al., 1998] Ferris, D. P., Louie, M., and Farley, C. T. (1998). Running in the real world: adjusting leg stiffness for different surfaces. In *IN PROC. R. SOC. LOND*, pages 989–993.

[Full and Koditschek, 1999] Full, R. J. and Koditschek, D. E. (1999). Templates and anchors: neuromechanical hypotheses of legged locomotion on land. *The Journal of experimental biology*, 202(Pt 23):3325–32.

[Gabrielli and Kàrmàn, 1950] Gabrielli, G. and Kàrmàn, T. v. (1950). What price speed? *Mechanical Engineering*, 72(10):775–781.

[Geyer et al., 2006] Geyer, H., Seyfarth, A., and Blickhan, R. (2006). Compliant leg behaviour explains basic dynamics of walking and running. *Proc. Biological sciences / The Royal Society*, 273:2861–2867.

[Hildebrand, 1959] Hildebrand, M. (1959). Motions of the Running Cheetah and Horse. *Journal of Mammalogy*, 40(4):481–495.

[Hodgins and Raibert, 1991] Hodgins, J. and Raibert, M. (1991). Adjusting step length for rough terrain locomotion. *IEEE Transactions on Robotics and Automation*, 7(3):289–298.

[Hung et al., 2013] Hung, V. Q., Hauser, H., Leach, D., and Pfeifer, R. (2013). A variable stiffness mechanism for improving energy efficiency of a planar single-legged hopping robot. In *Proc. of the 2013 IEEE International Conference on Advanced Robotics*, Montevideo, Uruguay. IEEE.

[Hutter et al., 2012] Hutter, M., Gehring, C., Bloesch, M., Hoepflinger, M., Remy, C., and Siegwart, R. (2012). Starleth: A compliant quadrupedal robot for fast, efficient, and versatile locomotion. In *Proc. of the 15th International Conference on Climbing and Walking Robots*, pages 483–490, Baltimore, USA. Climbing and Walking Robots (CLAWAR).

[Hutter et al., 2013] Hutter, M., Remy, C., Hoepflinger, M., and Siegwart, R. (2013). Efficient and versatile locomotion with highly compliant legs. *IEEE/ASME Transactions on Mechatronics*, 18(2):449–458.

[Hyon and Mita, 2002] Hyon, S. H. and Mita, T. (2002). Development of a biologically inspired hopping robot "kenken". *Proc. of the 2002 IEEE International Conference on Robotics and Automation*, pages 3984–3991.

[Iida et al., 2005] Iida, F., Gabriel, G., and Pfeifer, R. (2005). Exploiting Body Dynamics for Controlling a Running Quadruped Robot. *Proc. of the 2005 IEEE International Conference on Robotics and Automation*, pages 229–235.

[Iida et al., 2009] Iida, F., Minekawa, Y., Rummel, J., and Seyfarth, A. (2009). Toward a human-like biped robot with compliant legs. *Robotics and Autonomous Systems*, 57(2):139–144.

[Kimura and Fukuoka, 2000] Kimura, H. and Fukuoka, Y. (2000). Adaptive dynamic walking of a quadruped robot on irregular terrain by using neural system model. In *Proc. of the 2000 IEEE/RSJ International Conference on Intelligent Robots and Systems*, volume 2, pages 979–984. IEEE.

[Kimura and Fukuoka, 2004] Kimura, H. and Fukuoka, Y. (2004). Biologically inspired adaptive dynamic walking in outdoor environment using a self-contained quadruped robot: 'tekken2'. In *Proc. of the 2004 IEEE/RSJ International Conference on Intelligent Robots and Systems*, pages 986–991. IEEE.

[KITRoboticsLab, 2003] KITRoboticsLab (2003). The quadruped robot "tekken-ii". `http://robotics.mech.kit.ac.jp/kimura/research/Quadruped/photo-movie-tekken2-e.html`. [Online; accessed JUNE-2013].

[Kram and Dawson, 1998] Kram, R. and Dawson, T. J. (1998). Energetics and biomechanics of locomotion by red kangaroos (Macropus rufus). *Comparative biochemistry and physiology. Part B, Biochemistry & molecular biology*, 120(1):41–9.

[Lee and Farley, 1998] Lee, C. R. and Farley, C. T. (1998). Determinants of the center of mass trajectory in human walking and running. *Journal of Experimental Biology*, 201:2935–2944.

[McMahon and Cheng, 1990] McMahon, T. A. and Cheng, G. C. (1990). The mechanics of running: How does stiffness couple with speed? *Journal of Biomechanics*, 23:65–78.

[MITBiomimeticLab, 2013] MITBiomimeticLab (2013). MIT cheetah robot runs fast, and efficiently. `http://spectrum.ieee.org/automaton/robotics/robotics-hardware/mit-cheetah-robot-running`. [Online; accessed JUNE-2013].

[Muybridge, 2007] Muybridge, E. (2007). *Muybridge's Animals in Motion: CD-ROM & Book*. Dover Electronic Clip Art Series. Dover Publications.

[Papadopoulos and Buehler, 2000] Papadopoulos, D. and Buehler, M. (2000). Stable Running in a Quadruped Robot with Compliant Legs. *Proc. of the 2000 IEEE International Conference on Robotics and Automation*, pages 444–449.

[Peuker et al., 2012] Peuker, F., Seyfarth, A., and Grimmer, S. (2012). Inheritance of slip running stability to a single-legged and bipedal model with leg mass and damping. In *Proc. of the 4th International Conference on Biomedical Robotics and Biomechatronics (BioRob)*, pages 395–400, Rome, Italy. IEEE.

[Pfeifer et al., 2007] Pfeifer, R., Lungarella, M., and Iida, F. (2007). Self-organization, embodiment, and biologically inspired robotics. *Science (New York, N.Y.)*, 318(5853):1088–93.

[Pfeifer and Scheier, 1999] Pfeifer, R. and Scheier, C. (1999). *Understanding Intelligence*. MIT Press, Cambridge, MA, USA.

[Playter and Raibert, 1992] Playter, R. R. and Raibert, M. H. (1992). Control Of A Biped Somersault In 3D. *Proceedings of the IEEE/RSJ International Conference on Intelligent Robots and Systems*, 1:582–589.

[Pongas et al., 2007] Pongas, D., Mistry, M., and Schaal, S. (2007). A robust quadruped walking gait for traversing rough terrain. In *Proc. of the 2007 IEEE/RSJ International Conference on Robotics and Automation*, pages 1474–1479. IEEE.

[Poulakakis et al., 2004] Poulakakis, I., Smith, J., and Buchler, M. (2004). Experimentally validated bounding models for the Scout II quadrupedal robot. *Proc. of the 2004 IEEE International Conference on Robotics and Automation*, 3:2595–2600.

[Raibert, 1986a] Raibert, M. H. (1986a). Legged robots. *Communications of the ACM*, 29(6):499–514.

[Raibert, 1986b] Raibert, M. H. (1986b). *Legged robots that balance*. Massachusetts Institute of Technology, Cambridge, MA, USA.

[Raibert, 1990] Raibert, M. H. (1990). Trotting, pacing and bounding by a quadruped robot. *Journal of biomechanics*, 23 Suppl 1:79–98.

[Raibert, 2008] Raibert, M. H. (2008). BigDog, the Rough-Terrain Quadruped Robot. In Chung, M. J., editor, *Proc. of the 17th IFAC World Congress, 2008*, volume 17.

[Raibert et al., 1984] Raibert, M. H., Brown, H. B., and Chepponis, M. (1984). Experiments in Balance with a 3D One-Legged Hopping Machine. *The International Journal of Robotics Research*, 3(2):75–92.

[Rebula et al., 2007] Rebula, J. R., Neuhaus, P. D., Bonnl, B. V., Johnson, M. J., and Pratt, J. E. (2007). A controller for the littledog quadruped walking on rough terrain. *Proc. of the 2007 IEEE International Conference on Robotics and Automation*, pages 10–14.

[Robinson et al., 1999] Robinson, D. W., Pratt, J. E., Paluska, D. J., and Pratt, G. A. (1999). Series elastic actuator development for a biomimetic walking robot. In *Proc. of the 1999 IEEE/ASME international conference on advanced intelligent mechatronics*, pages 561–568.

[Saranli et al., 2001] Saranli, U., Buehler, M., and Koditschek, D. E. (2001). Rhex: A simple and highly mobile hexapod robot. *International Journal of Robotics Research*, 20:616–631.

[Sebastian and Seyfarth, 2011] Sebastian, R. and Seyfarth, A. (2011). Stance leg control: variation of leg parameters supports stable hopping. *Bioinspiration and Biomimetics*, 7(1):016006.

[Seipel and Holmes, 2007] Seipel, J. and Holmes, P. (2007). A simple model for clock-actuated legged locomotion. *Regular and Chaotic Dynamics*, 12:502–520.

[Seok et al., 2013] Seok, S., Wang, A., Chuah, M., Otten, D., Lang, J., and Kim, S. (2013). Design principles for highly efficient quadrupeds and implementation on the mit cheetah robot. In *Proc. of the International Conference on Robotics and Automation*, pages 3307 – 3312, Karlsruhe, Germany. IEEE.

[Sheikh, 2013] Sheikh, F. I. (2013). Towards fast running: Open-loop speed and direction control of a single-legged hopper. In *Proc. of the 2013 IEEE/RSJ International Conference on Intelligent Robots and Systems*, pages 5114–5120, Tokyo, Japan. IEEE.

[Sheikh et al., 2011] Sheikh, F. I., Hauser, H., Aryananda, L., Quy, H. V., and Pfeifer, R. (2011). SLIP-model-compatible and bio-inspired robotic leg with reconfigurable length. In *Proc. of the 5th International Symposium on Adaptive Motion of Animals and Machines (AMAM)*, pages 47–48, Awaji, Japan.

[Sheikh et al., 2014] Sheikh, F. I., Hauser, H., and Pfeifer, R. (2014). Significance of Foot Compliance For Fast and Energy-Efficient Legged Robot Locomotion. *IEEE Transactions on Robotics and Automation*.

[Sheikh and Pfeifer, 2012] Sheikh, F. I. and Pfeifer, R. (2012). Adaptive locomotion on varying ground conditions via a reconfigurable leg length hopper. In *Proc. of the 15th International Conference on Climbing and Walking Robots*, pages 527–535, Baltimore, USA. Climbing and Walking Robots (CLAWAR).

[Sheikh and Shams-Ul-Haq, 2013] Sheikh, F. I. and Shams-Ul-Haq, S. (2013). Dynamic Maneuverability Through Voluntary Morphosis in a Four-Legged Robot. In *Proc. of the 2013 IEEE International Joint Conference on Cybernetics and Intelligent Systems (CIS) & Robotics, Automation and Mechatronics*, pages 49–54, Manila, Philippines. IEEE.

[Spröwitz et al., 2013] Spröwitz, A., Tuleu, A., Vespignani, M., Ajallooeian, M., Badri, E., and Ijspeert, A. (2013). Towards dynamic trot gait locomotion: Design, control, and experiments with cheetah-cub, a compliant quadruped robot. *The International Journal of Robotics Research*, 32(8):932–950.

[Tsujita et al., 2001] Tsujita, K., Tsuchiya, K., and Onat, A. (2001). Adaptive gait pattern control of a quadruped locomotion robot. *Proc. of the 2001 IEEE/RSJ International Conference on Intelligent Robots and Systems*, 4:2318–2325.

[Vernaza et al., 2009] Vernaza, P., Likhachev, M., Bhattacharya, S., Chitta, S., Kushleyev, A., and Lee, D. D. (2009). Search-based planning for a legged robot over rough terrain. In *Proc. of the 2009 IEEE/RSJ International Conference on Robotics and Automation*, pages 2380–2387. IEEE.

[Webb, 2001] Webb, B. (2001). Can robots make good models of biological behaviour? *The Behavioral and brain sciences*, 24(6).

[Wyffels et al., 2010] Wyffels, F., D'Haene, M., Waegeman, T., Caluwaerts, K., Nunes, C., and Schrauwen, B. (2010). Realization of a passive compliant robot dog. In *Proc. of the 3rd International Conference on Biomedical Robotics and Biomechatronics (BioRob)*, pages 882 – 886, Tokyo, Japan. IEEE RAS.

Appendix A

Slip-Model-Compatible and Bio-Inspired Robotic Leg with Reconfigurable Length

Reprinted from:

Farrukh Iqbal Sheikh, Helmut Hauser, Lijin Aryananda, Hung Vu Quy and Rolf Pfeifer (2011). *Slip-Model-Compatible and Bio-Inspired Robotic Leg with Reconfigurable Length*, In Proceedings of 5th International Symposium on Adaptive Motion of Animals and Machines (AMAM), pages 47–48. Awaji, Japan.

Slip-Model-Compatible and Bio-Inspired Robotic Leg with Reconfigurable Length

[1]Artificial Intelligence Laboratory, Department of Informatics, University of Zurich, Switzerland
(Tel : +41-79-3747186; E-mail: fsheikh, hhauser, lijin, vqhung, pfeifer@ifi.uzh.ch)

Abstract: We present a novel robotic leg design with reconfigurable length. The design combines key features from bio-mechanical principles into a novel robotic leg with only two actuated degrees of freedom (DOF). The leg configuration with one rotary hip joint and one prismatic knee joint makes it compatible to the Spring Loaded Inverted Pendulum (SLIP) model and will therefore potentially allow direct transfer of suitable control parameters obtained by the simulation of the SLIP model [3]. We have implemented the first prototype and conducted preliminary hopping experiments based on energy-efficient hopping at optimal frequency in human experiment [1]. We measured the ground reaction force and electrical power consumption of the module over a range of hopping frequencies. Our results suggest that the leg driven at its optimal frequency is more dynamic and energy efficient. The externally measured ground reaction forces are very consistent with the results obtained in [1].

Keywords: Legged robots, energy efficiency, spring-mass model.

1. INTRODUCTION

Legged robot locomotion has been progressing over recent years supported by the fact that legged robots have the potential to traverse more efficiently rough terrain than the wheeled robots [2]. Inspiration for these designs mainly comes from nature as animal running, hopping and jumping yet present the most efficient and astonishing solution towards energy-efficient legged locomotion. The mechanics of legged animals are composed of many complex components. Some of the core properties of these mechanics can be captured by a simple spring-mass model (SLIP) [3], which makes this model is a promising solution towards building and controlling better legged robots.

Pioneering work has been demonstrated by Marc Raibert in his single legged planar hopper [2]. It uses two actuated DOFs, one rotary to control the forward and the backward motion and a second pneumatically powered telescopic leg for restoring energy and ground interaction. The SCOUT II quadruped robot is able to locomote in fast and dynamic gaits, with only one active rotary DOF and passive linear compliance [4]. Nevertheless, the use of one DOF limits its performance on rough terrain. In contrast, the Tekken robot utilizes three active DOFs per leg and is potentially capable to handle rough terrain up to certain extent [5]. However, with the accumulated motors weights, dynamically fast gaits are difficult to achieve.

In this paper, we present a novel robotic leg design with reconfigurable length using two actuated DOFs, which combines the strengths of the SCOUT II and Tekken robot, namely the lower DOF and the high motion flexibility. The design is based on a number of specifications, some of which are derived from bio-mechanical studies: light-weight, compact, high-speed and back-drivable vertical DOF with the ability to inject and regulate the required energy into the system, linear compliance that allows easy force measurement needed for impedance control, large range of joint motion, and variable-height ground clearance.

In the next section, we describe the design and implementation details of the leg prototype. We have performed some preliminary experiments with a single leg setup and report on our measurement results based on the electrical power consumption and ground reaction forces at varying hopping frequencies.

2. DESIGN AND IMPLEMENTATION

Based on the specifications listed above, we have designed and implemented the first leg prototype. As shown in Fig.1, The physical prototype uses two actuated DOFs, one rotary (the hip) to oscillate the leg within the range of 180^0 and a second (the knee) which is defined as a prismatic joint to alter and adjust the module length within the range of 100 mm. Both joints can be directly operated from the trunk segment. Thus, the weight of the leg segment can be considerably reduced.

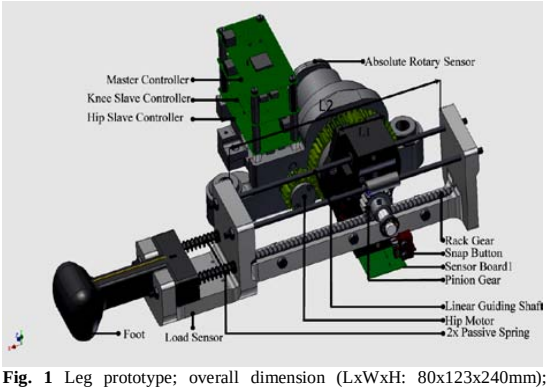

Fig. 1 Leg prototype; overall dimension (LxWxH: 80x123x240mm); weight: 0.75Kg; K per spring: 0.98 N/mm}; Translational speed (knee): 136.4 mm/s.

The prismatic knee motion is implemented by using a pinion and rack gear mechanism. We have also inserted two compression springs to introduce linear compliance in series with the leg segment. The combination of the prismatic knee joint and linear compliance provide the following capabilities: (i) The leg can inject and regulate the amount of energy needed for effective and efficient ground interaction during locomotion, (ii) It allows variable-height ground clearance, (iii) When integrated in a multi-legged robot, it provides the possibility for the robot to adapt its morphological parameters (leg length and center of mass), according to

the current environment or task, (iv) The linear spring allows energy storage through passive compliance and provides easy force measurement for impedance control, which can add active compliance to the system.

In addition to these capabilities, the leg configuration with one rotary hip joint and one prismatic knee joint makes it compatible to the Spring Loaded Inverted Pendulum (SLIP) model. This would allow direct transfer of suitable control parameters obtained by the SLIP model and significantly reduces the search space of optimal control parameters in the future. The current leg design is modular. Thus, the complete Quadruped robot can be realized by combining four such modules together with the trunk module.

3. EXPERIMENTAL RESULTS

The performance of the leg was tested in a sagittal plane against the gravity on a force plate. The hopping gait was selected to systematically perform experiment based on the measurements of optimal frequency in [1]. During the experiment, the straight posture of the module was maintained by actuating the hip motor at a constant angle and in-place hopping was carried out by operating the knee motor at different control frequencies. At each frequency, the total power consumption and the vertical ground reaction force (GRF) were measured.

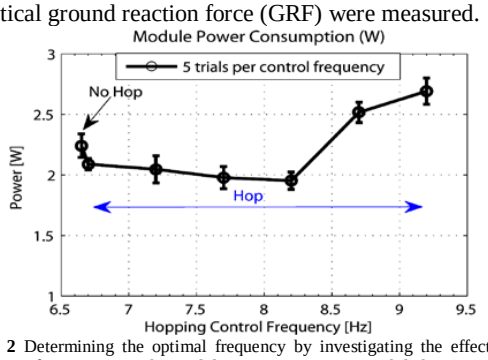

Fig. 2 Determining the optimal frequency by investigating the effect of different frequencies on the module power consumption while hopping.

Fig.2 shows the power consumption at different control frequencies (averaged over 5 trials per frequency). At 6.65 Hz, no hopping was observed and the average electrical power consumption of the module was about 2.242 ±0.096 W. When the control frequency was increased to 6.7 Hz, the module started to hop and the amount of power consumption dropped. When we increased the frequency further, the consumption decreased further until it reached a minimum at 8.2 Hz. At higher frequencies, the electrical power consumption increased again significantly. Thus, we concluded that 8.2 Hz is the optimal frequency of the leg module.

Fig. 3 (a) shows the vertical force exerted on the ground by the system during the ground contact phase, measured using a force plate, which is consistent with results obtained in human hopping in (b). According to [1], the time window, when the reaction force exceeded one body weight during landing and take-off is equivalent to half of the resonant period, i.e., T/2.

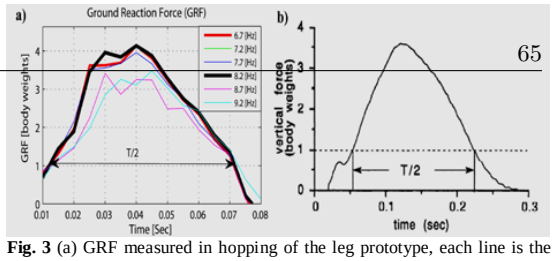

Fig. 3 (a) GRF measured in hopping of the leg prototype, each line is the mean GRF of five successive hops per control frequency; b) GRF measured in human hopping, taken from [1]

We obtained this time window by using the data shown in Fig.3 (a) 59.6 ±0.001 ms. Hence, the optimal frequency was $f\_res = 1/T$ = 8.39 ±0.087 Hz. Further, the effective stiffness of our robotic leg was computed by using the equation $k = m\omega^2$ = 2084.74 ±43.31 N/m, where m=0.75 kg is the mass of the module. Fig.4 shows a sequence of the hopping at the optimal frequency. About 20 mm ground clearance was observed.

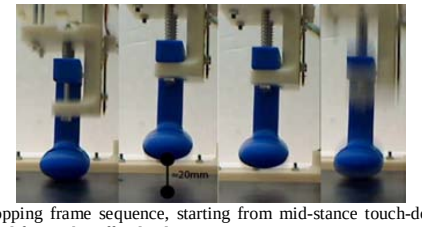

Fig. 4 Hopping frame sequence, starting from mid-stance touch-down to take-off and from take-off to landing.

4. CONCLUSION

We present a novel biologically inspired two-DOF leg with reconfigurable length, which is compatible to the SLIP model. We evaluated the preliminary performance of the leg module on the hopping gait based on the concept of energy-efficient hoping at optimal frequency [1]. We plan to further develop and investigate the dynamical properties and performance of the presented leg design in walking and running, and to validate the results in comparison to simulations based on the SLIP model.

5. ACKNOWLEDGMENT

This work was supported by the European Commission Seventh Framework Program, Theme ICT- 2007.8.5 as part of the project LOCOMORPH, under a grant no 231688.

6. REFERENCES

[1] Claire T. Farley et al., “Hopping Frequency in Humans: a test of how springs set stride frequency in bouncing gaits”, *The American Physiological Society*, 1991, pp 2127-2132.

[2] Marc H. Raibert, “Legged Robots that Balance”, *MIT press*, ISBN 0-262-681196.

[3] R. Blickhan, “THE SPRING-MASS MODEL FOR RUNNING AND HOPPING”, *Journal of Biomechanics*, Vol. 22, No. 11/12, 1989, pp 1217-1227.

[4] Ioannis Poulakakis, “On the Stability of the Passive Dynamics of Quadrupedal Running with a Bounding Gait”, *The international Journal of Robotics Research*, 2006, pp 669-687.

[5] Hiroshi Kimura et al., “Biologically inspired adaptive walking of a quadruped robot”, *Phil. Trans. R.Soc, 2007*, pp. 153-170.

Appendix B

Adaptive Locomotion on Varying Ground Conditions via a Reconfigurable Leg Length Hopper

Reprinted from:

Farrukh Iqbal Sheikh and Rolf Pfeifer (2012). *Adaptive Locomotion on Varying Ground Conditions via a Reconfigurable Leg Length Hopper*, In Proceedings of 15th International Conference on Climbing and Walking Robots (CLAWAR), pages 527-535. Baltimore, USA.

ADAPTIVE LOCOMOTION ON VARYING GROUND CONDITIONS VIA A RECONFIGURABLE LEG LENGTH HOPPER

FARRUKH IQBAL SHEIKH[†], AND ROLF PFEIFER

Artificial Intelligence Laboratory, University of Zurich, Andreastrasse 15 Zurich, 8050, Switzerland

In this paper, we present the concept of adapting to changes in ground conditions like stiffness, damping and friction, using a novel two degree of freedom reconfigurable leg length hopping robot with a fixed passive compliance. In such a robot, the change in the dynamics of the single legged hopper can be induced by the change in coupled stiffness and damping of the system, i.e., stiffness and damping of the ground coupled with the stiffness and damping of the robotic leg. It is experimentally shown by in-place hopping of a robotic leg on various grounds (stiff, less stiff and soft) that the leg can effectively adapt to changes in coupled stiffness and damping by the rate and the amplitude at which the leg length changes. This is true, while the leg hops in-place as the role of ground friction is negligible. However, in forward motion where the ground friction dominates, a change in initial effective leg length, i.e., shortening or lengthening can provide an additional support to the hip motor in overcoming even large variations in ground friction. This is demonstrated through a planar locomotion experiment on different ground surfaces. The overall results provide strong support for this concept.

Keywords: Varying ground conditions, changeable leg length.

1. Introduction

Animals and humans are capable to adapt to varying ground conditions (stiffness, damping and friction) while maintaining their balance on irregular surfaces [1]. This kind of adaptive behaviour is a great source of inspiration for designing legged robots. In general, ground surfaces can be characterized by their stiffness, damping and friction properties. In legged robot locomotion, one approach to adapting to varying ground conditions is by physically changing parameters of the robotic leg to counter-act the overall change. For example, in [2] mechanically adjustable compliance in the robotic leg was introduced to adapt to the change in stiffness of the underlying surface. However, it is not entirely clear how these changes can be incorporated in practice during fast running of a legged robot. Except for the pioneering work of Marc Raibert [1], most of the electrically actuated legged robots developed in the past were designed to exploit the potential of passive compliance [3], [4], together with the

[†] Work supported by the European Commission Seventh Framework Program, Theme ICT- 2007.8.5 as part of the project LOCOMORPH, under a grant no 231688. Video can be found at this link.

oscillatory motion of the robotic leg. However, due to exploiting limited degrees of freedom in [3], [4], the performances of these systems were mainly restricted to stiff grounds. In this study, we demonstrate that, in the context of adaptive legged robot locomotion, all three ground properties, namely stiffness, friction and damping, are equally important. In other words, efficient adaptation should consider all three ground conditions in a unified framework.

We developed a bio-inspired 2-DOF robotic leg whose design of [5] follows the spring loaded inverted pendulum (SLIP) model, also referred to as the bouncing motion [5]. In [5], the altering leg length feature was first introduced. In this paper, we propose a systematic approach, which is based on the concept of embodiment [6], in order to test the framework of [7] for varying ground conditions. According to [6], the dynamic coupling of the robot's body with its controls and the physical environment is important to investigate the overall behavior of the robot. By employing this concept, the effects of altering leg length are practically investigated on number of different grounds. Experimental results demonstrate that the reconfigurable leg length approach is suitable to efficiently adapt to varying ground conditions both for in-place and planar hopping.

The remainder of this paper is structured as follows: Section 2 describes the mechanical structure and the control of the robotic leg. Section 3 explains the proposed mathematical model. Experiments and results are provided and discussed in Section 4. Finally, Section 5 draws some conclusions and details the future research direction of this work.

2. Mechanical Design and Control

The 2-DOF reconfigurable leg length hopper (RLLH) module, as shown in Fig. 1, was designed and constructed based on the SLIP model [7].

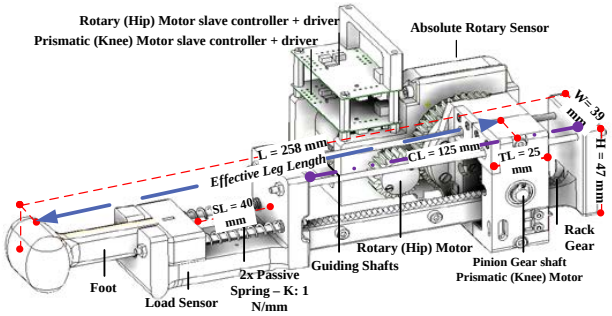

Figure 1. Reconfigurable Leg Length Hopper (RLLH) module. Leg segment dimension *(LxWxH: 258x39x47 mm^3)*; total weight (including the weight of the boom rod, which can be seen in Fig. 4 (a): *0.778 ± 0.001 kg*. Purple line shows the range of reconfigurable leg length (CL). Blue line indicates the effective leg length (i.e., It is a distance measured from the center of rotation to the ground).

However, in contrast to the standard SLIP model, the leg has an additional active DOF, i.e., a linear joint which works in series with the passive compliance, similar to a muscle-tendon mechanism in a biological system [8]. This additional DOF provides supplementary advantages over the SLIP model, i.e., it regulates the energy into the passive-spring by altering the amplitude and the rate at which the leg length changes. In addition, adjusting the initial leg length to the various settings, i.e., shifting the initial set position of the leg in order to make it shorter or longer, can now be achieved online. In order to make the design lighter, two electric DC brushed motors are used. The first DC motor drives the linear motion for changing the leg length while the second one allows for a rotary motion of the hip joint.

The control of the RLLH [7] consists of a two layer framework. At the lower level, two types of positional PID motor control loops, one each for the rotary and the linear motion, were implemented. The gains of each PID were experimentally tuned for good performance. On the higher level, an open-loop sinusoidal control scheme was programmed in a master controller. It computes the desired trajectory of each joint by processing control functions (see section 2.2) at the rate of *125 ± 2.4E-05 Hz.* The results from this computation are then transmitted to the low level PID control for the execution of joint motion.

2.1. *Control law*

The oscillator force F_m, due to the motion of the reconfigurable linear joint, for a given operating time t is defined as follow:

$$F_m = -\frac{I_l}{d^2}\left(\Delta l {\omega^2}_p\right)\sin\left(\omega_p t + \varphi_p\right), \tag{1}$$

where, I_l is the moment of inertia of the leg, d is the radius of the pinion gear, Δl is the change in leg length (amplitude), $\omega_p = 2\pi f_p$ is the angular frequency of the oscillator, and φ_p is the phase shift in the oscillator. Furthermore, $v_p = \omega_p * d$ and $\Delta l = v_p * t$. F_m acts such that, when the leg length increases during the first phase of the control signal, the body moves up consequently performing positive work at the passive spring. This work is done by pushing the leg against the ground thus storing some energy in the spring. During the next phase of the control signal, when the applied torque is in the counter-clockwise direction, the leg length reduces by effectively taking the energy from the system (the negative work). Hence, by applying a simplified oscillatory control signal of various amplitudes and frequencies, the required energy in the passive spring can be regulated.

Similarly, the torque τ_r produced by the rotary joint during the oscillatory motion in the sagittal plane, is defined as

$$\tau_r = I_l * \ddot{\theta_r} = -\Delta\theta_r \omega_r^2 \sin(\omega_r t + \varphi_r), \tag{2}$$

where, $\ddot{\theta}_r$ is the joint angular acceleration, $\Delta\theta_r$ is the amplitude of the rotary motion, ω_r is the angular frequency of the oscillator, and φ_r is the phase offset of the oscillations. By adjusting the parameters $\Delta\theta_r$, ω_r and φ_r in the above equation, the forward and backward motion of the leg is controlled.

3. Mathematical Model

The dynamics of the in-place hopping of the RLLH can be described by the mass-spring-damper model, as shown in Fig. 2. By conducting a force analysis of the model, a differential equation describing the motion of the center of mass of the robotic leg, when the ground stiffness is high, is obtained as,

$$m\ddot{y} + D_l\dot{y} + k_l y = F_m + mg, \tag{3}$$

where, y is the motion of the body in the vertical axis, D_l is the damping while k_l is the stiffness constant of the leg, F_m is the oscillatory force produced by the motion of the prismatic joint, as defined in (1), and $m.g$ is the weight of the module. According to (3), when the ground surface is highly stiff, the natural frequency of the system can be defined as,

$$f_0 = \frac{1}{2\pi}\sqrt{\frac{k_l}{m}}, \tag{4}$$

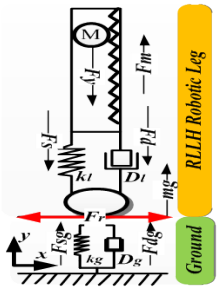

Figure 2. A mass-spring-damper representation of the robotic leg during in-place hopping.

However, for varying ground conditions, the resulting natural frequency f_0 of the system is not only a function of the stiffness and the damping of the robotic leg but it becomes a function of the coupled properties of the two, i.e., stiffness and damping of the ground coupled with the stiffness and damping of the robotic leg (see Fig.2, a model of RLLH (orange) in connection with the model of the ground (green)). These coupled properties affect the overall system dynamics when the leg is in contact with the varying ground conditions. In this case, the coupled stiffness k_c is defined as,

$$k_c = \frac{k_l * k_g}{k_l + k_g}, \tag{5}$$

where, k_l is the leg stiffness and k_g is the ground stiffness. The resulting natural frequency of this coupled interaction can be represented as,

$$f_0 = \frac{1}{2\pi}\sqrt{\frac{k_c}{m}}, \tag{6}$$

In case of very stiff grounds, i.e., $k_g \gg k_l$, the natural frequency of the system (6) mainly depends on k_l, because the coupled stiffness k_c reduces to k_l.

On the other hand, when the ground is soft, i.e., $k_g \ll k_l$, the ground stiffness dominates the system behavior and the coupled stiffness k_c reduces to the ground stiffness k_g. Thus, in this case k_g defines the natural frequency of the coupled system. Since, for soft grounds, k_g is lower than that of k_l, the required operating frequency of the actuator in order to adapt to surface changes will also be lower than in the case of stiff ground. This is advantageous, since, the electric actuators such as the DC brushed motors typically have a limited operational bandwidth. At the lower operating frequency, such motors can potentially be more efficient.

The presence of the dissipative forces, such as friction is very common in real systems. It causes a decrease in mechanical energy during the motion. This effect is modeled as a damper in our system that depends on the speed of the body. In a coupled system, its effect will be additive and can be compensated by injecting more energy (see Equation 1).

These two ground properties (stiffness and damping) lead to a change in the natural frequency and the amplitude of the power consumption of the system for varying grounds, which is shown in number of experiments (see Section 4.1).

The ground friction comes into play during the forward motion of the robotic leg. Due to varying nature of the ground, friction also varies and one way to compensate this change in friction is to reduce the length of the leg such that the rotary joint requires less torque to efficiently negotiate with the ground friction. This relation of the rotary joint torque τ_r and the leg length is defined as

$$\tau_r = F_r * \{L_0 + \Delta l \sin(\omega_p t + \varphi_p)\}, \quad (7)$$

where, L_0(initial leg length), Δl (change in leg length), and ω_p (rate of change). Thus, the shorter leg can theoretically negotiate better both the high and the low friction grounds compared to the longer leg. However, a longer leg can be useful in situations where an increased locomotion speed is required. The latter can be achieved by increasing the leg length during the steady state locomotion when the effect of the static friction becomes smaller. This is experimentally verified in section 4.2.

4. Experiments and Results

To test the role of the reconfigurable leg length for different ground conditions, two types of dynamic motions of the RLLH were studied: one, when the leg hops in-place on various grounds (see Section 4.1) and second, when the leg ran in hopping gait over different grounds, while being fixed to a boom (see Section 4.2).

4.1. *Hopping In-Place*

This experiment was conducted while the robot was in an upright posture with respect to the ground. Hopping was achieved by actuating the hip motor at a

constant position (i.e., the hip angle is fixed at $\pi/2$ *rad*). In-place hopping was performed by varying two parameters, the amplitude (Δl) and the frequency (f_p) in equation (1) that controls the force produced by the prismatic motion. For each change in amplitude and frequency, the total electrical power consumption of the RLLH was measured. The same experiment was repeated on three types of ground surfaces: stiff (force plate), less stiff (gym training mat) and soft (foam), as shown in Fig. 3 (a). In total, *152* combinations including *4* different amplitudes *(4-28 mm in steps of 8 mm)* and *38* different frequencies *(0.5-10 Hz in steps of 0.25 Hz)* were experimentally tested per ground surface.

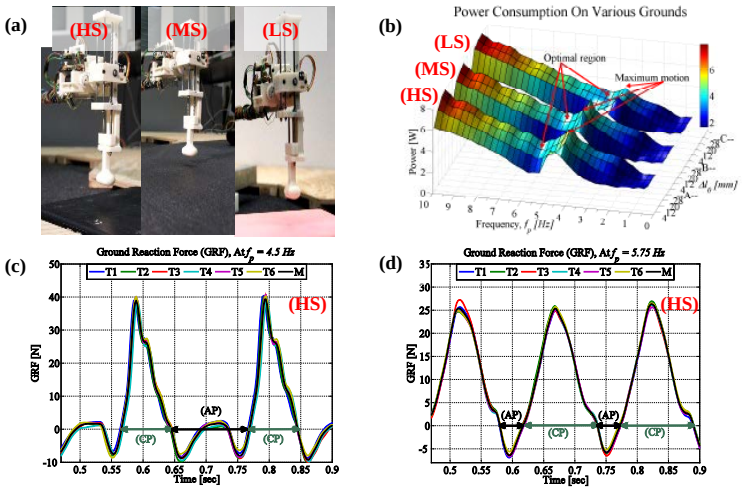

Figure 3. Hopping in place experiments. **(a)** Photographs taken during the experiment over (HS) very stiff ground (force plate), (MS) medium stiff ground (gym training mat), and (LS) soft, low-stiff ground (foam). **(b)** The power consumption plot for HS, MS, and LS. The x-axis represents the frequency ranging from *(0.5-10Hz in steps of 0.25Hz)*, the y-axis the amplitude of change in leg length *(4-12-20-28mm)* relative to the initial effective leg length of *135.5mm*, and the z-axis represents the electrical power consumption averaged over *6 trials* per control parameter. The duration of each trial was *7 sec*. **(c)** The ground reaction force (GRF) measured at a forced frequency (f_p) of *4.5 Hz* on ground (HS). At this frequency the robotic leg achieved the maximum aerial phase (AP) – see the duration of contact phase (CP) and aerial phase (AP) in Fig. 3 (c). This reflects the increase in the ground impact, thus the power consumption- see Fig. 3 (b), (HS). **(d)** The GRF measured at the optimal forced frequency *5.75 Hz* on ground (HS), where the lowest power consumption was observed. At this point the aerial phase decreases to the value shown in Fig. 3 (c). These results from c) and d) also indicate that the duration of the contact phase (CP) and the aerial phase (AP), can be actively modulated by the rate of change in leg length to adapt to varying ground conditions. As we formulated in (5) that on stiff ground such as (HS), the coupled stiffness k_c reduces to the leg stiffness, i.e. $k_c = k_l$ = *1 N/mm* – see Fig. 1. By substituting this value of k_l and *m: 0.778 ± 1E-3* k_g in equation (5), the natural frequency f_0 is computed, which yields *5.70 Hz*. This theoretical f_0 approximately matches the optimal frequency of (HS), which is *5.75 Hz*, where the robotic leg is energy efficient in maintaining steady-state hops.

It can be observed in the respective plot that the power consumption over different grounds (HS), (MS), and (LS) follows nearly the same pattern. On each of these surfaces, the power consumption is low at lower frequencies and it increases proportionally with the frequency. Interestingly, a sharp peak in the power curve is observed just after the frequency, where the in-place hopping started (see Fig. 3 (b), (HS) it is *4.25 Hz*). This peak represents the point where the contact phase (duration on ground) is less than the aerial phase (duration in air), i.e., high ground clearance, as can also be seen in Fig. 3 (c). Right after that, the power consumption sharply drops again as the frequency increases further and the contact phase (CP) increases compared to the aerial phase (AP) (see Fig.3 (d)). This frequency is the optimal frequency of the coupled system as it consumes least power. By further increasing the frequency above the optimal frequency, the power consumption increases too due to the decrease in aerial phase (AP). This shows that by altering the rate of change in leg length caused by the change in the frequency (f_P) of the actuation control signal in equation (1), the passive spring can be actively tuned to work in two different modes: First, in the energy efficient mode (optimal region), where the system can consume the least power and, second, an energy inefficient mode (maximum motion), where the system consumes more power but achieves high ground clearance. These modes are essential in designing the optimal control by exploiting the use of the passive compliance for locomotion.

As can be observed further, the optimal frequency for the soft ground (LS) shifted to a lower frequency as compared to the stiffer grounds (HS) and (MS). This shift in the frequency of overall system was caused by the change in the coupled stiffness and damping properties of the robotic leg with the ground surface, as formulated in equation (6). However, the proposed design is potentially able to adapt to it by varying the rate of change in leg length (see in Fig. 3 (a) In addition, it was observed that to efficiently adapt to the soft ground by mitigating the effect of deformation, higher ground clearance will also be needed. This can be obtained by increasing the amount of change in leg length at the optimal frequency.

4.2. *Planar Locomotion in a Hopping Gait*

This experiment was performed by operating both the rotary (at the hip) and prismatic motors (to change the leg length) at the frequency of *5 Hz*, which has been previously obtained from the in-place hopping experiment (see Fig. 3). For the planar locomotion, the amplitude of the oscillation of rotary hip joint was kept constant at *0.1745 ± 0.035 rad*. In addition, the phase shift between the rotary and the prismatic actuation signals was set to *0.92* rad with the change in leg length (i.e., Δl_0) to *10 mm and 18 mm*, during all trials. Only the initial effective leg length was altered (see Fig. 1), thereby the initial distance between the hip and the ground was changed (i.e., simulating different heights of the leg). In each trial, the angular velocity ω_s (see Fig. 4 (a)) about the boom fixed

coordinate system was measured using the gyro and it was then converted into planar velocity.

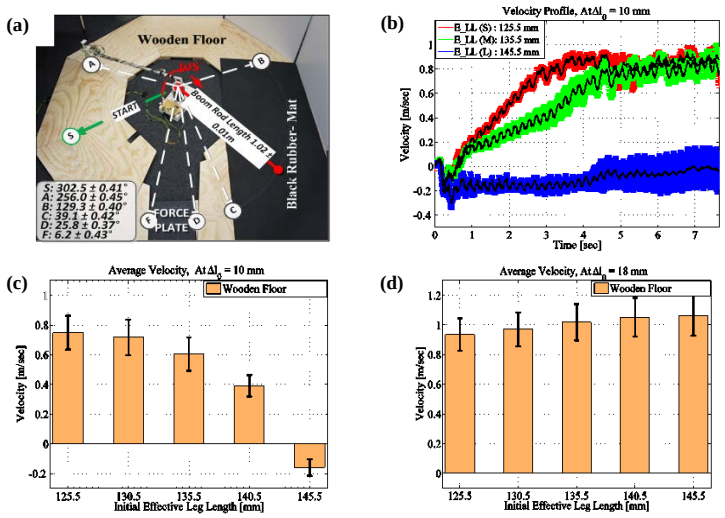

Figure 4. Forward hopping experiment. **(a)** A top view of the experimental-setup. Each trial ends after completing one revolution about the fixed boom axis. **(b)** The velocity profile with respect to the different initial leg lengths *(125.5 (short), 135.5(medium) and 145.5(long) in mm)*. For each leg length settings 5 trails were performed; the shaded region indicates the error about the mean value. **(c)** The measures of the change in forward velocity on wooden grounds with respect to the different initial leg settings. **(d)** The measures of change in forward velocity on wooden ground, when the amplitude of change in leg length Δl_0 increases to *18mm* than Fig. 4 (c).

As shown in Fig. 4 (b) and (c), the velocity at the smaller leg length (red curve) increases faster to the maximum than to the medium (green) and longer leg length (blue). Since the starting point for all these experiments were on wooden floor, we showed that the robotic leg in the short leg configuration was able to recover faster from the static-friction, than in the larger leg length condition, as described by equation (7). However, when the amplitude of change in leg length increases to 18 mm than 10 mm, then it enables the robotic leg to recover faster from the effect of friction, maintaining an increase in overall average locomotion speed with respect to increase in leg length, as shown Fig. 4 (d).

5. Conclusion and Future Work

We have practically demonstrated, that the reconfigurable second DOF of the RLLH that works in series with the passive compliance, is potentially useful to adapt to the changes in ground conditions like stiffness, damping and friction. It

can be simply achieved by adapting the amplitude of the linear leg movement and its rate of change in the leg length. Both changes can be rapidly applied to compensate for the change in the overall system behavior, i.e., the change in coupled stiffness and damping between leg and ground. In addition, shortening and lengthening the leg makes this design equally suitable for compensating the varying ground friction. Moreover, the speed of the locomotion, which also depends on the leg length, is also controllable. Furthermore, we highlighted in the in-place hopping experiments that our robotic leg can function in two modes, the optimal energy efficient mode *(aerial phase < contact phase)* and the high bounce energy in-efficient *(aerial phase > contact phase)* mode.

In the near future, these results will be incorporated in a closed loop control for the RLLH. Similar concept will be extended towards controlling a state of the art robot called DTAR that consists of 4 of the presented robotic legs (RLLH).

Acknowledgment

This work is supported by the European Commission Seventh Framework Program, Theme ICT- 2007.8.5 as part of the project LOCOMORPH, under a grant no 231688.

References

[1] M. H.Raibert, "Legged Robots," *Communications of the ACM,* vol. 29, no. 6, June 1986.

[2] Jonathan W.Hurst, et al., "Series Compliance for an Efficient Running Gait," *IEEE Robotics & Automation Magazine,* pp. 42-51, 2008.

[3] Fumiya Iida, et al., "Exploiting Body Dynamics for Controlling a Running Quadruped Robot," pp. 229-235, 2005.

[4] Ioannis Poulakakis, et al., "On the Stability of the Passive Dynamics of Quadrupedal Running with a Bouncing Gait," *IJRR,* pp. 669-687, 2006.

[5] R.Blickhan, "The Spring-Mass Model For Running And Hopping," *Journal of Biomechanics,* vol. 22, pp. 1217-1227, 1989.

[6] Rolf Pfeifer, et al., "Self-Organization, Embodiment, and Biologically Inspired Robotics," *Science,* vol. 318, p. 1088, 2007.

[7] Farrukh Iqbal Sheikh, et al., "SLIP-Model-Compatible and Bio-Inspired Robotic Leg with Reconfigurable Length," in *Adaptive Motion in Animals and Machines (AMAM),* 2011.

[8] R.M.Alexander, "Elastic Mechanisms in Animal Movement," *Cambridge University Press,* 1988.

Appendix C

Towards fast running: Open-loop speed and direction control of a single-legged hopper

©2013 IEEE. Reprinted, with permission, from:

Farrukh Iqbal Sheikh (2013) *Towards fast running: Open-loop speed and direction control of a single-legged hopper*, In Proceedings of 2013 IEEE International Conference on Intelligent Robots and Systems (IROS), pages 5114–5120. Tokyo, Japan.

This is the final accepted version. Final version of this article can be found at http://ieeexplore.ieee.org (doi=10.1109/IROS.2013.6697096).

Towards fast running: Open-loop speed and direction control of a single-legged hopper

Farrukh Iqbal Sheikh

Abstract— **Traditional 2D single-legged hoppers were able to demonstrate stable bi-directional running in a closed-loop approach. In contrast, we employ an open-loop control to achieve high-speed (≈0.8 m/sec or 1.78 mph) bi-directional dynamic running of the reconfigurable leg length hopper (RLLH). Our hopper has variable linear joint in series with a passive spring that allows changing its effective leg length in real-time. Furthermore by instantaneously changing the leg length at a particular amplitude and frequency. The required "thrust-forces" can be produced. We hypothesize that the direction and the speed of our hopper can be smoothly controlled by only changing the phase of the thrust-forces being applied to the ground, i.e., the change in phase between the leg-reconfiguration and the leg-oscillation. This is experimentally evaluated by varying the phase of leg-reconfiguration up-to the range of 0-2π rad (0-360 deg). Our results show a large region of a symmetric running. Moreover, a novel gait called "in-place running[1]" is found, where the speed of running is zero. We demonstrate that by only altering the phase of applying thrust-forces together with a constant leg oscillation can robustly control the speed and transition in the direction of locomotion.**

Keywords: Thrust-forces, in-place running, and bi-directional running.

I. INTRODUCTION

Wheeled robots can accelerate in a forward and a backward direction by simply changing the rotational phase of the wheels. Despite the limited performance of the wheeled robots in an unstructured environment, the control of wheeled robots is fairly simple compared to many existing legged robots. On the other hand legged robots have complex dynamics and control. Perhaps by advancing a simple open-loop approach in a legged robot, a fast and a stable bi-directional locomotion can be achieved.

Dynamically stable legged robot locomotion is being researched to understand the underlying mechanics of animals and humans locomotion [1]. In addition this research may lead us to develop a legged vehicle that will not be restricted to a particular terrain. A step towards a practical prototype that bounce over obstacles and run on legs, Raibert and his colleagues [1] built a series of legged robots: single-legged, two-legged, and four-legged. Each of these robots was controlled in hierarchy of three closed-loop control laws: one corrects the hopping height, second controls the forward speed, and third ensures the balance. These three control laws were coupled together in a state machine to achieve a stable running with varying speed. Moreover, by applying the rules of body and leg symmetry [2], the control was simplified further to achieve locomotion in a specified direction. However, how the principle of symmetry holds in a physical single-legged robot locomotion is not experimented in detail.

Existing legged robots [1], [3], [4] are designed to demonstrate the role of a closed-loop approach to achieve stable running; however, the dynamically self-stable running of a legged robot can also be achieved in an open-loop without any sensory feedback [5], [6]. The open-loop requires no sensory feedback; therefore, it is more suited to exploit inherent self-stability of a robot morphology during locomotion that results in a rapid dynamic running [7]. By employing this simple open-loop approach many under-actuated robots [8], [9] were successfully controlled. These robots exploit the passive-dynamic function of the compliant element in a single and a bipedal configuration to demonstrate a stable walking and hopping; nevertheless, the motion of these robots [8], [9] were optimized for a unidirectional locomotion, i.e., the importance of controlling the speed and the direction of locomotion was rarely addressed in an open-loop control. In this work, we explore the basis of a rapid bi-directional dynamic running of a single-legged robot in an open-loop control because this exploration may serve as a better foundation for a robust closed-loop control [10] of a legged robot.

Legged animals use muscles to exert forces on a ground through tendons to achieve bouncing (running) locomotion in varying directions [11]. Such bouncing or running locomotion in animals and humans can be described by the motion of a point mass in series with the mass less spring - SLIP model [12]. Similarly, this model also describes the bouncing locomotion of a robot that rebounds its body by exerting force to the ground. However, it is unable to explain that how the multiple joints in a robotic leg should actuate that accelerates the robot body in a specified direction. Inspired by the SLIP model, we developed a single-legged 2D hopper, called the "Reconfigurable Leg Length Hopper (RLLH)" [13] because the linear joint in series with the mechanical spring is a variable (reconfigurable) that functions as a biological muscle [14]. This joint can shorten and lengthen the robotic leg, such that the required forces can be exerted to the ground through a mechanical spring (tendon). We used this bio-inspired 2D hopper (RLLH) to conduct experiments based on our hypothesis that the speed and the direction of motion can be smoothly controlled in a simple open-loop control.

*This work was supported by the EU Project Locomorph.

[1]Farrukh Iqbal Sheikh is working at the Artificial Intelligence Laboratory, Department of Informatics, University of Zurich, Andreastrasse 15, 8050, Zurich. fsheikh@ifi.uzh.ch

[1]In-place running is like an in-place jogging, in which the motion of the body is mainly restricted in-place by the continuous movement of each joints of the leg.

This paper is organized in following sections: Section II briefly explains the mechanics and electronics of the robotic leg. Section III describes a feed-forward control approach. Section IV illustrates the concept of thrust-forces in a legged locomotion. Section V provides a detail of the experimental setup. Section VI discusses results of the experiments performed. Finally, Section VII draws a conclusion and highlights the future work.

II. MECHATRONIC DESIGN

The reconfigurable leg length hopper (RLLH) prototype [13] was designed to be modular in mechanics and electronics such that wide range of different morphologies and their influence on control, and vice-versa can be physical experimented.

A. Mechanical Design

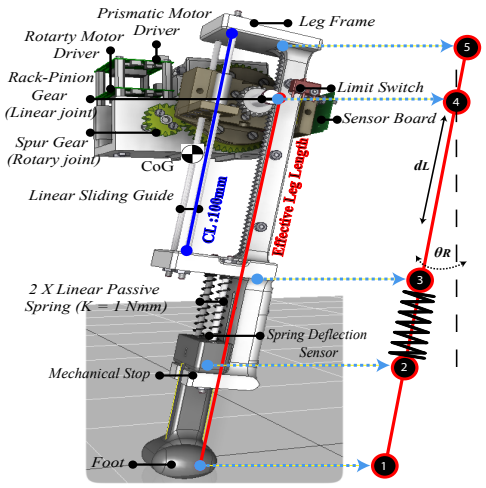

Fig. 1. Reconfigurable Leg Length Hopper (RLLH). The volumetric dimension of the robotic leg is LxWxH: 258x39x47 mm^3; total weight (including the weight of the boom rod (see section V)) is 0.870 $\pm$ 0.001 kg. Red-line indicates the leg length at rest, which is defined as the effective leg length of the robotic leg. Blue-line indicates a distance within which leg length can be changed, CL: 100 mm. The kinematic-stick shown in right, is used in Fig. 7 to describe the dynamic motion of forward and in-place running of the RLLH over time. Each circle over the red-stick represents a joint that corresponds to the joint of the physical platform, as indicated by the dotted light-blue arrows.

The mechanical design of the robotic leg consist of two active joints (revolute and prismatic) and a passive joint (linear spring). The active joints are powered by the conventional DC brushed motors that permit a fixed joint rotary and a reconfigurable joint linear motion. As shown in Fig. 1, the linear motion in our design is obtained by the pinion-rack gear mechanism that enables us to accommodate both the actuators (DC motor) and their electronics on the trunk (body). This allows us to considerably reduces the weight of the leg and its inertia, which is very essential to use low-cost actuators. In addition, the motion of the linear joint is coupled in series with a mechanical spring (passive compliant element) through a rigid single-segment leg-frame. This mechanical configuration work in three ways: it can exert required forces to the ground by doing an oscillatory work on a passive spring, to reduce ground impact at touch-down by shortening the robotic leg and by changing the effective leg length of the robotic leg a speed can be adjusted.

B. Custom Motor Driver

Each active joint in the RLLH is controlled by the custom developed motor control board, as shown in Fig. 2. This motor control board (MCB) uses a 16 bit high performance micro-controller to execute low-level motor control algorithms, such as the low-level positional PID (proportional, integral and differential). Each MCB board is capable of communicating with other boards on a long distance half duplex RS-485 protocol in a master-slave configuration.

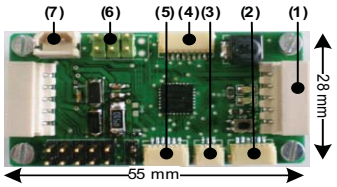

Fig. 2. Motor control board (MCB), (1) Power and RS-485 communication bus, (2) Programming connector, (3) 1 Analog input, (4) 4 DIO/ANA, (5) Secondary UART/I2C/SPI, (6) motor encoder, (7) 2 pins motor connector.

Four MCB boards are used in the construction of the experimental platform (see section V). Two MCB boards are responsible to control the rotary (leg-oscillation) and the linear (leg-reconfiguration) motion of the reconfigurable leg length hopper (RLLH) and other two, executes high-level tasks, e.g., foot trajectory. They are all mounted on the trunk. Moreover numbers of sensors are added to the mechanical design to monitor the internal state of motion of the robotic leg in time. These sensors are as follows: two limit switches, one rotary position sensor and one linear potentiometer.

III. FEED-FORWARD POSITIONAL CONTROL

The control of the two active joints in the RLLH is feed-forward (open-loop). The open-loop control means, no external sensory information is utilized to modify the prescribed shape of a command signal. This reduces the control-loop bandwidth to achieve a fast dynamic legged robot locomotion. This minimalistic feed-forward positional control signal of each active joint, namely the rotary and the linear joint, is sinusoidal, as defined in equation 1 and programmed in a master-controller 1 (see Fig. 4 b)). Master controller 1 processes equation 1 to produce a desired motion trajectory for the linear and the rotary joint respectively. The result of equation 1 is then transmitted to their respective

low-level PID motor controller (slave) on a connected RS-485 bus to execute desired motion.

$$\begin{bmatrix} \theta_R \\ d_L \end{bmatrix} = \begin{bmatrix} A_R + O_R + \Delta A_R \sin(\omega_R t + \phi_R) \\ d_0 + O_L + \Delta d_L \sin(\omega_L t + \phi_L) \end{bmatrix} \quad (1)$$

where, θ_R is the high-level oscillatory positional commands for the fixed rotary joint, O_R is the offset in leg oscillation (offset), A_R is the reference position of the robotic leg, ΔA_R is the amplitude of change in leg oscillation, $\omega_R = 2\pi f_r$ is the angular frequency of the oscillator, and ϕ_R is the phase shift in the oscillator. d_L is the high-level oscillatory positional commands for the reconfigurable linear joint, d_0 is the initial effective leg length of the robotic leg at rest, O_L is the offset in change in leg length (offset), Δd_L is the change in leg length (amplitude) during motion, $\omega_L = 2\pi f_L$ is the angular frequency of the oscillator, and ϕ_L is the phase shift in the oscillator. Note that $-\theta_R$ swing the leg in forward direction and $-d_L$ reduce the leg length.

IV. CONCEPT OF THRUST-FORCES IN FORWARD RUNNING

Thrust-forces in legged human locomotion are the result of external forces that act in the direction of movement during a ground contact phase [15]. These forces are also known as the propelling forces. In this particular design of the robotic leg, the thrust-forces can be generated by doing an oscillatory positive (increasing leg length) and negative (decreasing leg length) work at the passive mechanical spring. We previously [13] demonstrate that the dynamically stable vertical in-place hopping can be achieved by applying a simple sinusoidal control function to the reconfigurable linear joint. Using this similar control signal with zero phase-shift between the rotary and linear actuation, results in running forward.

A concept of thrust-forces in a single stride of forward running is graphically shown in Fig. 3. As can be seen in Fig. 3, the control signal (LM) that alters the leg length of the robotic leg, decreases during the negative half duration of the control signal. When the robotic leg touches the ground surface at point (1), the following sequence of events occurs: the linear joint start increasing the robotic leg length by doing a positive work at the mechanical spring, spring starts accumulating elastic energy by the compression against the ground, and finally the ground reaction force starts increasing by reflecting all the external forces during the contact phase. This duration from the touch-down point (1) to the lift-off point (3) is known as a "contact phase or stance". The forces exerted by the robotic leg, from point (2) to (3) are defined as the duration of thrust-forces. In short, it can be identified where Fx is positive by looking the ground reaction force after the mid-stance (see the GRF plot in Fig.3). The motion of the robotic leg along the direction of these thrust-forces defines the direction of locomotion. We hypothesize that by simply changing the phase ϕ_L of the sinusoidal LM (Linear Motor) control signal d_L, i.e., change in the phase of exerting force to the ground, at constant leg oscillation θ_R, the direction and the speed of running hopper can be controlled.

Similar concept is well described theoretically in [2] by a simple mechanical model that uses a mass-less leg and a point-foot. In this model [2] the effect of the rotary joint's torques and the leg forces are considered on the robot CoG that describes the rules of symmetry in dynamic running.

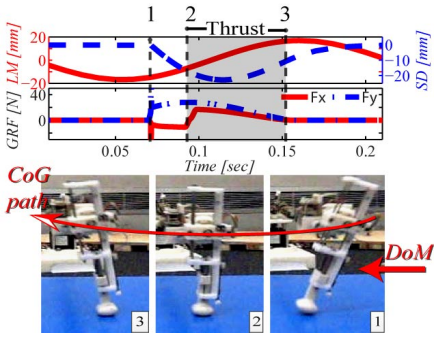

Fig. 3. Thrust-forces in a single cycle of actuation. First plot shows the compression of the spring (SD) and a single cycle of sinusoidal control signal (LM or d_L) over time. While the second plot shows the vertical and horizontal components of the GRF (ground reaction force). The duration of thrust-forces is indicated by the duration from mid-stance$-(2)$ to lift-off$-(3)$. DoM means the direction of motion.

V. EXPERIMENTAL SETUP

The concept of controlling the direction and the speed of running hopper is experimentally evaluated using the platform shown in Fig. 4. As can be seen in Fig. 4, a). The single-legged 2D reconfigurable leg length hopper module is attached to the fixed boom that constrains the motion of the robotic leg in two DOF (degrees of freedom), namely a yaw (about z-axis) and a pitch (about y-axis) axis of the fixed boom coordinate.

The base-shaft of the fixed boom, that permits a rotary (yaw) motion around the wooden-floor is physically coupled to the high-power-slip ring. The high-power-slip ring in our construction provides an uninterrupted electrical power up to N number of revolutions to the electronics placed at the upper-body of the robotic leg, i.e., prevent wire folding in multiple revolutions during N number of experiments. While the pitch motion about the boom-fixed coordinate is achieved by connecting the boom-rod of length 1.02 m in perpendicular to the rotary base shaft. The motion of the robotic leg relative to the fixed-boom is measured by the following sensors: IMU (6 DOF inertial measurement unit equipped with 3 axes accelerometer and 3 axes gyro sensors), and a rotary-position-sensor around the pitch axis. The Z-axis component of the IMU-gyro measures the speed about z-axis, which later converted in to the planar speed for compiling results, and the rotary-position sensor attached to the y-axis which measures the motion of the robotic leg body or in other words motion of the CoG (Center of Gravity). Moreover, a

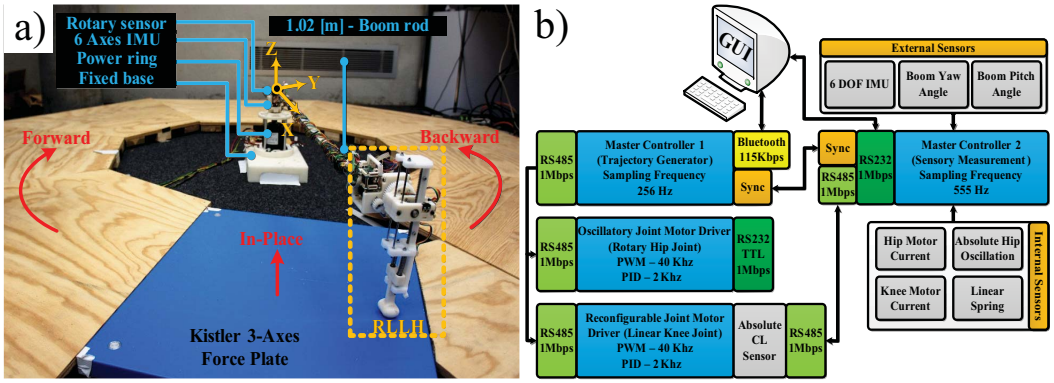

Fig. 4. Experimental setup of a two dimensional bi-directional running. a) The robotic leg is tethered to the fixed boom that constrained the motion of the robotic leg in a circular path (yaw and pitch) around a stiff-wooden-floor. A clockwise motion of the robotic leg about the z-axis of boom fixed coordinate is defined as the forward motion and the anti-clockwise motion is indicated as backward. An average speed of the robotic leg in either direction is measured by the 3D gyro of IMU (Inertial Measurement Unit), which is mounted at the boom fixed coordinate. b) shows the embedded feed-forward control and sensor data acquisition architecture. This setup uses four 16-bit custom developed micro-controller boards, two of them act as master and remaining two act as slave; Master controller 1 generates trajectory command by processing the equation 1 and transmits its result to the respective slave controllers on RS-485 Bus at the data transmission rate of 1 Mbps. Each slave controller receives the data packet and decodes its commanded signal to execute the desired motion command; Master controller 2 samples the internal sensors and external sensors at the sampling frequency of 555 Hz. Both master controller 1 and 2 are connected to the main computer, where GUI (graphical user interface) supervises the execution of control commands and records all the sensory data for further analysis.

3-axes kistler force plate was placed in the motion path of the RLLH to measure the ground reaction forces during each trial of the experiment per control parameter.

The control parameters are derived from our previous work in [13], where the frequency and the amplitude of sinusoidal leg reconfiguration for the energetic vertical in-place hopping were experimented. In [13], we showed the importance of two frequency values: one where the robotic leg exhibit higher ground clearance by consuming more power (maximal) and other where the robotic leg consumes less power (optimal). In this study, we specifically chose the operating frequency of the maximal power consumption, i.e., $4.5Hz$. Additional control parameters for the sinusoidal rotary and linear joint command signal were set to the following values: $f_R, f_L = 4.5Hz$, ΔA_R = 0.056π $\pm$ 0.005 rad (10 deg), Δd_L = 15 $\pm$ 1 mm, and d_0 = 135.5 $\pm$ 1 mm. Only the phase parameter (ϕ_L) of the linear actuation control signal was varied, as defined in equation 1 to establish the relation between the phase of exerting force to the ground with respect to the change in speed and direction of running hopper. This ϕ_L parameter is systematically changed starting from 0-2π rad with an increment of step-size 0.027π rad. At each change in control parameter four trials were performed and at each trial the robotic leg completes two revolutions around the fixed-boom on a stiff wooden-floor that has a frictional coefficient of $\approx$ $0.4 - 0.5$. The total distance covered by the robotic leg in two revolutions about the fixed boom frame is approximately equivalent to the planar distance of about 12.8 m in length. We use this as a criterion to quantify the robustness of stable running per control parameter in our experiment. As all the trial per experiment are synced, therefore the standard deviation among trials per control parameter can be used to quantify stability.

VI. RESULTS AND DISCUSSION

Fig. 5 shows the planar speed of running as a function of different phase (ϕ_L) that starts from 0 to 2π rad. As it can be seen in Fig. 5, at zero phase-shift (ϕ_L = 0) between the active rotary and the linear joint control signal, running in a forward direction occurs with an average speed of ≈0.8 m/s. By systematically increasing the phase-shift further from 0 to 0.53π rad, no change in the average running speed was observed. Thus, the phase duration from 0 to 0.53π rad is defined as the forward hopping (FH) region. Further increase in the phase-shift starting from 0.53π to 0.805π rad, decreases the average speed of locomotion until the point, where the in-place running was achieved (zero locomotion speed, despite the time varying sinusoidal actuation of each active joint) and then additional increase in phase-shift causes increase in speed by changing the direction of motion. This duration is indicated as the phase transition (PT) region in Fig. 5 and 6. By increasing in the phase values further from 0.805π to 1.53π rad, flatten out the average speed of locomotion at -0.8 m/s in reverse direction. The effect of the change in phase shift until 1.53π rad indicates that the direction of hopping is changed by the change in phase of exerting thrust-forces to the ground surface. However, if the mechanical design of the robotic leg is symmetric then the phase-transition region should repeat again. In order to confirm the symmetry of a thrust-cycle, the effect of phase-shift was further explored up to 2π rad. As it can be seen in Fig. 5, the thrust-cycle is symmetric, as the robotic leg design.

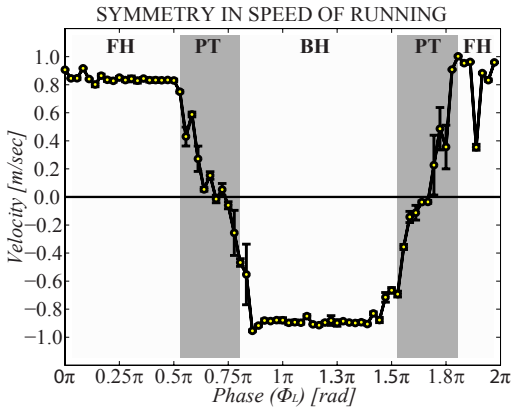

Fig. 5. Symmetry in speed of running. This shows the change in locomotion speed over different phases of applying external forces (thrust-forces) to the ground surface. X-axis indicates the change in the phase parameter (ϕ_L). Y-axis indicates the average speed taken over 3 synced trials per control parameter. The change in running speed and direction with respect to different phase (ϕ_L) values are categorized in three regions: FH (forward hopping) region, PT (phase transition) region, and BH (backward hopping) region. The forward hopping (FH) region is defined as the region, where the speed of locomotion remains constant in the clockwise direction about fixed boom. Its is highlighted by the phase duration $0-0.52\pi$ rad and $1.8\pi-2\pi$ rad. The phase transition (PT) region is indicated by the phase duration $0.52\pi-0.80\pi$ rad and $1.5\pi-1.8\pi$ rad, where the speed of locomotion changes significantly by passing through a zero speed (as shown by the speed transition from $+$ve speed values to $-$ve and vice versa). Similarly the backward hopping (BH) starts from phase (ϕ_L) 0.8π rad and ends at 1.5π rad, where the speed remains constant (-0.8 m/s) in an opposite direction.

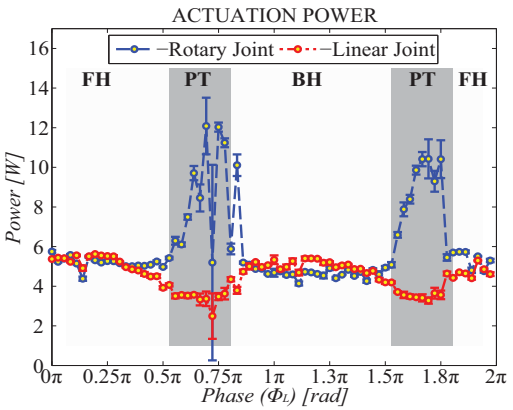

Fig. 6. Electrical power consumed by the active (fixed rotary) and variable (linear) joints per change in phase (ϕ_L) parameter is shown. The electrical power used by each active joint (DC motors) are nearly constant during forward (FH) and backward (BH) hopping region. However, the electrical power changes significantly during the phase transition region, where the speed starts dropping to zero before changing the direction of motion. It can be noted that the total power was mainly increased by the rotary joint power that limits the motion in-place by counteracting to the thrust-force.

It is important to note that the phase of in-place running in our experiments occurred approximately at phase 0.66π and 1.64π rad. But can it be influenced further? As the in-place running is a result of highly non-linear dynamical interaction between the robotic foot and the ground; therefore, the phase at which the in-place running was achieved, can easily be affected by the following factors: shape of the foot, friction of the ground, asymmetrical position of the robot CoG (Center of Gravity), and gains of the low-level PID control etc.

Fig. 6 shows the electrical power consumption of each active joint with respect to various thrust phases. This allows us to determine the overall cost of transport to change the direction of motion. As it can be seen in Fig. 6, each active joint power consumption was nearly constant during the forward (FH) and the backward (BH) region, same as the magnitude of running speed (see Fig. 5). While in phase transition region, the power consumption of the rotary joint was significantly affected. Especially at the phase value of the in-place running, where the electrical power consumption of the rotary joint reaches its peak. This indicates that the torque applied by the rotary joint, were acting against the thrust-forces that caused an increase in electrical power consumption of this joint. Based on these results, we can characterize the in-place running as a highly energy inefficient gait because the speed of locomotion becomes zero (v = 0), i.e., specific resistance ($\epsilon = p/mgv = \infty$), where p is the electrical power consumption, mg is the weight, and v is the velocity.

As it can be observed further in Fig. 5, the speed and the direction of the single-legged hopper was mainly affected in the phase transition region (PT). Operating the robotic leg within this region also affected the total power consumption. Therefore, we can conclude that the change in speed and the direction by using the phase transition parameters is costly but it provides a way to smoothly control the speed and the direction of locomotion in open-loop control. The role of the phase transition parameters, as a control to alter the speed and the direction of dynamic running online, is further demonstrated in section VI-C).

A. Forward and In-place Running

Instantaneous dynamic motion of each joint in the RLLH during two strides of a forward and an in-place running are shown in Fig. 7 a) and b) respectively. First two plots of Fig. 7, a) the motion of body joint, i.e., the motion of the robot CoG (Center of Gravity), is indicated by the red line, while the compression of the passive spring is shown by the green line. Both of these plots describe the dynamics of a forward and an in-place running in time, whereas the third plot (foot motion) is depicted with respect to the distance covered by the robotic leg during two strides. In Fig. 7, a) The vertical motion of the body joint (CoG motion) with respect to the foot in forward running decreases at the beginning of a ground contact phase, then it decreases further until mid-stance; from where it starts increasing again in the direction of thrust-forces. This motion of the robot CoG that acts in the direction of thrust-force, causes the robotic

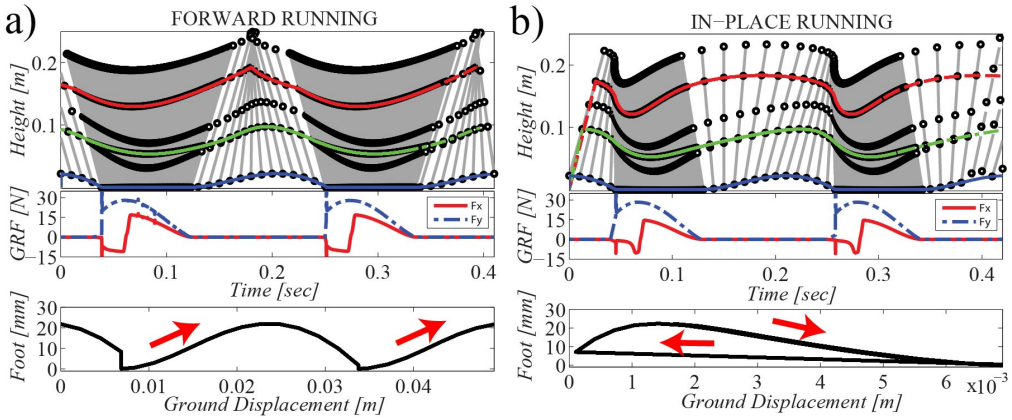

Fig. 7. 2D dynamics of the forward and the in-place running of the RLLH. First two plots in a) and b) show the dynamic motion of each joint with respect to the time duration of two strides. The first plot is a stick diagram that the motion of robot CoG (Center of Gravity) is shown by a red line and the deflection of spring is indicated by a green line. While the foot motion is indicated by a blue line. Second plot shows the vertical (Fy) and the horizontal (Fx) component of the GRF (ground reaction forces). These two plots (stick diagram and GRF) in column a) and b) are synchronized in time. This illustrates a complete dynamic of the robotic leg with respect to the thrust-forces (GRF, where Fx is positive) exerted on the ground surface. However, the third plot in a) and b) indicates the foot motion of the robotic leg with respect to the ground displacement covered during two strides. Moreover, this also provides a measure of ground clearance in an aerial phase. The contact phase and the aerial phase can be identified by the GRF plot in a) and b), i.e., aerial phase is the duration where GRF is zero ($Fx = 0$ and $Fy = 0$), and ground contact phase is the duration, where GRF is not zero ($Fx \neq 0$ and $Fy \neq 0$). Red arrows inside the foot motion plot of a) and b) indicate the direction of motion before and after touch-down.

leg to run in a forward direction. During in-place running joints motion of the robotic leg act against the direction of thrust-forces that causes the robotic leg to lift-off in a backward direction before retracting the robotic leg back at the same position (see foot motion in Fig. 7, b)). This behavior emerges, when the phase difference between the continuous joint motions constrains the direction of motion against the thrust-forces. Thus, the power consumption of the rotary joint increases (see Fig. 6), because the motion of the active rotary joint is acting against the thrust-forces of the GRF. As a result of this, the robotic leg runs in-place, while maintaining the ground clearance. It is very interesting to note that the motion of passive spring in both the cases (forward and in-place running) is nearly same, hence the vertical component of the ground reaction forces (GRF) is same as well. However, the horizontal (Fx) component of GRF and the body motion change significantly. Furthermore, the foot motion with respect to the planar distance per stride is indicated in Fig. 7, a) and b). Fig. 7, a) shows the robotic leg hop in a forward direction by covering a ground distance of approximately 27 mm in length per stride, whereas Fig. 7, b) indicates the robotic leg jump first in a backward direction and then bring the foot forward to the same location from where it lifts off.

B. In-place Running and In-place Hopping

The in-place running is different from the vertical in-place hopping, as shown in Fig. 8. The vertical in-place hopping can be achieved by the following steps: by keeping the robotic leg vertically straight to the ground, i.e., fixed angle of attack $\alpha_R = 90\ deg$ or $\theta_R = A_R$, and by actuating the reconfigurable linear joint in a feed-forward control. Consequently, the force exerted to the ground by the motion of the reconfigurable joint in series with the mechanical spring directly translated into straight vertical jumps. On the other hand, in the in-place running both joints (rotary and linear) of the robotic leg are operated by a continuous time-varying sinusoidal command signal, whose phase difference mainly restricts the foot motion of the robotic leg in-place while running at high-sped. In this way, we can characterize the in-place hopping gait further into the vertical and the oscillatory in-place running.

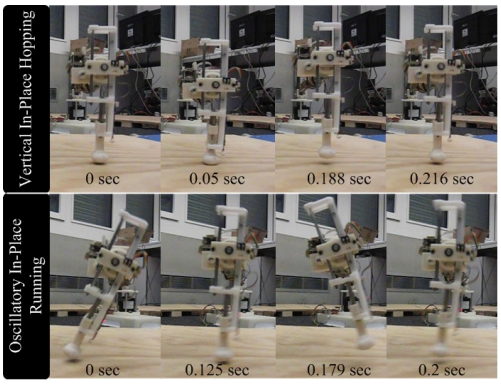

Fig. 8. High-speed video frame sequences of the vertical in-place hopping and the oscillatory in-place running.

C. Online Speed and Direction Control

Fig. 9 demonstrates the effect of varying the phase parameter (ϕ_L) online as a control of speed and transition in direction of a single-legged running. As it can be seen in the first plot of Fig. 9, at phase $(a) - (\phi_L = 0)$ the running speed of the hopper increases in the forward direction and reaches the steady-state speed of 0.8 m/sec. When the phase (ϕ_L) advances to the value 0.53π rad or enters into the phase transition (PT) region, decreases in the speed of locomotion by increasing in the electrical power consumption of the active rotary joint. However, at phase of the in-place running $(b) - (\phi_L = 0.66\pi\ rad)$, the speed gradually drops to zero and causes further increase in the rotary joint power, as also described in section VI-A. Additional increase in phase (ϕ_L) to the value $(c) - (\phi_L = 1.3\pi\ rad)$, causing the robotic leg to smoothly switch its direction of motion, as indicated by the negative sign of speed. It can be noted that the total actuation power is affected in phase transition region, which is indicated by the PT in Fig. 9. However, at phase (a) and (c) the actuation power of each joint is at the nominal value.

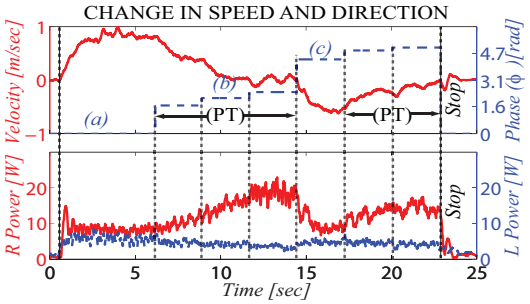

Fig. 9. Online speed control of bi-directional running. First plot shows the effect of different phase values to control the speed and the direction with respect to time. Second indicates the progression of the change in electrical power of each active joint with respect to time. The phase values used in this process are the following: Phase (a) $\phi_L = 0$ rad shows forward running, (b) $\phi_L = 0.53\pi$ rad indicates in-place running, and (c) $\phi_L = 1.38\pi$ rad shows backward running. PT defines the region of phase transition parameters.

VII. CONCLUSION AND FUTURE WORK

We demonstrated a simple way of controlling the speed and the direction of high-speed single-legged running. It is achieved by only altering the phase relation between the linear and the rotary joint in open-loop control. Initially, we explore a complete effect of this parameter on the speed and the electrical power consumption of each active joint and later we demonstrate this as a control to alter the speed and transition in the direction in real-time. A complete exploration reveals that the designed robotic leg exhibits a large stable region of forward and backward running, where the speed of locomotion and the total electrical power consumption are nearly constant. While the speed and the direction of locomotion are only affected by operating the robotic leg in a phase-transitional (PT) region, where the robotic leg starts changing its direction of motion from forward to backward and vice versa. This phase transition (PT) region can be described as: firstly at the phase; where the speed of locomotion starts decreasing, secondly at the phase; where the speed of locomotion becomes zero, and thirdly; where it increases the speed in an opposite direction of locomotion. The phase parameter at which the speed of locomotion becomes zero, is defined as "the phase of a novel gait called In-place running". The in-place running is another form of the vertical in-place hopping that restricts the motion of the robotic leg in-place by the continuous sinusoidal actuation of each active joint. Overall results strongly suggest that the proper phase relation among number of active joints in a robotic leg is a highly important parameter that can be used to smoothly control the speed and the dynamic transition in particular direction of a legged robot locomotion.

We intend to extend this control approach to design and control dynamic gaits of our four-legged robot that may run at high-speed without using any external sensory feedback. Perhaps this approach may be useful to achieve gait transitions in a four-legged system in future.

ACKNOWLEDGMENT

The author would like to extend his gratitude to Prof. Dr. Rolf Pfeifer for his kind guidance and constructive feedback.

REFERENCES

[1] M. H. Raibert, "Legged robots," *Communications of the ACM*, vol. 29, no. 6, pp. 499–514, May 1986.
[2] M. H. Raibert, "Running with symmetry," *The International Journal of Robotics Research*, vol. 5, no. 4, pp. 3–19, Dec. 1986.
[3] M. Ahmadi and M. Buehler, "The ARL monopod II running robot : control and energetics," *Proc. of the 1999 IEEE International Conference on Robotics and Automation*, vol. 1, pp. 1689–1694, 1999.
[4] S. H. Hyon, "Development of a biologically inspired hopping robot "kenken"," *Proc. of the 2002 IEEE International Conference on Robotics and Automation*, pp. 3984–3991, 2002.
[5] J. G. Cham and M. R. Cutkosky, "Dynamic Stability of Open-Loop Hopping," *Journal of Dynamic Systems, Measurement, and Control*, vol. 129, no. 3, pp. 275–284, 2007.
[6] J. Seipel and P. Holmes, "A simple model for clock-actuated legged locomotion," *Regular and Chaotic Dynamics*, vol. 12, no. 5, pp. 502–520, Oct. 2007.
[7] R. J. Full and D. E. Koditschek, "Templates and anchors: neuromechanical hypotheses of legged locomotion on land." *The Journal of experimental biology*, vol. 202, no. Pt 23, pp. 3325–3332, Dec. 1999.
[8] F. Iida, Y. Minekawa, J. Rummel, and A. Seyfarth, "Toward a human-like biped robot with compliant legs," *Robotics and Autonomous Systems*, vol. 57, no. 2, pp. 139–144, Feb. 2009.
[9] J. Rummel, F. Iida, J. A. Smith, and A. Seyfarth, "Enlarging regions of stable running with segmented legs," *Proc. of the 2008 IEEE International Conference on Robotics and Automation*, pp. 367–372, May 2008.
[10] S. Schaal and C. Atkeson, "Open loop stable control strategies for robot juggling," *Proc. of the 1993 IEEE International Conference on Robotics and Automation*, pp. 913–918, 1993.
[11] M. H. Dickinson, C. T. Farley, R. J. Full, M. A. Koehl, R. Kram, and S. Lehman, "How animals move: an integrative view." *Science (New York, N.Y.)*, vol. 288, no. 5463, pp. 100–106, 2000.
[12] R. Blickhan, "The spring-mass model for running and hopping," *Journal of Biomechanics*, vol. 22, no. 11-12, pp. 1217–1227, Jan. 1989.
[13] F. I. Sheikh and R. Pfeifer, "Adaptive locomotion on varying ground conditions via a reconfigurable leg length hopper," *Proc. 15th International Conference on Climbing and Walking Robots*, pp. 527–535, 2012.
[14] A. A. Biewener, *Animal Locomotion*. Oxford University Press, 2003.
[15] V. M. Zatsiorsky, *Kinetics of Human Motion*. Human Kinetics, 2002.

Appendix D

Significance of Foot Compliance For Fast and Energy Efficient Legged Robot Locomotion

Submitted article:

Farrukh Iqbal Sheikh, and Helmut Hauser (2014) *Significance of Foot Compliance for Fast and Energy Efficient Legged Robot Locomotion*, is submitted to IEEE Transactions on Robotics and Automation.

1

Significance of Foot Compliance for Fast and Energy-Efficient Legged Robot Locomotion

Farrukh Iqbal Sheikh and Helmut Hauser

***Abstract*—This paper addresses the significance of foot compliance. We experimented with two robotic legs. Each has a different foot. A stiff foot robotic leg is called the "S-RLLH" and a compliant foot robotic leg named the "C-RLLH". The length and mass properties of the two robotic legs are the same, but they differ in number of segments, shape and compliance because of different foot. First, we explored the maximal speed of the S-RLLH robot in open-loop by systematically altering two control parameters: stride frequency f_s and amplitude of leg oscillation ΔA_R. Latter, we investigated the C-RLLH robot by applying the control parameters of the S-RLLH robot. By comparing their speed and electrical power consumption, we observed that the S-RLLH robot can run up to ≈ 1.22 m/s at a stride frequency of 7.0 Hz, whereas the C-RLLH robot exhibits a similar speed of ≈ 1.23 m/s at a stride frequency of 4.8 Hz. Moreover, the total electrical power consumption of the C-RLLH robot is less than the S-RLLH. Overall results suggest that the foot compliance is important to increase the leg compliance, thereby it reduces the electrical power consumption and shifts the maximal speed of legged locomotion to the lower stride frequency.**

***Index Terms*—Legged locomotion, hopping, foot morphology, speed, energy efficiency, stiff foot, and compliant foot.**

I. Introduction

THE physical properties of feet in animals play an important role in terrestrial locomotion for a number of reasons. First, it is the part of the leg that directly interacts with the ground during legged locomotion. Second, it transfers required forces to the ground, and, third, it provides better traction for stable locomotion. In general, the foot morphology of legged animals is complex as it varies in number of joints, shape, adhesiveness, elasticity and size. Thus, to quantify the role of a particular foot morphology poses a great challenge in practice. The field of embodied robotics [1] in combination with evaluation in form of real-world platforms can help us to understand such complex systems because it promotes the concept of combining the robots body, its control and the physical environment to study the overall behavior of the robot.

Following the embodiment approach, we have designed and constructed a robotic leg called reconfigurable leg length hopper (RLLH) [2]. It can change the length of the leg in real-time. The original design of the RLLH (as described in [2]) employed a telescopic-stiff foot in series with a pair of linear springs (see S-RLLH in Fig. 1). The design was built to mimic the dynamics of the spring loaded inverted pendulum model. However, feet in biological system are typically composed of multiple segments. Based on this observation, we developed another foot morphology for the RLLH, which is comprised of two segments. It uses a torsional compliant element (spring) in between the two segments (called C-RLLH, see Fig. 1). Both foot morphologies were physically embedded in leg structure of the reconfigurable leg length hopper (RLLH) such that the role of each can be compared with each other in terms of speed and energy efficiency.

II. Background

Legged animals run by bouncing along the ground. Numerous studies suggest that the mechanics of running animal can be described by the spring-mass model [3]–[5]. This model is known as "spring loaded inverted pendulum" model. The SLIP model is rather simple and consists only of a point mass (body mass), a mass-less spring (leg) and a point contact (foot). Despite its simplicity, its interaction with the ground is in fact non-linear [3]. By simulating this model, the researcher report that the leg stiffness is a key parameter to characterize animal locomotion [6], [7].

Humans change their leg-stiffness to maintain a similar dynamic locomotion on various surfaces [8]. Following similar studies, a mechanism that significantly affects the leg-stiffness, was investigated in [9]. Their simulation results suggest that the ankle joint stiffness affects the leg-stiffness more than the stiffness of the knee joint [9]. As the ankle joint is the part of the foot, the foot compliance plays a prominent role to alter the stiffness of the whole leg (leg-stiffness). Another study shows that the toe and ankle act together as a variable gear changer to increase extensors muscle performance about the ankle joint [10]. These findings can be an important inspiration for building fast and energy-efficient legged robots. However, their implementation in a legged robot system have been so far limited. For example, many advancements have been made in developing variable stiffness actuators [11], [12], but rarely these actuators were tested at the ankle joint in a legged robot configuration. One exception is the jack spring variable stiffness actuator [13], which has been successfully tested on human subjects as a lower ankle prosthesis. In general there is a need for more research to understand the role of feet for legged locomotion. In this study, we aimed to find out the advantages of two different foot morphologies that are different in compliance and shape.

A. Existing Legged Robots

Compared to the bio-mechanics, research in the field of developing legged robots are focused on understanding legged locomotion with the help of machines that move in similar

fashion as legged animal [14]. Having this motivation, e.g., researchers from MIT built numerous legged robots [14]: single-legged, bipedal and four-legged. Each of these robots can stably hops in-place and runs forward, while balancing the tipping of the robot in a closed-loop control. On the basis of this control running speed and complex maneuvers, such as somersault [15], were successfully controlled and demonstrated. Later, Lee et al. [16], applied a similar control approach to the one proposed by Raibert [14] to control an articulated single-legged hopper. He found that due to its particular robot morphology the hoof-foot rolls over the surface during stance phase that affects the stability of the robot running. He proposed that limiting the inertial loading during contact phase is essential to control this hopper [16]. Later instead of using hydraulic and pneumatic actuator, the ARL II [17] was developed. It uses conventional DC brushed motor and mechanical spring to design a compliant robotic leg. The ARL II incorporated two mechanical springs: one along the leg axis and another about the hip joint. It was controlled in a closed-loop approach that exploits the passive dynamic of the robot for energy-efficient running up to the speed of 1.25 m/sec [18].

These single-legged robots [14], [16], [17], either used a compliant telescopic leg or a compliant segmented leg, to demonstrate the importance of control for stable locomotion. However, the morphology of all these robots were rarely consider to simplify the control task. In contrast to the closed-loop control approach that relies on a global sensory feedback, a stable running can also be realized in simple open-loop control that exploits intrinsic dynamical properties of the physical system. This control approach is highly minimalistic. By applying this similar control approach Juergen et al., [19] studied the locomotion of a compliant two-segmented leg that uses a torsional spring in between the two leg segments of equal length. They demonstrated in simulations that the robot with segmented leg and compliance can increase the region of self-stable single-legged hopping. Next to this theoretical result one can observe in nature that the leg design of many four-legged animals that run fast, e.g., cheetah, dog, cat, etc., is also consisted of different segments.

Inspired by the leg segmentation, the robotic leg designs of more recently developed legged robots [20]–[22] are employing segmented leg to target fast locomotion. In contrast to a simple leg segmentation, we introduced the idea of a reconfigurable leg length segment to achieve leg of various lengths (voluntary morphosis) in our hopper. While studying the role of changeable leg length, we demonstrated in [23] that this robotic leg is also suitable to adapt to the changes in various ground conditions (stiffness, damping and friction) without changing the stiffness of the passive spring. Although, the closed-loop control is essential for stable legged locomotion in highly unstructured environment, the open-loop control can be useful for fast running on level ground. We demonstrated in [24], by exploiting the natural dynamics of the robotic leg in open-loop control, speed and direction of single-legged fast running can be controlled. Following the same approach, we now aim to advance the performance of our robotic leg by investigating different foot morphologies.

The remainder of this paper is structured as follows. Section III illustrates the mechanics of the two robotic legs (S-RLLH and C-RLLH) that used different foot. Section IV describes our open-loop control approach. Section V introduces the experimental setup. Section VI explains our systematic exploration process of determining the maximum forward speed of the S-RLLH, which we applied later to evaluate the C-RLLH. Section VII discusses the experimental results. Finally, section VIII draws a conclusions. Furthermore, we add some supporting results in Appendix C to illustrate our data processing approach.

III. Mechanical Design of the Robotic Legs With Different Foot Morphologies

The reconfigurable leg length hopper, which was presented in [23], is utilized in this study. The mechanical design of this robotic leg is composed of four major components: trunk, reconfigurable leg length segment, passive linear spring and modular foot. The robotic leg has been designed to be light in weight by moving heavier components to the trunk, e.g., DC motors (actuators), mechanical gears and interface electronics. As a result, the trunk mass (body) becomes 3.5 times heavier than the leg mass (see Table I), which is essential for fast and energy-efficient legged locomotion, because a light weight leg can oscillates faster. The trunk is equipped with two active joints: one is rotary and the other one is linear joint. Both are powered by a conventional low cost DC brushed motor. The rotary joint swings the robotic leg in the fore-aft directions and the linear joint changes the length of the leg. The total change in leg length caused by the linear joint is mechanically realized by a pinion-rack gear mechanism. It is attached to the DC motor located at the trunk, whereas the rack gear is located on the reconfigurable leg length segment (see Fig. 1).

TABLE I: Technical specification of the two robotic legs

Physical parameters	***Metric Unit***
Rotary joint motor	2232R024SR22/2K (57.5:1)
Linear joint motor	2232R024SR22/2K (30.7:1)
leg length transmission ratio	104.16 rad/m
Overall height (L_A, L_B)	297.17 $\pm$ 0.1 mm
Overall width (W_A, W_B)	81 $\pm$ 0.1 mm
Total mass-SF (m_A)	917 $\pm$ 0.1 g
Total mass-TCF (m_B)	918 $\pm$ 0.1 g
Mass of the trunk (m_T)	714 $\pm$ 0.1 g
Mass of the stiff foot (m_{A_L})	203 $\pm$ 0.1 g
Mass of the compliant foot (m_{B_L})	204 $\pm$ 0.1 g
Body mass to leg mass ratio	3.5 / 1
Linear leg spring (k_L)	1 N/mm
Linear foot spring (k_F)	$4 \times k_L$ N/mm

This particular mechanical configuration of the robotic leg allows the linear joint to move the trunk (body mass) up and down on the reconfigurable leg length segment. This motion of the trunk acts in series with the linear mechanical spring k_L in such a way that the required forces act through the mechanical spring during the ground contact phase (CP). This principle of transmitting forces is similar to the function of a biological muscle that works on tendon [4], [25]. It provides following set of functions: it can perform the mechanical work

3

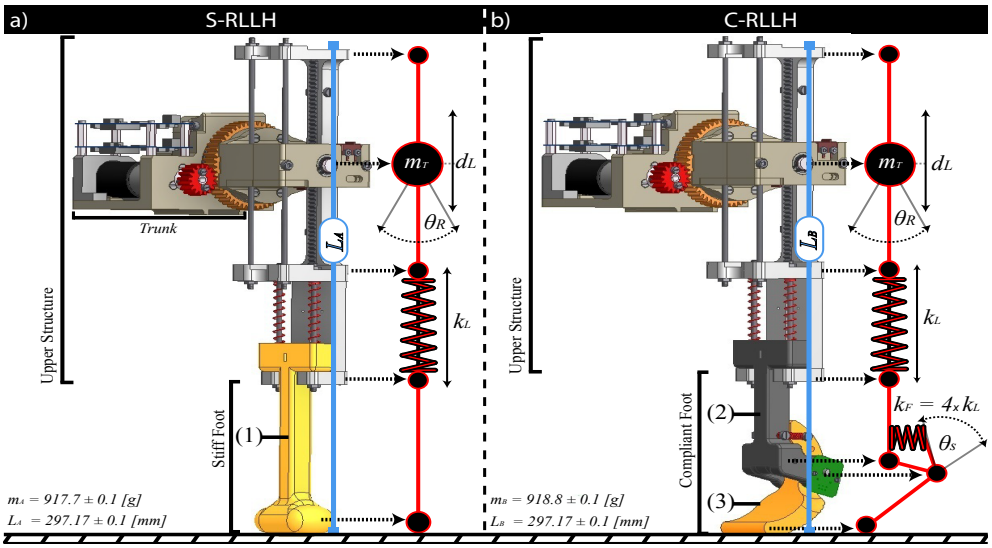

Fig. 1: Reconfigurable leg length robotic leg with two foot morphologies. a) is the S-RLLH that uses a single-segmented stiff foot (see label (1) in a) . b) is the C-RLLH that uses a two-segmented compliant foot (see label (2) and (3) in b)). Both the S-RLLH and the C-RLLH are nearly equal in total weight and length, but are significantly different in shape and compliance at the foot. It is important to note that the foot part in a) and b) does not include k_L spring, which is the spring in series with the reconfigurable joint.

on the passive spring during the contact phase, it can minimize ground impact by reducing leg length at touch-down, it can increase ground clearance by retracting the leg during aerial phase, and it can increase and decrease the nominal leg length of the robotic leg to mimic a robotic leg of various leg lengths.

Compared to the other components, the foot of the robotic leg is modular, which enables us to conduct experiments with different foot morphologies. For this study, we constructed two foot morphologies that can be physically embedded in the RLLH. This resulted into two different robotic leg configurations: the stiff reconfigurable leg length hopper (S-RLLH); which uses a stiff foot (see Fig. 1a)), and the compliant reconfigurable leg length hopper (C-RLLH); which uses a compliant foot (see Fig. 1b)). The stiff foot morphology is a single-segmented telescopic, which is highly stiff, i.e., no passive mechanical spring at the foot segment, whereas the compliant foot morphology is a two-segmented structure including a foot spring k_F. Both the foot morphologies are attached in series with the linear leg spring k_L of the existing robotic leg design. As the compliant foot morphology has an additional mechanical spring k_F, it has a capacity to store more elastic strain energy than the stiff foot. It is important to note that the stiffness constant of the foot spring k_F is four times the stiffness constant of the leg spring k_L, i.e., $k_F = 4 \times k_L$. Moreover, the foot spring k_F is attached to the rolling motion of the foot-segment, which mimics the function of a torsional spring under-load.

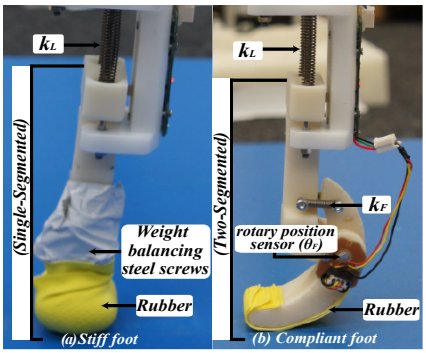

Fig. 2: Two foot morphologies. (a) is the stiff foot morphology and (b) is the compliant foot morphology. Both has the same (yellow) rubber material to prevent slippage during running.

A. Morphological Similarities and Differences

The benefits of the two foot morphologies were experimentally compared by keeping the mass and length of the two robotic legs (S-RLLH and C-RLLH) identical. To keep the total mass of both designs as close as possible, we added few steel-screws to the stiff foot morphology (see Fig. 2). Nevertheless, the geometry of the two foot morphologies and their compliant properties clearly remained different. As can be seen in Fig. 2, the stiff foot morphology has a fixed ball

shaped curve morphology at the bottom, which is highly rigid (stiff), whereas the compliant foot morphology has a compliant arched shaped curve morphology that bends during ground contact by some angle θ_s (see Fig. 1b). This bending of the foot is connected to the linear spring k_F to store elastic strain energy under stress.

IV. Actuation Method

The two active joints of the S-RLLH and C-RLLH are driven in a feed-forward positional control loop. This implies the following: no force control, no damping control, and no global sensory feedback were used. This particular choice of controlling the robot is simple and minimalistic, which is purposefully chosen to understand the role of two foot morphologies for the self-stable, fast and energy-efficient locomotion. The control function for the two active joints can be mathematically represented as,

$$\begin{bmatrix} \theta_R(t) \\ d_L(t) \end{bmatrix} = \begin{bmatrix} A_R + O_R + \Delta A_R \sin(\omega_R t + \phi_R) \\ d_0 + O_L + \Delta d_L \sin(\omega_L t + \phi_L) \end{bmatrix} \quad (1)$$

where, θ_R is the oscillatory positional command for the fixed rotary joint, which is a simple sinusoidal function comprising following variables: O_R is the offset in leg oscillation, A_R is the angular reference position of the robotic leg, ω_R is the angular frequency of oscillating leg, and ϕ_R is the phase shift. Similarly, d_L is the sinusoidal oscillatory positional command for the reconfigurable linear joint. It is a function of following variables: d_0 is the initial effective leg length of the robotic leg at rest, O_L is the offset in change in leg length, Δd_L is the amplitude of change in leg length, ω_L is the angular frequency of change in leg length, and ϕ_L is the phase shift of d_L.

Equation 1 is programmed in the dedicated master controller 1 (see Fig. 3). It is responsible of generating the positional commands for the active rotary and variable (reconfigurable) linear joint (see section V). It is important to note that the S-RLLH has an additional joint, which is passive, i.e., the mechanical spring k_L in series with the active linear joint. Thus, the final foot trajectory is the result of coupled interaction between the active joints and the passive joint. Similarly, the C-RLLH has two passive joints (k_L and k_F). We explore this coupled interaction between active and passive joints in section VI.

V. Experimental Setup

The experimental setup of this study is similar to the one presented in [24]. However, it included an additional measurements which is the passive deflection of the compliant foot (see in Fig. 3). This complete experimental setup consists of two parts, namely the single-legged running platform, and the embedded control and data acquisition architecture.

A. Single-legged Running Platform

Fig. 3a) shows the physical layout of the experimental platform. It consisted of a light weight metal rod (boom-rod), an electrical power-slip, the robotic leg (RLLH), a 3 axes force-plate, and a wooden-floor. The rod (boom-rod) constrained the motion of the robotic leg to two dimensions: about the Z-axis of the fixed boom coordinate (yaw) and about the Y-axis of the fixed boom (pitch). This forced the robotic legs to run in a circular path around the stiff wooden-floor. An integrated power-slip allowed the robot to take multiple revolutions about the Z-axis without damaging the power/data cable.

B. Embedded Control and Data Acquisition Architecture

The embedded control and data acquisition architecture can be seen in Fig. 3b). It consists of a computer, four micro-controller boards and two groups of sensors. The computer ran a custom designed graphical user interface containing high-level control functions for the robot. This GUI was able to communicate with the embedded firmware running inside the master controller 1 and 2. The master controller 2 acted as a high-speed data acquisition unit. It simultaneously sampled each sensor at the sampling frequency of 555 ± 1 Hz before transmitting all the sensory data back to the main computer. It was interfaced with the main computer through a dedicated 1 Mbps RS-232 serial interface. The master-controller 1 processed Eq. (1) to generate the positional commands for the two active joints. It iterated the control function at the sampling frequency of 256 ± 1 Hz, which is suitable to generate a sinusoidal control signal of up to 10 Hz. Once the targeted position data was ready, then the master controller 1 sent the positional commands signal to the motor driver boards of each active joint over the 1 Mbps RS-485 data transmission bus. Since our robotic leg had two active joints, we used two separate motor driver boards to seamlessly control the leg-oscillation and leg-reconfiguration. Each motor driver board ran internally at 11 kHz positional PID motor control loop that awaited for the positional command transmitted by the master controller 1 to move the leg. By this arrangement of the controllers, we were able to simultaneously control and sense the dynamics of the robotic leg in real-time.

Dynamic states of the 2D planar motion of the robot were measured in real-time by sampling two groups of sensors: external sensors and internal sensors. The external sensors consisted of a 6-axis inertial measurement unit (IMU), two rotary sensors (pitch any yaw), and a 3 axes force-plate. The 6-axis IMU unit measured the 3-axis of angular speed and 3-axis acceleration of the robot with respect to the boom as the fixed coordinate, which we transformed later into the horizontal speed of running V_x and the vertical speed of the robot trunk B_v. Similarly, the two rotary sensors that were attached to the boom, measured the absolute angular displacement of the boom-rod about Z-axis (yaw) and Y-axis (pitch). These two measurements were converted into the horizontal distance covered by the robot x and the vertical displacement of the robot trunk B_d. Moreover, the force-plate provided the exact measure of the ground reaction forces (GRF), i.e., the amount of force exerted by the robot to the ground. Its measurement was synced with the other sensory measurements and recorded separately by the commercial "Kistler Bioware software". The internal sensors measured the internal states of the robot. The internal sensors consists of two spring-deflection sensors,

5

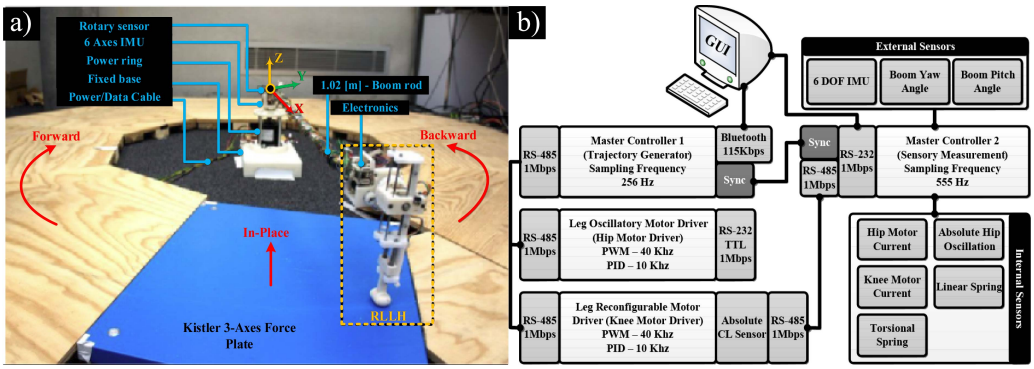

Fig. 3: Experimental setup (adapted from [24]). In a) the physical layout of the experimental platform is shown. b) depicts the embedded control and data acquisition architecture.

two motor current sensors and one rotary joint positional sensors (see Appendix C). The two spring-deflection sensors measured the deflection of the springs k_L (leg spring) and k_F (foot spring), which we translated into the spring force F_{s_i} by applying Hooke's law, i.e., $F_{s_i} = k_i \Delta x$, where Δx is the amount of compression of a mechanical spring with the stiffness constant k_i and $i = L$ or F (either the linear leg spring or the torsional foot spring). Similarly, the two motor current sensors measured the amount of current drawn by the active motors during the experiments. Finally, the rotary position sensor measured the absolute leg-oscillation. Both the external and internal sensors produced their outputs within the voltage range of $0 - 3.3\ V$, which we sampled by the on-chip 16-bit ADC (analog to digital convertor) of the master controller 2 (see in Fig. 3).

VI. Exploration Approach

The role of the stiff foot morphology and the compliant foot morphology for fast and energy-efficient running were explored in open-loop control. First, we systematically explored the effect of the stride frequency f_s and the amplitude of leg oscillation ΔA_R on the forward speed of the S-RLLH. It is performed by using the two stages of exploration (see Fig. 4). Second, we ran the C-RLLH at the optimal control parameter space of the S-RLLH. The two stages of determining the maximal forward speed of the S-RLLH were as follows: Stage 1 - Range of stride frequencies, and Stage 2 - Maximal speed of forward running.

A. Stage 1 - Range of stride frequencies

As described previously, the robotic leg uses the linear joint in series with the passive spring. The linear motion acts as a source to supply energy for the system, i.e., it moves the robot trunk along the leg axis to perform the mechanical work on the passive spring. It is similar in function, when the muscles generate forces to make use of biological tendons [4], [25]. Inspired by this fact, we conduct in-place hopping experiment to study the relation between the active variable linear joint (muscle) and passive mechanical spring (tendon). As illustrated in Fig. 4a, the robotic leg was placed in upright posture by keeping the amplitude of leg oscillation θ_R constant to 90 deg ($\pi/2$ rad) and forced to hop the robotic leg in-place by applying a sinusoidal actuation of the variable linear joint, i.e., periodic up-down motion of the robot trunk. This motion of the trunk at particular amplitude and frequency generate forces that excites the mechanical spring to achieve hopping in-place [23].

Following the same approach [23], we obtained the range of stride frequencies for forward hopping experiments. As shown in stage 1 exploration, we systematically varied the frequency parameter f_L from 0 – 8 Hz in steps of 0.1 Hz by keeping the amplitude of leg reconfiguration Δd_L constant to 15 mm. At each change in control parameter, we recorded the following states of the robot: the electrical power consumed by the two active joints P_R and P_L and the time response of the mechanical spring k_L as F_{s_U}. The results of this experiment shows that the S-RLLH consumes less power, when it is operated close to the leg resonance frequency (see Fig. 5). In addition, it provides the information about the suitable range of frequencies for the next stage of the speed exploration, which we discuss further in section VII.

B. Stage 2 - Maximal speed of forward running

In general, the speed of legged robot locomotion can be described as,

$$V_x = \Delta x_s f_s \tag{2}$$

where, V_x is the running speed, Δx_s is the step-length or distance covered during single step, and f_s is the stride frequency or number of steps in a second. Eq. (2) indicates that the single-legged robot can run fast either by taking long-steps (step-length) at lower stride frequencies or by taking short-steps at higher stride frequencies. Thus, both parameters step-length and stride frequency should be considered to achieve the maximal speed of forward running in legged locomotion. Accordingly, we explored the effect of two control parameters: amplitude of leg oscillation ΔA_R, and stride frequency f_s

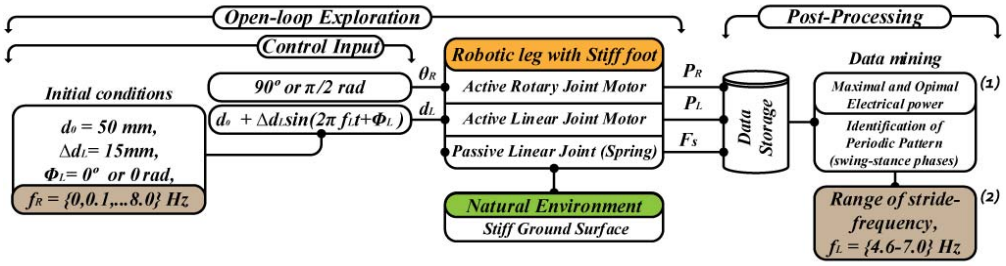

(a) Stage 1 - systematic exploration for the range of stride frequencies.

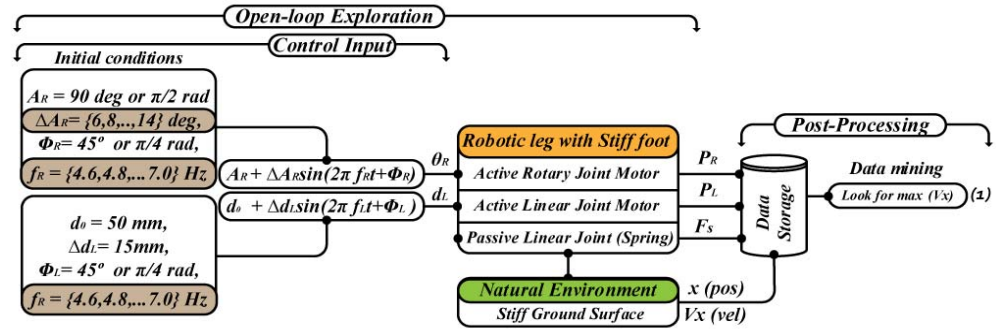

(b) Stage 2 - systematic exploration for the maximum speed of locomotion.

Fig. 4: Stages of systematic exploration for the S-RLLH. a) shows the first stage of exploration in which we study the relation between the active linear joint (muscles) and the passive mechanical spring (tendon) for the power efficient and in-efficient in-place hopping. This also provides the range of stride frequencies. b) indicates the second stage of exploration that determines the maximum speed of locomotion.

(see Fig. 4b). The change in amplitude of leg oscillation ΔA_R directly affects the step-length, while the change in stride frequency f_s alters the frequency of oscillating the leg f_R together with the frequency of reconfiguring the leg f_L. These two control parameters were systematically altered to investigate the effect on average speed with the S-RLLH. As mentioned in the last section, we selected the range of stride frequencies f_s from the in-place hopping experiments (see section VI-A). Within that range, we varied the stride frequency in steps of 0.2 Hz. At each stride frequency, we varied the amplitude of leg oscillation ΔA_R from 6 – 14 deg (0.033π – 0.078π rad) in steps of 2 deg (0.011π rad). The result of this exploration reveals a surface of forward speed with respect to the control parameters ΔA_R and f_s. In this surface, each column of the stride frequency depicts the averaged maximal speed of the S-RLLH running (see Fig. 6a). We utilized this parameter space to evaluate the C-RLLH. This way, we compared the two robotic legs with different feet. It is important to note that there are other parameters that could potentially affect further the speed of forward running, e.g., O_L and Δd_L, but we did not explore the effect of these parameters because by changing them will result in an additional change in the robot morphology, i.e., leg length. As this work is based on studying the effect of the two foot morphologies in a particular leg configuration. Therefore, the effect of the stride frequency and the amplitude of leg oscillation were only considered for the speed exploration.

VII. Results and Discussion

We ran the S-RLLH based on the two stages of exploration. It consisted of two types of experiments: in place hopping and forward hopping. The in-place hopping experiments were performed first based on the approach described in [23]. It is useful to extract a suitable range of stride frequencies for forward running. While the forward running experiments were executed later to obtain the speed of the S-RLLH running with respect to ΔA_R and f_s. Following these two types of experiments, we conducted in total 950 experiments. The detail of the total number of experiments that we performed with each design, can be found in Appendix A.

A. Selecting the Range of Stride Frequencies

Fig. 5 illustrates open-loop response of the robotic leg with respect to the operating frequency f_L. In Fig. 5a), we show the total electrical power consumed by the robotic leg with respect to various operating frequencies f_L that starts from 0 – 8 Hz in steps of 0.1 Hz. In Fig. 5b), we depict the time-frequency

response of the leg spring force F_{s_L} to identify the region of stride frequency (see grey highlighted area in Fig. 5).

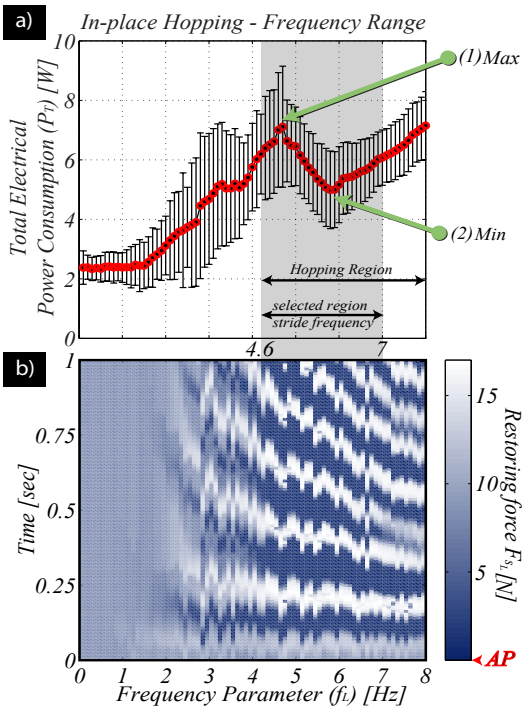

Fig. 5: Range of the stride frequencies. a) is the electrical power of the module with respect to the operating frequency $f_L = 0$ – 8 Hz. b) indicates the behavior of the spring force F_{s_L}, which is plotted over time of the duration 1 sec (see y-axis) and operating frequency (see x-axis). The spring at lower operating frequency shows the weight of the robotic leg (no-aerial phase), the aerial phase (AP) emerges with the increase in operating frequency, and third indicates the increase and decrease of the aerial phase duration; In a) the label (1) and (2) are the in-efficient and efficient hopping respectively.

As can be seen in Fig. 5a), initially the total electrical power consumed by the robotic leg stayed nearly constant up to the operating frequency range from 0 – 1.5 Hz and then it started rising gradually. During this range of operating frequencies $0 \geq f_L \leq 1.5$ Hz, the spring force F_{s_L} showed no aerial phase; thus its value reflected to the total weight of the robotic leg, i.e., $F_{s_L} = mg \approx 9$ N or in other words, there was no ground clearance. Additional increase in operating frequency f_L until 4.3 Hz increased the total power consumption and gradually develops the aerial phase. However, when the operating frequency increased from 4.3 – 4.7 Hz, the module power consumption increases further until it reached to its peak 7 W at 4.7 Hz. This particular frequency is defined as the maximum frequency point at which the time duration of the aerial phase is greater than the contact phase (see label (1) in Fig. 5a). Further increased in the operating frequency from 4.6 – 5.8 Hz linearly decreased the total electrical power consumption of the module until it reached a minimum power consumption of ≈ 5 W at 5.8 Hz. This frequency is defined as the minimum frequency point, where the total power consumption is minimum with ground clearance (see label (2) in Fig. 5a). Any additional increase in operating frequency beyond the optimal frequency gradually increased the total electrical power consumption of the module and decreased the aerial phase. By this result, we can state that the in-place hopping at the maximum frequency point is power in-efficient while at the minimum frequency point is power efficient. Considering this, we select the range of stride frequencies $f_s = 4.6$ – 7.0 Hz for the forward speed exploration of the S-RLLH.

B. Forward Speed Exploration of the S-RLLH

After selecting a range of stride frequencies, we performed the exploration stage-2 to determine the forward running speed of the S-RLLH. In this exploration, we varied two control parameters: ΔA_R, and f_s. It is important to note that varying f_s means changing the f_R and f_L together. Both are the frequency parameters of the control function (1), e.g., $\omega_R = 2\pi f_R$ and $\omega_L = 2\pi f_L$. The stride-frequency changed within this range $f_s = 4.6$ – 7.0 Hz in steps of 0.2 Hz, whereas, the amplitude of leg oscillation ΔA_R was incremented in steps of 2 deg (0.11 rad) about the reference leg position A_R until the maximum speed per stride frequency was achieved. The result of this exploration can be seen in Fig. 6a that shows the averaged step-length and the averaged speed of running with respect to the two control parameters: amplitude of leg oscillation ΔA_R and stride frequency $f_s = f_R$ and $f_s = f_L$.

As can be observed in Fig. 6a, each column of the stride frequency has an optimal step-length, where the speed of running is also maximum. It is interesting to note that for some stride frequencies 4.6 – 6.0 Hz and 6.4 Hz the optimal step-length occurred at $\Delta A_R = 12$ deg (0.067π rad). However, for the other stride frequencies 6.2, 6.8 and 7.0 Hz, the optimal step-length was obtained at $\Delta A_R = 14$ deg (0.077π rad). For these stride frequencies, we explored ΔA_R up to 16 deg (0.88π rad) to confirm the optimal step-length. By running the S-RLLH within this parameter range, we can observed that the highest speed of running is up to 1.22 m/sec or 2.72 mph at the highest operating frequency of 7.0 Hz (see Appendix C). It is also important to note that the maximum averaged step-length $\bar{x}_{SF}$ defines the maximum averaged speed $\bar{V}x_{SF}$ of running in the S-RLLH. In addition, we observe the total electrical power consumption P_T because the energetics (specific resistance) of legged robots mainly depend on two variables (power and speed), if the mass of the robot is constant (see Eq. (3)).

As can be observed in Fig. 6b, the total electrical power consumption P_T with respect to different amplitudes of leg oscillation ΔA_R at a particular stride frequency f_s is fixed, i.e., linearly increasing. It is also repetitive over different stride frequencies. We analyzed this fixed pattern of the total electrical power consumption at particular stride frequency by

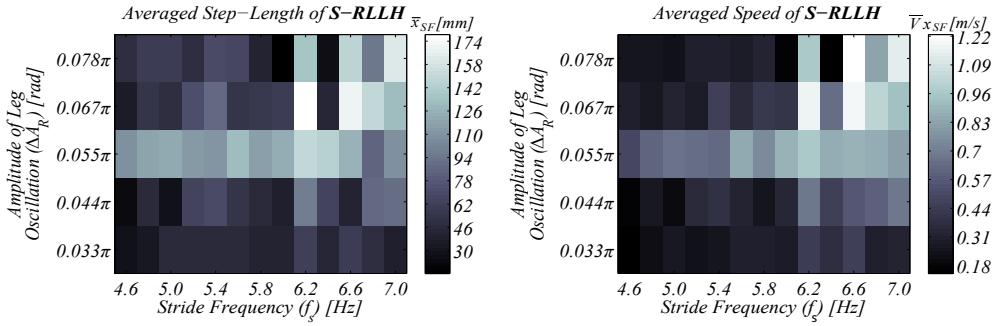

(a) Averaged step-length and speed of running of the S-RLLH.

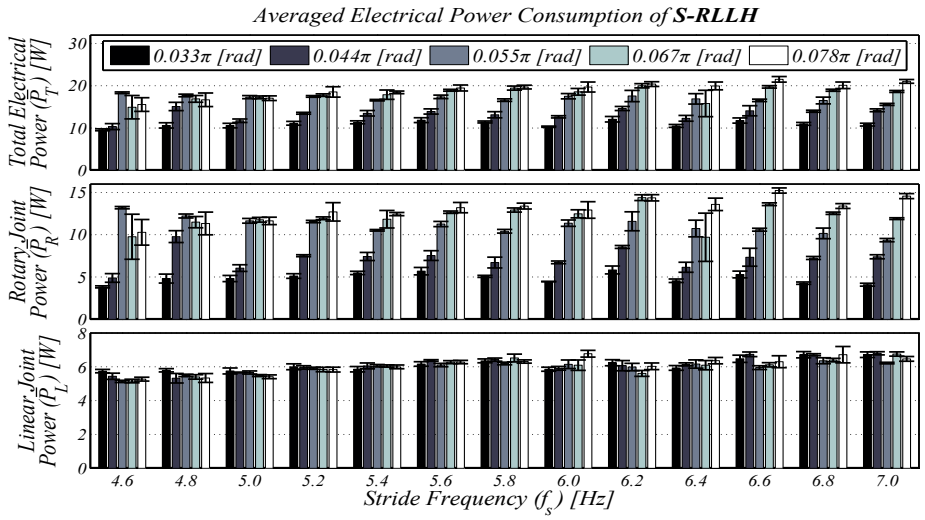

(b) Averaged electrical power consumption of the S-RLLH.

Fig. 6: Speed and electrical power consumption of the S-RLLH. a) shows the average step-length $\Delta\bar{x}_{s_{SF}}$ and the average speed of running $\bar{V}_{x_{SF}}$ with respect to the two control parameters ΔA_R and f_s. b) indicates the average electrical power consumptions of the total $\bar{P}_T$, rotary joint $\bar{P}_R$ and linear joint $\bar{P}_L$.

further observing the electrical power of the individual joint (see Fig. 6b). It is interesting to observe that the total electrical power at each stride frequency within which the amplitude of leg oscillation was altered, increased proportionally with the amplitude of leg-oscillation ΔA_R. This particular pattern was shaped by the electrical power consumption of the rotary joint (see Fig. 6b). On the other hand, the electrical power consumed by the linear joint, stayed nearly constant at approximately 6 W. The total electrical power was less affected by the increase in stride frequency.

C. Forward Speed Exploration of the C-RLLH

To establish a comparison between the S-RLLH (i.e., with the stiff foot) and C-RLLH (i.e., with the compliant foot) based on speed and energy efficiency, we conducted a forward running experiments with the C-RLLH in which we utilized the same control parameter space for the S-RLLH. Following the same experimental procedure and systematic exploration stage 2 (see section VI-B), we measured the step-length, speed and electrical power consumption. Fig. 7a shows the averaged step-length and averaged speed of running of the C-RLLH with respect to the two control parameters: amplitude of leg oscillation ΔA_R, and stride frequency f_s. Fig. 7b depicts the total and the individual electrical power consumption of the module and two active joints respectively.

As can be observed in Fig. 7a, the averaged step-length and averaged speed of running of the C-RLLH show no clear pattern. Nevertheless, it indicates a significant boost in the averaged step-length and the averaged speed of forward running at the lower stride frequency compared to the S-RLLH

9

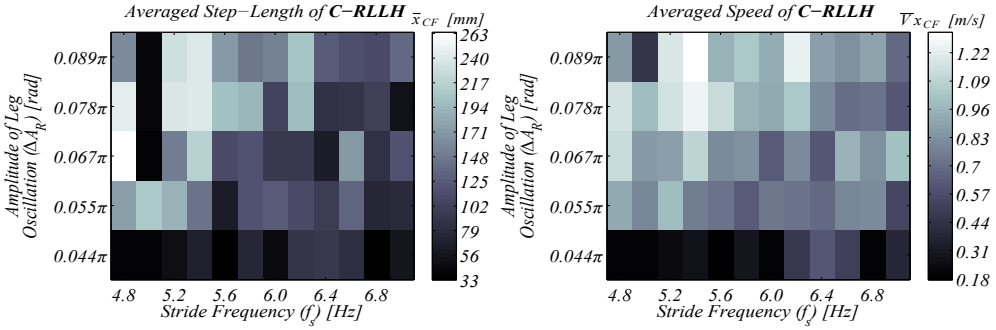

(a) Averaged step-length and speed of running of the C-RLLH.

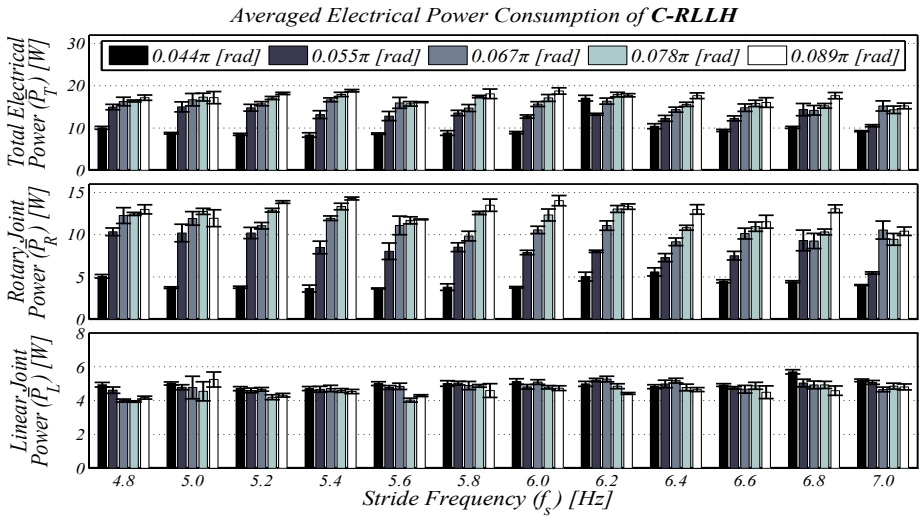

(b) Averaged electrical power consumption of the C-RLLH.

Fig. 7: Speed and electrical power consumption of the C-RLLH. a) shows the average step-length $\Delta\bar{x}_{s_{CF}}$ and the average speed of running $\bar{V}_{x_{CF}}$ with respect to the 2D optimal control parameter space ΔA_R and f_s of the S-RLLH; b) shows the average total electrical power consumption $\bar{P}_T$ of the robot along with the average electrical power consumption of the active joints $\bar{P}_R$ and $\bar{P}_L$.

(see Fig. 7a). This boost in speed of running can be considered as the effect of the passive compliant element (k_f), which is torsional in series with existing linear compliant (k_L). Compared to the S-RLLH, the C-RLLH is able to store additional elastic strain energy during stance phase that results in increase in the step-length at the lower stride frequency. However, this raises a question, why the higher speed occur at lower stride frequency in the C-RLLH? A possible explanation can be derived by looking at the elementary relation between the two mechanical springs that are connected in series. Consider the two mechanical springs $k1$ and $k2$ that are attached in series then the resulting spring k can be mathematically expressed as "$k = \frac{k1k2}{(k1+k2)}$". By applying a similar analogy, we see that the C-RLLH configuration is more compliant than the S-RLLH. This implies that the leg resonance frequency of the C-RLLH is also less compared to the S-RLLH. Hence, operating the C-RLLH at lower operating frequency results in a higher speed of running (≈ 1.23 m/s). We also looked the total electrical power including the individual power consumptions of each active joint. As we can observed in Fig. 7b, the total electrical power consumption follows nearly the same pattern as observed in the result of the S-RLLH (see Fig. 6b). This pattern shows that the increase in total electrical power of this robotic leg is mainly influenced by the amplitude of leg oscillation ΔA_R.

D. Comparison between the S-RLLH and C-RLLH

Fig. 8 shows a complete comparison between the S-RLLH and the C-RLLH. As we can clearly observe in Fig. 8a,

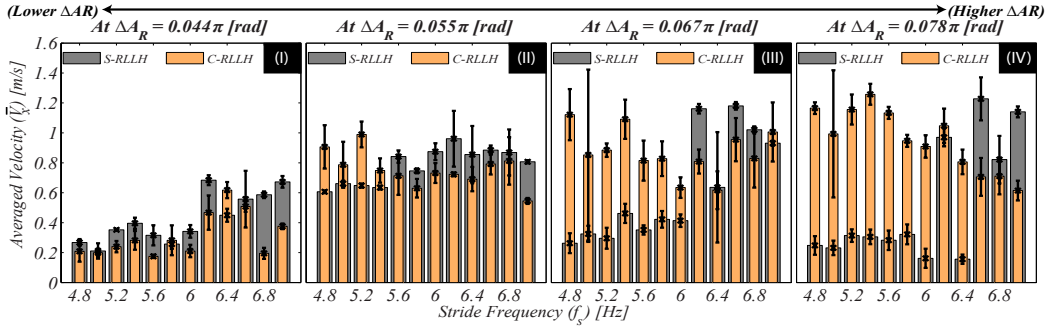

(a) Averaged speed comparison.

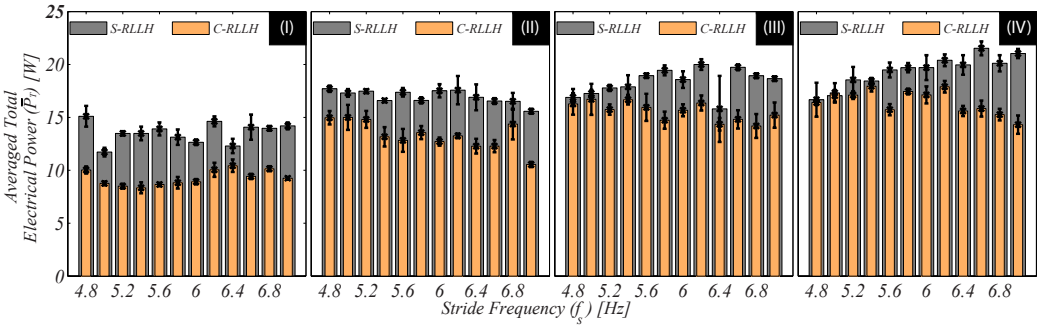

(b) Averaged electrical power consumption comparison.

Fig. 8: Comparison between the S-RLLH and C-RLLH. a) shows the speed comparison between the S-RLLH and the C-RLLH. In a) left most figure shows the comparison at the lowest amplitude of leg oscillation ΔA_R. Right most indicates the result at the highest amplitude of leg oscillation ΔA_R. b) depicts the electric average total electrical power consumption of the two robotic legs S-RLLH and the C-RLLH.

regardless of any choice of the stride frequency at the lowest amplitude of leg oscillation (right graph in Fig. 8a), the C-RLLH is lowered in the averaged speed of running than the S-RLLH. However, higher amplitudes of leg oscillation the averaged speed of the two robotic leg with respect to the stride frequency becomes comparable as follows (see Fig. 8a, II, III and IV). At lower stride frequency f_s, the averaged speed of the C-RLLH is higher compared to the S-RLLH and at higher stride frequency f_s, the averaged speed of the S-RLLH is higher than the ones obtained with the C-RLLH. Interestingly, the maximal averaged speed of running of both the robotic legs are similar.

In Fig. 8b, we compare the total electrical power consumption of the S-RLLH and C-RLLH. In contrast to the results with respect to speed, we can see that the C-RLLH is better than the S-RLLH. It consumed less electrical power over the full range of the investigated parameter space. Based on this result, we may infer that the foot compliance is important to increase the leg compliance of the robotic leg as it considerably reduced the electrical power consumption.

The results demonstrate that the averaged speed of running similar to the S-RLLH, can be achieved at lower stride frequency. This shows that by adding another compliant element at the foot, which works as the torsional spring, we can achieve higher speed of running at lower operating frequency, which is also useful to increase the actuator performance.

VIII. Conclusion

This paper presented a comparison between two foot morphologies: a stiff foot and a compliant foot. Both were identical in mass and length properties, but they were different in shape and compliance. By embedding these two foot morphologies in the existing design of the reconfigurable leg length hopper, we obtained two corresponding robotic leg configurations: S-RLLH and C-RLLH. With both, we conducted experiments by varying two control parameters: amplitude of leg oscillation (ΔA) and stride frequency (f_s). By comparing the results in terms of speed and electrical power consumption, we observed that with the C-RLLH, which uses a compliant foot, we can obtain a maximum averaged speed of ≈ 1.23 m/s (2.75 mph) at a stride frequency of $f_s = 4.6$ Hz, whereas the S-RLLH, which has a stiff foot, can result a maximum averaged speed of ≈ 1.22 m/s (2.72 mph) at a stride frequency of $f_s = 7.0$. Hence, both robotic legs exhibited approximately the

same maximum speed, but at different stride frequencies. This implies that the maximal speed of locomotion can be shifted to lower operating frequency by adding a compliant foot. Furthermore, if we would design a foot with the capability to change its stiffness (e.g., variable compliant mechanisms), we would get a device, which would be able to obtain high speed over a wider range of stride frequencies. The C-RLLH consumes less electrical power than the S-RLLH, which shows that the compliant foot configuration (C-RLLH) is more energy-efficient compared to the S-RLLH. The results suggest that the foot compliance is an important physical parameter for fast and energy-efficient legged robot locomotion.

APPENDIX A
STATISTICS OF THE TOTAL NUMBER OF EXPERIMENTS

Table below summarizes the total number of experiments.

Foot/ Leg Type	*Experiment Type*	*Control Parameter*	*Number of Experiments*
Stiff/S-RLLH	in-place	f_L	5x8/0.1 = 400
Stiff/S-RLLH	Forward	ΔA_R and f_s	275
Compliant/C-RLLH	Forward	ΔA_R and f_s	275

APPENDIX B
SPECIFIC RESISTANCE

The specific resistance of a legged robot locomotion can be mathematically represented as,

$$\epsilon = \frac{P_T}{mgV_x} \tag{3}$$

where, ϵ is the specific resistance or energy efficiency, m is the mass of the robot, g is the gravitational constant, P_T is the electrical power consumed by the robot, and V_x is the running speed of the robot.

APPENDIX C
ADDITIONAL RESULTS AND DATA PROCESSING APPROACH

This appendix shows additional results and describes our methodology to process sensory data for the two robotic legs (S-RLLH and C-RLLH). Both robots ran up to 12 m planar horizontal distance during each trial. In total, we performed five trials per control parameter. In each trial, we measured the following state variables: θ_R, d_L, L_U, θ_F, B_d, B_v, P_T, x and V_x.

The instantaneous speed and the total power consumption of 5 trials per control parameter can be seen in Fig. 9a and Fig. 9b. Fig. 9a shows the result of the S-RLLH at the control parameter, where running speed is maximum. Similarly, Fig. 9b indicates the result of the C-RLLH. As can be seen in Fig. 9a and Fig. 9b, the robotic leg (S-RLLH), which uses a stiff foot, can move at the averaged speed of up to 1.2 ± 0.032 m/s at higher stride frequency $f_s = 7.0$ Hz, whereas the robotic leg (C-RLLH), which uses compliant foot, can result the similar averaged speed of running at lower stride frequency $f_s = 4.8$ Hz. Moreover, the average total electrical power consumption of the C-RLLH is approximately 30% less than the average total electrical power consumption of the S-RLLH. We obtained these results were by processing the number of samples within the rectangular grey highlighted area (see Fig. 9a, 9b, 9c and 9d). The width of the grey highlighted area contains 20% of the total samples. It starts from 60% of the total samples and ends at 80%. This ensures that the averaged results $\bar{V}_x$ and $\bar{P}_T$ are computed from the steady-state speed. However, if the robot stumble while running as observed mostly in the C-RLLH then the measure of standard deviation over five successive trials can qualitatively characterize the stability of running. As can be seen in the title of Fig. 9c, the standard deviation of the C-RLLH at the control parameters $f_s = 4.8$ Hz and $\Delta A_R = 0.078\pi$ rad is less than the standard deviation of the C-RLLH at the control parameters $f_s = 4.8$ Hz and $\Delta A_R = 0.067\pi$ rad (see title of Fig. 9d). Hence, the running of the compliant foot robotic leg (C-RLLH) at the control parameters $f_s = 4.8$ Hz and $\Delta A_R = 0.078\pi$ rad is stable than the running of the compliant foot robotic leg (C-RLLH) at the control parameters $f_s = 4.8$ Hz and $\Delta A_R = 0.067\pi$ rad.

The averaged speed of running $\bar{V}_x$, the averaged step-length $\Delta\bar{x}$ was measured by taking the average over 20 consecutive step-lengths of the steady-state running (see Fig. 10a and Fig. 10b). These 20 steps were identified based on the stride frequency of the control signal d_L. Each step is highlighted by the diamond shape point in the state variables plot Δx (see Fig. 10). It shows the internal sensory information of the S-RLLH and C-RLLH. It can be noted that Fig. 10b has an additional sensor, whose value is represented by the θ_F. This θ_F indicates the torsional deflection of the compliant foot spring k_F. Similarly, L_U shows the linear deflection of the leg spring k_L. By comparing the sensor values of the leg spring k_L (see second graph from the top in Fig. 10a) with the leg spring k_L and the foot spring k_F (see second graph from the top in Fig. 10b), we can observe that the C-RLLH can store more elastic energy than the S-RLLH at this control parameter, thereby the C-RLLH consumes less electrical power than the S-RLLH.

ACKNOWLEDGMENT

This work is supported by the European Commission Seventh Framework Program, Theme ICT- 2007.8.5 as part of the project LOCOMORPH, under a grant no 231688.

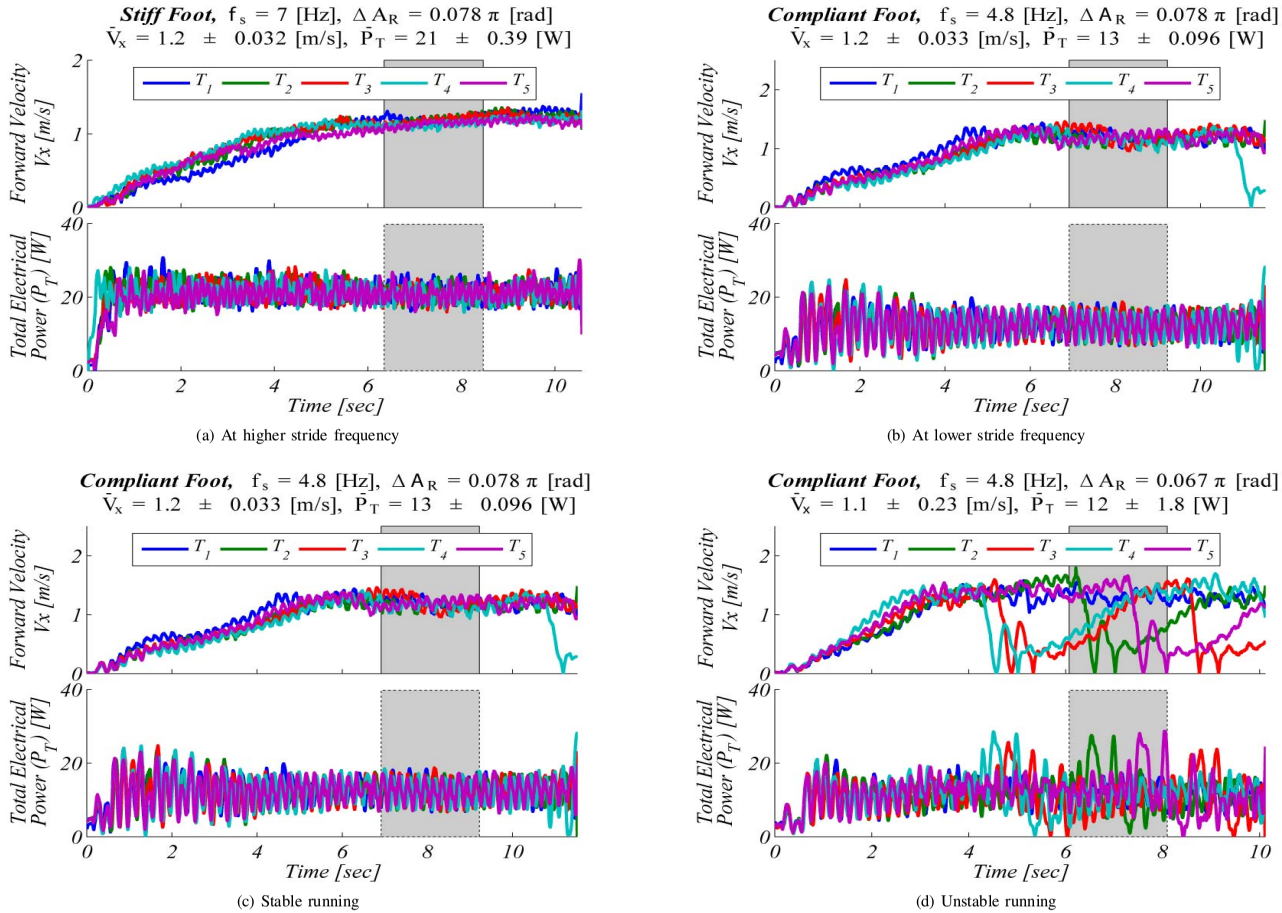

(a) At higher stride frequency

(b) At lower stride frequency

(c) Stable running

(d) Unstable running

Fig. 9: Instantaneous speed and electrical power consumption of the S-RLLH and C-RLLH. a) shows the running speed and the electrical power consumption of the S-RLLH over time at higher stride frequency $f_s = 7.0$ Hz, whereas b) indicates the running speed and the electrical power consumption of the C-RLLH with respect to time at lower stride frequency $f_s = 4.8$ Hz; the grey highlighted region shows the number of samples that were processed to compute the average speed $\bar{V}_x$ and the average electrical power $\bar{P}_T$; c) and d) shows the stable and unstable running on different control parameters. It can be explained by the standard deviation over 5 successive trials. Lower standard deviation means running is stable as can be seen in the title c) and higher standard deviation means running is unstable as indicated in the title d).

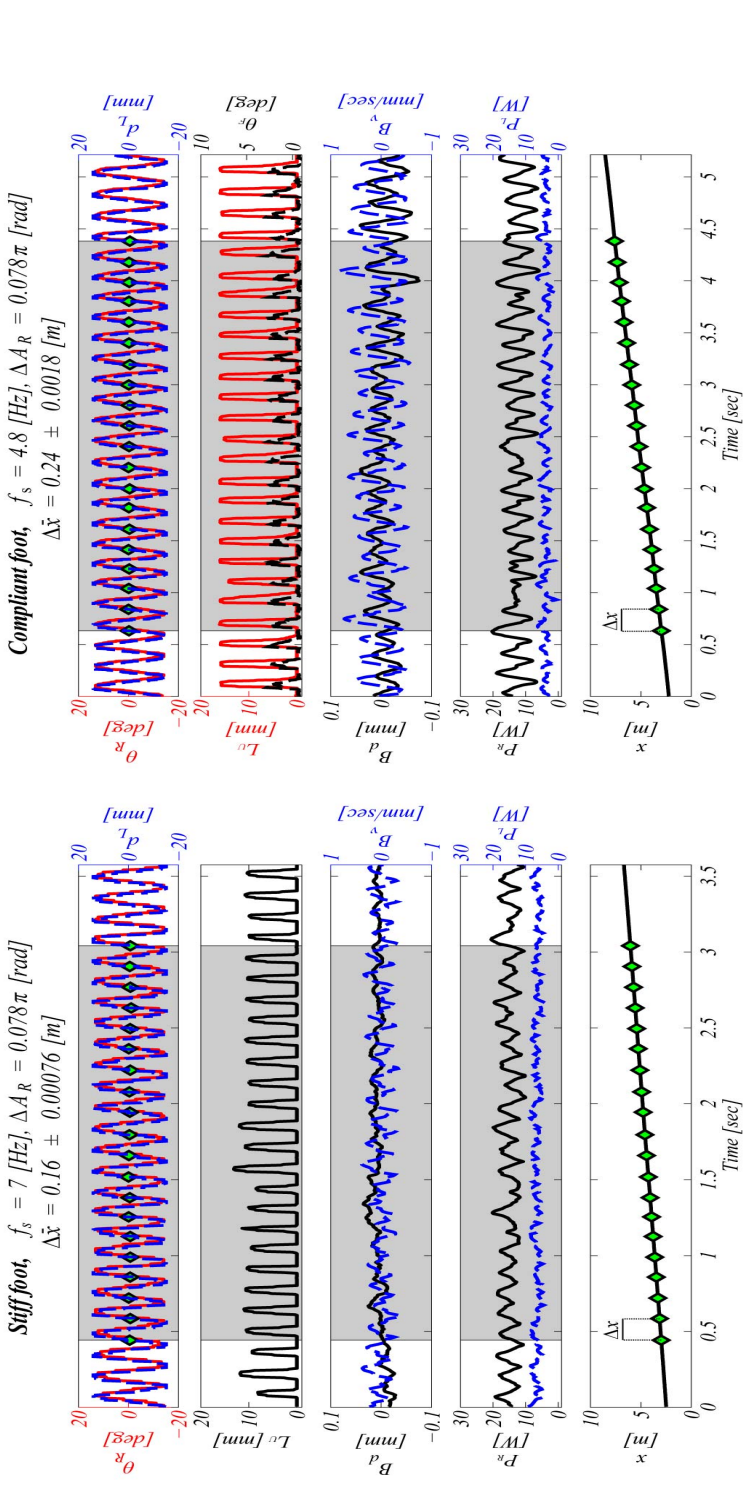

(a) The internal sensory information of the S-RLLH

(b) The internal sensory information of the C-RLLH

Fig. 10: Internal sensory measurements of the two robotic legs (S-RLLH and C-RLLH). a) shows the internal sensory information of the S-RLLH and b) shows the internal sensory information of the C-RLLH. In both a) and b), the bottom plot indicates the step-length Δx that samples based on the stride frequency of d_L control signal. The sensor values B_d and B_v are associated with the motion of the robot trunk where the robot CoG (center of gravity) is located. As can be seen in a), both B_d and B_v are noisy due to small aerial phase, whereas in b) both B_d and B_v are exhibiting clear periodic pattern because the aerial phase in the C-RLLH is greater than aerial phase of S-RLLH. Note that the average step-length and control parameters can be found in the title of each figure. Moreover, the grey highlighted region is comprised of 20 consecutive steps.

REFERENCES

[1] R. Pfeifer, M. Lungarella, and F. Iida, "Self-organization, embodiment, and biologically inspired robotics." *Science (New York, N.Y.)*, vol. 318, no. 5853, pp. 1088–93, Nov. 2007.

[2] F. I. Sheikh, H. Hauser, L. Aryananda, H. V. Quy, and R. Pfeifer, "SLIP-model-compatible and bio-inspired robotic leg with reconfigurable length," in *Adaptive Motion of Animals and Machines*, no. October, 2011, pp. 47–48.

[3] R. Blickhan, "The spring-mass model for running and hopping," *Journal of Biomechanics*, vol. 22, no. 11-12, pp. 1217–1227, Jan. 1989.

[4] Alexander, *Principles of Animal Locomotion*. Princeton University Press, 2003.

[5] T. McMahon, "The role of compliance in mammalian running gaits." *The Journal of experimental biology*, vol. 115, pp. 263–82, Mar. 1985.

[6] Y. Blum, S. W. Lipfert, and A. Seyfarth, "Effective leg stiffness in running." *Journal of biomechanics*, vol. 42, no. 14, pp. 2400–5, Oct. 2009.

[7] R. Blickhan, A. Seyfarth, H. Geyer, S. Grimmer, H. Wagner, and M. Günther, "Intelligence by mechanics." *Philosophical transactions. Series A, Mathematical, physical, and engineering sciences*, vol. 365, no. 1850, pp. 199–220, Jan. 2007.

[8] D. P. Ferris, M. Louie, and C. T. Farley, "Running in the real world: adjusting leg stiffness for different surfaces," in *Proceedings of the Royal Society, B (Biological Sciences)*, 1998, pp. 989–993.

[9] C. T. Farley and D. C. Morgenroth, "Leg stiffness primarily depends on ankle stiffness during human hopping," *Journal of Biomechanics*, vol. 32, no. 3, pp. 267 – 273, 1999.

[10] D. R. Carrier, N. C. Heglund, and K. D. Earls, "Variable gearing during locomotion in the human musculoskeletal system." *Science (New York, N.Y.)*, vol. 265, no. 5172, pp. 651–3, Jul. 1994.

[11] J. W. Hurst, J. Chestnutt, and A. Rizzi, "Design and philosophy of the bimasc, a highly dynamic biped," in *Proc. of the 2007 IEEE International Conference on Robotics and Automation*, April 2007.

[12] R. Ham, T. Sugar, B. Vanderborght, K. Hollander, and D. Lefeber, "Compliant actuator designs," *Robotics Automation Magazine, IEEE*, vol. 16, no. 3, pp. 81–94, Sep. 2009.

[13] K. W. Hollander, T. G. Sugar, and D. E. Herring, "Adjustable Robotic Tendon Using a 'Jack Spring'," *Proc. of the 2005 9th International Conference on Rehabilitation Robotics*, pp. 113–118, 2005.

[14] M. H. Raibert, "Legged robots," *Communications of the ACM*, vol. 29, no. 6, pp. 499–514, May 1986.

[15] R. Playter and M. Raibert, "Control Of A Biped Somersault In 3D," *Proc. of the 1992 IEEE/RSJ International Conference on Intelligent Robots and Systems*, vol. 1, pp. 582–589, 1992.

[16] W. Lee and M. Raibert, "Control of hoof rolling in an articulated leg," *Proceedings. 1991 IEEE International Conference on Robotics and Automation*, pp. 1386–1391, 1991.

[17] M. Ahmadi and M. Buehler, "The ARL Monopod 11 Running Robot : Control and Energetics," vol. 1, no. May, pp. 1689–1694, 1999.

[18] M. Ahmadi and M. Buehler, "Controlled passive dynamic running experiments with the ARL-monopod II," *IEEE Transactions on Robotics and Automation*, vol. 22, no. 5, pp. 974–986, 2006.

[19] J. Rummel and A. Seyfarth, "Stable running with segmented legs," *Int. J. Rob. Res.*, vol. 27, no. 8, pp. 919–934, Aug. 2008.

[20] M. Hutter, C. Remy, M. Hoepflinger, and R. Siegwart, "Efficient and versatile locomotion with highly compliant legs," *IEEE/ASME Transactions on Mechatronics*, vol. 18, no. 2, pp. 449–458, 2013.

[21] A. Sprowitz, A. Tuleu, M. Vespignani, M. Ajallooeian, E. Badri, and A. Ijspeert, "Towards dynamic trot gait locomotiondesign, control, and experiments with cheetah-cub, a compliant quadruped robot," *The International Journal of Robotics and Research*, vol. 32, no. 8, pp. 932–950, 2013.

[22] A. Ananthanarayanan, M. Azadi, and S. Kim, "Towards a bio-inspired leg design for high-speed running," *Bioinspiration and Biomimetics*, vol. 7, no. 4, pp. 1–12, 2012.

[23] F. I. Sheikh and R. Pfeifer, "Adaptive locomotion on varying ground conditions via a reconfigurable leg length hopper," *Proc. 15th International Conference on Climbing and Walking Robots*, pp. 527–535, 2012.

[24] F. I. Sheikh, "Towards fast running: Open-loop speed and direction control of a single-legged hopper," in *Proc. of the 2013 IEEE/RSJ International Conference on Intelligent Robots and Systems*. Tokyo, Japan: IEEE, 2013, pp. 5114–5120.

[25] T. J. Roberts, "The integrated function of muscles and tendons during locomotion." *Comparative biochemistry and physiology. Part A, Molecular & integrative physiology*, vol. 133, no. 4, pp. 1087–99, Dec. 2002.

Farrukh Iqbal Sheikh is currently a Ph.D. Candidate at the Artificial Intelligence Laboratory (AiLab), Dept. of Informatics, University of Zurich, Switzerland. He completed his M.Sc. in Space Science and Technology on EU scholarship Erasmus Mundus, from the Aalto University, Helsinki, Finland. He received the B.S. degree in Electronics Engineering with distinction from the Sir Syed University of Engineering and Technology, Karachi, Pakistan.

His research interests are bio-inspired robotics, machine learning, real-time control, embedded systems, micro-electronics, and educational technology.

Dr. Helmut Hauser Helmut Hauser received his masters degree in electrical engineering with specialization in control engineering from Graz University of Technology, Austria. From the same university he received his PhD on bio-inspired control paradigms for robots.

Since Nov. 2010 he is postdoc at the Artificial Intelligence Laboratory at the University of Zurich (Switzerland). He was project manager of the EU project Locomorph, he was editor of a special issue on morphological computation in Artificial Life (MIT Press), and he co-organized a number of international events regarding this topic. He is interested in soft robotics, embodiment, morphological computation, and bio-inspired robotics; mostly in the context of locomotion. Dr. Helmut Hauser is a member of the Review Editorial Board of Frontiers in Bionics and Biomimetics and he is the coordinator of the working group on "Control Architectures and Paradigms for Soft Robots" in the european coordinated action RoboSoft. He won with his co-authors the best paper award at the IEEE-RAS international conference on Humanoid Robots (HUMANOIDS 2007), Pittsburgh.

Appendix E

Dynamic Maneuverability Through Voluntary Morphosis in a Four-Legged Robot

©2013 IEEE. Reprinted, with permission, from:

Farrukh Iqbal Sheikh and Syed Shams-Ul-Haq (2013) *Dynamic Maneuverability Through Voluntary Morphosis in a Four-Legged Robot*, In Proceedings of 2013 IEEE International Joint Conference on Cybernetics and Intelligent Systems (CIS) & Robotics, Automation and Mechatronics (RAM), pages 49–54. Manila, Philippines.

This is the final accepted version. Final version of this article can be found at http://ieeexplore.ieee.org (10.1109/RAM.2013.6758558).

Dynamic Maneuverability Through Voluntary Morphosis in a Four-Legged Robot

Farrukh Iqbal Sheikh and Syed Shams-Ul-Haq

Abstract— **Dynamic maneuverability is an inherent skill of any legged animal locomotion. Thus it is useful and challenging for a physical four-legged robot that runs in open-loop control. This paper presents a concept of dynamic maneuverability in a four-legged system that can alter its morphology through leg reconfiguration, i.e., voluntary morphosis[1]. By exploiting this unique feature of the robot body, we designed a dynamic maneuverability control in open-loop that changes the leg length of the ipsilateral pairs of legs to smoothly control the turning of the robot on a particular gait. We verified our control approach on trot gait locomotion. Our results demonstrate that the maneuverability in a four-legged robot is mainly the result of an active change in robot morphology.**

Keywords: Differential change, Maneuverability and Voluntary Morphosis.

I. INTRODUCTION

Dynamic maneuverability is a key attribute of any legged animal locomotion [1] that enables them to avoid obstacles and dodge predator for the survival. This particular behavior is very much inspiring and essentially useful for any physical legged robot locomotion that has to move from location A to B in natural environment.

Legged robots have the potential to traverse over unstructured terrain better than wheeled robots. However, the complex interaction of the robotic legs with the ground surface, still makes the control of some desirable behavior such as various gaits and dynamic maneuverability, very difficult to achieve, even on a level ground surface. Especially in case of four-legged robotic systems, where the stability during the locomotion is of main concerned. Moreover to achieve maneuverability in open-loop control also poses a great challenge for four-legged systems because the uncontrolled body rolling and pitching at particular gait in an open-loop may easily compromise stability as well as the direction of locomotion. Despite the challenges lie in clock-driven open-loop approach, still open-loop approach is suitable to obtain rapid legged robot locomotion [2] that exploits the passive mechanical stability of the legged robots for the dynamically fast locomotion. In addition, by studying a behavior of the robot in simple open-loop control, may provide a better foundation of formulating a robust closed-loop control [3] that may use least number of parameters to control a high-dimensional non-linear system, such as legged robots, for a robust and an energy-efficient locomotion in an unstructured natural environment.

In contrast to this open-loop control strategy, many existing legged robots developed by Raibert and his team in ranging from single, bipedal and four-legged, were controlled in a closed-loop approach. This similar control approach is extended to demonstrate the maneuverability of a 3D-single legged hopper [4] in various directions. Further more, the same approach had been implemented to produce stable dynamic gaits in a four-legged robot [5]. However, how this control approach may help to achieve dynamic maneuverability on various gaits in four-legged system was not experimented. Perhaps, the same control approach is being utilized to steer far most advanced quadruped robots, the Big dog and the Alpha dog [6] but somehow their control scheme is not really known to many researchers.

The quadruped robot built [7] later, was mainly focused to advance control scheme by using non-linear neural oscillator with reflex feed-back to achieve stable dynamic walking and running. But the simple open-loop sinusoidal actuation can also be used [8], [9] to obtain dynamic running in four-legged robots that exploits the passive dynamic of the under-actuated four-legged system to demonstrate stable running in open-loop. However, due to limited actuation in [8], [9], only single stable running gait (bounding) was demonstrated. Moreover, the concept of dynamic maneuverability in open-loop for a four-legged system remains elusive to date.

Compared to the existing quadruped robots [5], [7]–[9], many cockroach inspired hexapedal (six-legged) robots, the Rhex [10], the whegs II [11], and the DynaRoACH [12] are inherently more stable and capable to take dynamic turn at high-speed using a simple feed-forward control approach. For example the Whegs II [11] can turn on a tripod gait by simply operating the lateral pair of legs in opposite phases. While the DynaRoACH [12] demonstrated, the dynamic maneuverability can be achieved by tuning the stiffness of the robotic leg during running on a tripod gait. Contrary to the fixed gait pattern with tunable leg stiffness to achieve dynamic maneuverability as observed in many hexapedal robots, we aimed to understand the concept of dynamic maneuverability in our four-legged system called DTAR (Differential Terrain Adaptive Robot) using a simple model of turning. This robot uses un-coupled (independent) 2 DoF per leg. In these 2 DoF, one is linearly reconfigurable that permits an active change in the leg length of the robotic leg. Having this feature of the active leg reconfiguration, our robot is potentially capable to produce wide range of gaits as any four-legged animals and be able to maneuver by an

*This work is supported by the EU Project Locomorph.

F.I Sheikh is working at the Artificial Intelligence Laboratory, Department of Informatics, University of Zurich, Andreastrasse 15, 8050, Zurich. fsheikh at ifi.uzh.ch

[1]Voluntary morphosis is an inherent ability of a robot to self-adjust its own morphology to adapt to the current tasks and environments.

active change in its morphology, i.e., define as a voluntary morphosis through leg-reconfiguration. It is important to note that this robot does not change the stiffness of the passive spring to maneuver the robot, as demonstrated in [12].

Number of insect studies [13], [14] suggest that cockroach uses no sensory feedback while turning and moving forward at the speed of 50 body length per second. Therefore, in this study we intentionally used fairly less-control (open-loop) to demonstrate maneuverability in our four-legged robot (DTAR). In other words, we exploited an inherent feature of the robot body for the task of maneuverability. Further we proposed a maneuverability control based on a simple conceptual model of turning that can be applied on wide range of gaits of a four-legged system.

This paper is structured as follows: section II briefly explains the mechanical design and describes the conceptual model of maneuverability in a four-legged robots, section III illustrates the practical implementation of the maneuverability control, section IV describes the details of the experimental setup, section V presents results, and section VI comments on conclusion and future work.

II. MECHANICAL DESIGN AND CONTROL MODEL

The physical prototype of the four-legged robot, which we named DTAR (Differential Terrain Adaptive Robot), can be seen in Fig. 1. The robot structure consists of the four decoupled two DoF reconfigurable length modules (RLLH) [15] and the rigid trunk. Each leg module features the one rotary joint and the reconfigurable linear joint which is connected in series with the passive mechanical spring. The rotary joint permits the leg oscillation in the fore-aft direction. While motion of the reconfigurable joint works in series with mechanical spring that enables us to alter leg-length of each leg during dynamic running on a particular gait. By considering this inherent attribute of the robotic leg which is an active change in leg-reconfiguration, we developed a conceptual model of the dynamic maneuverability (turn right, left and move straight) that can potentially work on wide-range of gaits, however, for this study we only demonstrated the principle of dynamic maneuverability on trot gait.

A. Conceptual Model of Maneuverability

A free body diagram that describes the concept of maneuverability through a differential change in ipsilateral pairs of legs, is shown in Fig. 2. As can be seen in Fig. 2, the front side of robot shows the following: the width of the trunk, as l_T; the nominal leg-length of the right pair of legs (FR, HR), as l_{BR}; and the nominal leg-length of the left pair of legs (FL, HL), as l_{BL}. By applying Newtonian mechanics to this particular case, when $l_BR > l_BL$, shown in Fig. 2, the forces are acting on the robot CoG (Center of Gravity) can be analyzed to obtain a relation between the radius of turn (r) and the body-tilt angle (θ) as,

$$r = v^2/(g.\tan(\theta)) \quad (1)$$

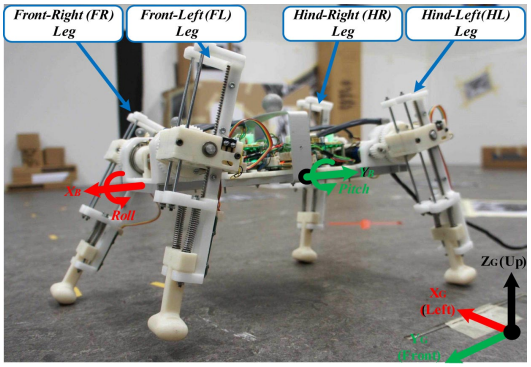

Fig. 1. Four-legged robot "DTAR (Differential Terrain Adaptive Robot)". Total weight of the robot is $2.3 \pm 0.6\ Kg$. Volumetric dimension of the robot is $337 \times 270 \times 256\ mm^3$. Robot has 8 active joints that are powered by the eight DC-brushed motors. Each motor is controlled by the custom developed motor drivers board that uses dsPiC33FJ128MC804 μ-controller.

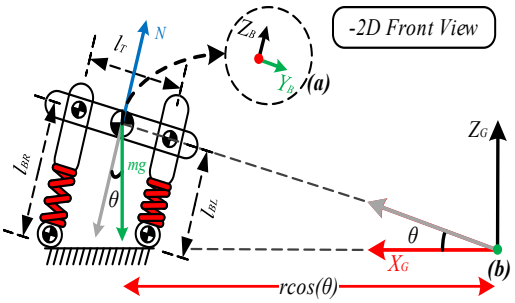

Fig. 2. Free-body diagram of the 2D front view of "DTAR (Differential Terrain Adaptive Robot)". a) points the location of the robot body reference frame which is situated at the robot CoG (Center of Gravity). b) shows location of the fixed ground reference frame. l_{BR} means the length of the leg on body-right side that comprises of two legs (FR and HR). l_{BL} means the length of the leg on body-left side that consists of two legs (FL and HL). l_T is the width of the trunk. Initial conditions for this particular case are $l_{BL} = l_{FL} = l_{HL}$ and $l_{BR} = l_{FR} = l_{HR}$.

where, r is the radius of turn, v is the velocity of the robot, and θ is the body-tilt angle. Similarly, by considering the geometry of the robot structure, we can define the body-tilt angle θ as,

$$\theta = tan^{-1}((l_{BR} - l_{BL})/l_T) \quad (2)$$

Both parameters r and θ can be estimated online using these two equations 1 and 2. The difference between l_{BR} and l_{BL} is defined as the differential change in robot morphology which is denoted by ΔD (see section III). By increasing and decreasing ΔD, maneuverability control in open-loop is practically realized.

III. FEED-FORWARD POSITIONAL CONTROL

The control of the eight decoupled active joints in four-legged DTAR robot, is feed-forward control (open-loop).

Contrary to a closed-loop approach, an open-loop approach provides two main advantages: simple to implement and requires no sensory information. The prescribed shape of the open-loop control signal for each active joint is sinusoidal function, whose amplitude, offset, frequency and phase parameters can be adjusted online. As can be seen in Fig. 1 this robot uses two active degree of freedoms per leg, namely the fixed-rotary and the variable-linear joint; therefore to control four such legs, we programmed eight sinusoidal control signals that are grouped in two types: the actuation signal for the rotary joints (θ_{R_i}), and the actuation signal for the linear joints (d_{L_i}). The actuation signal of rotary joint controls the fore-aft movements of each leg while the actuation signal of linear joint controls the leg reconfiguration of each leg. These two groups of the control signals can be mathematically described as,

$$\begin{bmatrix} \theta_{R_i}(t) \\ d_{L_i}(t) \end{bmatrix} = \begin{bmatrix} O_{R_i} + \Delta\theta_{R_i} \sin(\omega_{R_i} t + \phi_{R_i}) \\ O_{L_i} + D_i + \Delta d_{L_i} \sin(\omega_{L_i} t + \phi_{L_i}) \end{bmatrix} \quad (3)$$

Where, i is the leg index, θ_R is the instantaneous angle at which each leg oscillates in the fore-aft direction, and d_L is the instantaneous change in leg-length. O_R and O_L are the offsets, $\Delta\theta_R$ and Δd_L are the amplitudes, ϕ_R and ϕ_L are the phases, ω_{R_i} and ω_{L_i} are the angular frequencies, and D is the differential change factor. Each of these parameters can be adjusted online to generate a desired foot trajectory of a particular leg. Note subscript $i = 1$ is the leg index number of "Front-Right Leg", $i = 2$ "Hind-Right Leg", $i = 3$ "Hind-Left Leg", and $i = 4$ "Front-Left Leg". Similarly subscript R indicates, this control signal is for the rotary joint, and L points the control signal is for the linear joint.

A. Embedding of Differential Maneuverability Control

Each leg in our robot has the reconfigurable leg-length joint that allows us to change the nominal leg-length per leg, i.e., voluntarily morphing the height of robotic leg. By harnessing this feature, we designed the maneuverability control that introduces the differential change in nominal leg-length of the ipsilateral pairs of legs. This differential change causes the change in robot's body posture, such that it can be inclined online either to the left or the right while moving on a particular gait. This maneuverability control that embedded on the top of existing open-loop control layer, can be defined as,

$$\Delta D = l_{BR} - l_{BL} \quad (4)$$

Where, ΔD defines differential change factor that controls the change in robot body morphology. By adding and subtracting ΔD from the nominal leg length of ipsilateral pairs of legs as $D_{1,2} = \Delta D$ and $D_{3,4} = -\Delta D$, the robot morphology can be adjusted for the task to achieve maneuverability in open-loop.

A voluntary change in our robot morphology by the differential change factor ΔD, introduces three conditions to steer the direction of locomotion. These conditions are as follows:

1) When $\Delta D = 0$: This condition implies the robot-body symmetry ($l_{BR} = l_{BL}$), i.e., all legs are equal in length. If the robot body is initially symmetrical then by applying this condition on a particular gait moves the robot in straight direction.

2) When $\Delta D < 0$: This condition introduces negative asymmetry in the robot-body posture ($l_{BR} < l_{BL}$), i.e., the nominal leg-length of the right pair of legs (FR and HR) is less than the nominal leg-length of the left pair of legs (FL and HL). This inclines the robot body to the robot's right side, thereby the robot turns to its right side on a particular gait.

3) When $\Delta D > 0$: This means positive asymmetry in the robot-body posture ($l_{BR} > l_{BL}$). This shifts the (body-CoG) footprint to the robot's left side. As a result of this, the robot turns to its left side while moving forward on a particular gait.

These conditions of maneuverability are only applicable, when the initial posture of the robot is perfectly symmetrical that means the projection of the robot body-CoG perfectly lies at the center of support polygon.

IV. EXPERIMENTAL SETUP

The maneuverability through voluntary change in the robot morphology was systematically experimented on trot gait, in which the diagonal pairs of legs move $180°$ out of phase from each other (see Fig. 4). We performed these experiments in the room equipped with 10 IR motion capture cameras, as shown in Fig. 3A. These IR cameras form a "motion capture system" that can record the motion (position and orientation) of the reflected markers at $120\ fps$ within its visible volume of $L \times W \times H : 5 \times 4.5 \times 2.6\ m^3$. To record the motion of our robot, we placed five IR reflected markers on the robot's trunk (see Fig. 3B). A cluster of these 5 markers was defined as one rigid body whose motion (position and orientation) is measured relative to the fixed coordinate frame of the motion capture system.

The differential change in robot morphology factor ΔD was altered systematically within a range of $-20\ mm$ to $20\ mm$ in steps of $5\ mm$. The control parameters that were used to achieve stable trot gait, were as follows: the amplitude of four legs oscillation was set to $\Delta\theta_{R_i} = 10°$, the amplitude of four legs reconfiguration was fixed to $\Delta d_{L_i} = 10\ mm$, the phase of leg reconfiguration was set to $\phi_L = 45°$, and the stride frequency (f_{R_i}, f_{L_i}) was fixed to $1\ Hz$. In order to produce trot gait motion sequence, the front right (FR) and the hind left (HL) legs were forced to oscillate at $180°$ out of phase than the leg oscillation of the front left (HR) and the hind right (HL) legs. At each differential change in parameter ΔD we performed 3 trials. At the completion of every trial, robot was physically brought back to the same starting position (see Fig. 3A, point a)), such that the dynamically coupled effect of the robot morphology and the control in natural environment can be quantified. During each ran, we measured the following parameters: position and orientation of the robot body relative to the coordinate of motion capture system (see Fig. 5), the total amount of

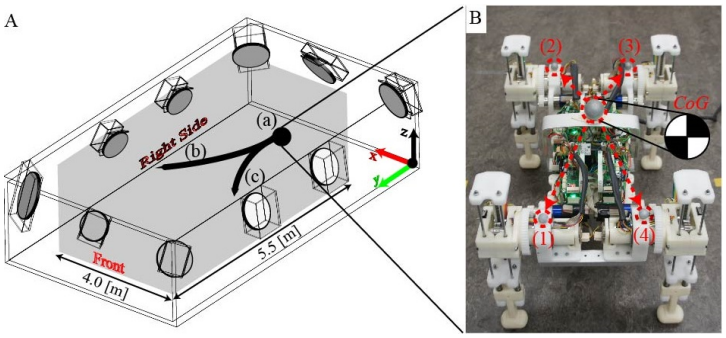

Fig. 3. Experimental setup for the dynamic maneuverability. A) shows the layout of opti-track motion capture system that is equipped with 10 IR (infrared) cameras, B) indicates the placement of 5 IR reflective markers on the robot body. a) indicates the location from where the robot starts running. b) indicates the direction of motion to the right and c) shows the left direction of locomotion.

electrical power consumption (see Fig. 7), the restoring force per leg, i.e., force exerted by the spring to the ground (see Fig. 6), the absolute leg oscillation of each leg, and the angular rate (see Fig. 4) at which body pitches in the fore-aft direction.

V. RESULTS AND DISCUSSION

Four-legged robots can propel their body in a forward direction on wide range of gaits (walk lateral, walk diagonal, trot, bound, gallop etc). These gaits can be quantified either by looking phase of each leg oscillation in the fore-aft direction or by observing the foot-fall pattern of the individual legs. As described in the previous section, we implemented trot gait to study the dynamic turning through voluntary change in robot morphology. We quantify the pattern of trot gait by observing the absolute leg-oscillation of the pairs of legs with respect to time, as shown in Fig. 4. As we know, when four-legged animals move forward on trot gait then they oscillate their diagonal left pairs of legs ((FL,HR), and (FR,HL)) 180° out of phase. Considering this fact, we can evaluate trot gait in Fig. 4 that shows FL and HR legs move in sync together with almost 0° phase shift. As pair they move 180° out of phase from FR and HL legs. In order to clearly observe turning per differential change in leg-length of the ipsilateral paris of legs, we operated four legs at the frequency of $1\ Hz$.

Fig. 5 shows the turning of DTAR robot on a stiff-level ground-floor with respect to the positive and negative differential change in leg-length of the ipsilateral pairs of legs, i.e., ΔD. As can be seen in the result of three trials, at zero differential change, the robot moves nearly straight on trot gait. The turning increases in both the direction from left to right with respect to decrease and increase in differential change in morphology respectively. It can be noted that when the differential change ΔD is less than the amplitude of leg reconfiguration, then the robot makes a gradual turn, i.e., the radius of turn is very large. However, when differential change ΔD is greater than the amplitude of leg reconfiguration then robot turns sharply to the left

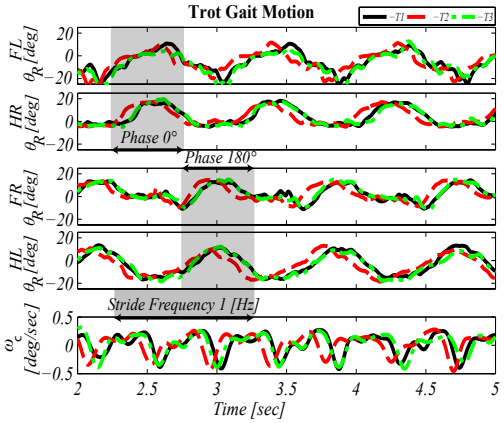

Fig. 4. Trot gait motion at zero differential change, i.e., $\Delta D = 0$. First four plots from the top show the oscillation of each leg over time, while the fifth plot indicates the angular rate of body-pitching.

and right (see the result of -20, -15, 15, and 20 mm). This is indeed true from the model as well, because the large differential change increases the angle of inclination, which is inversely related to the radius of turn. As can be observed the turning to the right at $\Delta D = 20\ mm$ is not resembled to the turning to the left in terms of radius of turn. The reason of this is slight shift in dynamic equilibrium (see section V-A) or asymmetry in the initial conditions.

A. Restoring Forces

Averaged restoring forces of the lateral pairs of legs are measured and plotted with respect to the differential change ΔD in Fig. 6. Fig. 6 indicates the effect of differential change in morphology on the production of restoring forces in the ipsilateral pairs of legs, i.e., the average force exerted by the leg spring (FL and HL) and (FR and HR) to the ground. As can been seen in Fig. 6, the negative ΔD inclines the

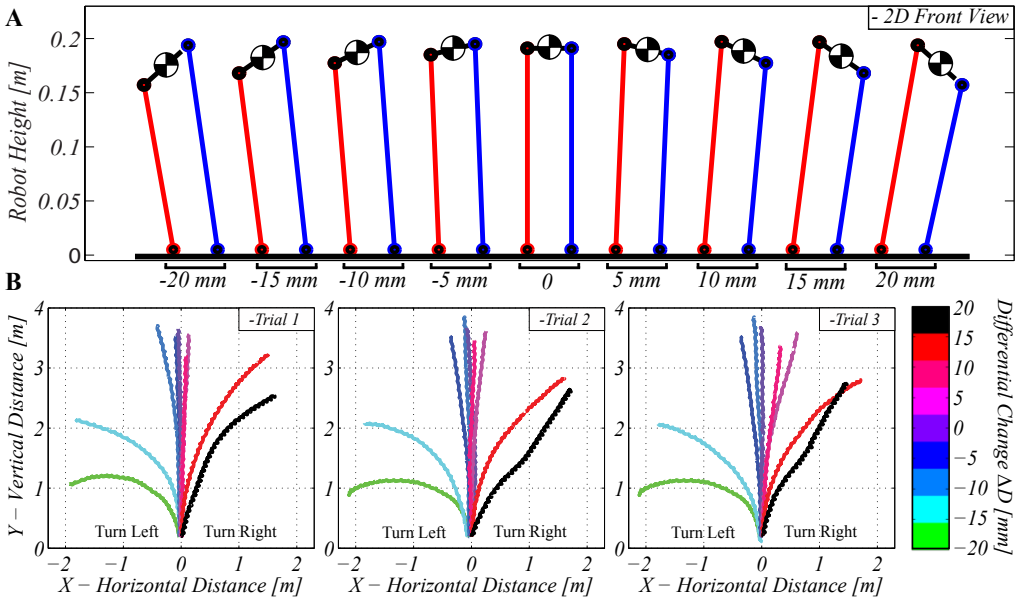

Fig. 5. Maneuverability through a differential change in robot morphology. A) shows the robot front view that describes the change in morphology at various value of ΔD and B) shows the results of three successive trials at fixed change in morphology ΔD. Each color line in B) represents the 2D motion of the robot body on trot gait. Differential change ΔD can be seen in color bar on the right-side.

body to the left or shift the robot CoG to the left that results an increase in weight to the left-side. As a result of this negative asymmetry, the average restoring force on the left-side during locomotion on trot gait, becomes greater in magnitude than the restoring forces of the right-side of the legs. This magnitude of force increases proportionally with the increase in the magnitude of the differential change (see the duration from -5 to -20 mm). This unbalance of restoring forces in the ipsilateral pairs of legs turns the robot to the left. Thus, by the negative differential change the robot motion can be directed to the left side using simple open-loop control.

Conversely, when the differential change is positive. The robot body inclines to the right-side and causes the weight transfer to the right-side of the legs. As a result the average restoring force on the right-side of the leg increases in magnitude than the left-side of the legs. This change increases linear with the increase in positive differential change (see the duration from 5 to 20 mm). By this way the turning of our robot to the right-side on trot gait is achieved.

Interestingly, this figure also shows the dynamic equilibrium, where the straight locomotion at this particular gait can be obtained. It can be noted that the point of dynamic equilibrium, where the average restoring force of the left-side legs becomes equal to right-sides legs, is slightly shifted to the negative side of the differential change (see Fig. 6). This shows the initial asymmetry in the robot CoG, which is usually occurred by the following factors: error in applying the initial conditions (software), and asymmetry in the physical construction of the robot (hardware). By this ipsilateral force distribution analysis at particular gait, we can calibrate the robot to eliminate the effect of initial asymmetry that may affect the unnecessary turning in a four-legged system. It is important to note that due to this initial asymmetry in the robot CoG. The turning of robot in right direction is not exactly same in magnitude as the turning to the left side because of this slight shift in the dynamic equilibrium. There are two potential possibilities to compensate for the shift in dynamic equilibrium: by accurately measuring the body-tilt angle θ, and by measuring the force-distribution per leg.

B. Total Actuation Power

Fig. 7 summarizes the effect of differential change in robot morphology, i.e., change in ipsilateral leg pairs, on the average total actuation power, and the restoring forces. As can be seen in Fig. 7, the average total power consumed by the robot remains unaffected by the active change in the robot morphology. This is also true in case of the total average restoring forces of the four legs. Moreover, it is important to note that the standard deviation in total average restoring force increases with the amount of differential change. This shows the difference of restoring forces in ipsilateral pairs of leg increases (see Fig. 6).

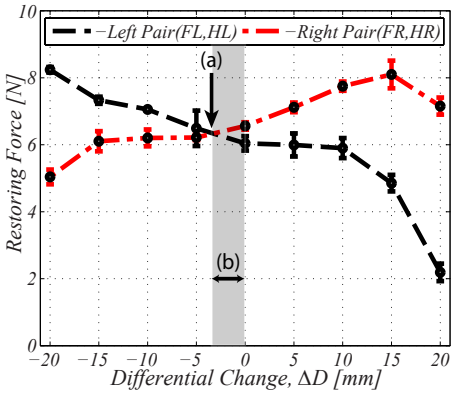

Fig. 6. Averaged restoring forces of the ipsilateral leg pairs with respect to the differential change ΔD. Black line shows the average restoring forces in the FL and HL legs or simply left pair of legs. While the green (dotted) line indicates the change in restoring force in the FR and HR legs or right pair of legs. Point a) shows the point of dynamic equilibrium, and b) indicates the amount of the shift in dynamic equilibrium.

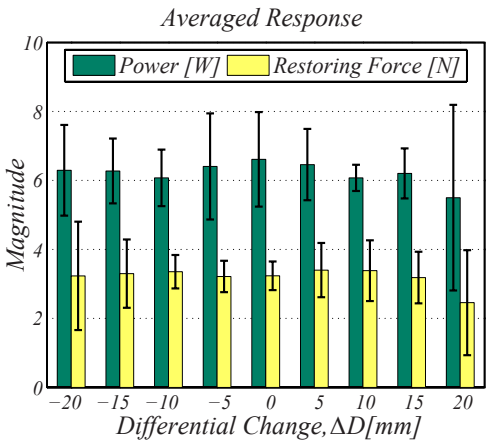

Fig. 7. Averaged total actuation power and restoring forces.

VI. CONCLUSIONS AND FUTURE WORK

Our work demonstrated the concept of maneuverability in a four-legged system in open-loop control. The maneuverability is achieved by utilizing the intrinsic feature of the robot structure, i.e., active leg reconfiguration. By exploiting this feature the differential change in the ipsilateral pairs of legs is implemented as a maneuverability control. This differential change is defined as voluntary morphosis. It simplifies the task of turning our four-legged robot (DTAR) on trot gait in simple open-loop control (no force and damping control). We experimentally verified this concept by systematically introducing the differential change ΔD (-20 to 20 mm in steps of 5 mm) on stable trot gait. Our results suggest that by using this approach the task of dynamic maneuverability can be easily achieved on wide-range of gaits. We intend to advance this approach further on fast dynamic gait (pronk, bound and gallop) to understand the effect of high-speed turning on a four-legged robot.

ACKNOWLEDGMENT

Author would like to extend his gratitude to Prof. Dr. Rolf Pfeifer for his kind guidance, constructive feedback, and immense support. Many thanks to my friend Engr. Sarmad Rashid who helped me in conducting practical experiments.

REFERENCES

[1] M. H. Dickinson, C. T. Farley, R. J. Full, M. a. Koehl, R. Kram, and S. Lehman, "How animals move: an integrative view." *Science (New York, N.Y.)*, vol. 288, no. 5463, pp. 100–6, Apr. 2000.

[2] J. Seipel and P. Holmes, "A simple model for clock-actuated legged locomotion," *Regular and Chaotic Dynamics*, vol. 12, no. 5, pp. 502–520, Oct. 2007.

[3] S. Schaal and C. Atkeson, "Open loop stable control strategies for robot juggling," *Proc. of the 1993 IEEE International Conference on Robotics and Automation*, pp. 913–918, 1993.

[4] M. H. Raibert, H. B. Brown, and M. Chepponis, "Experiments in Balance with a 3D One-Legged Hopping Machine," *The International Journal of Robotics Research*, vol. 3, no. 2, pp. 75–92, Jun. 1984.

[5] M.H. Raibert;M. Chepponis; H.B. Brown, "Running on four legs as though they were one," *IEEE Robotics and Automation*, vol. 2, no. 2, pp. 70–82, 1986.

[6] B. Dynamic. (2013, Jun.) Four legged robots, big dog and alpha dog @ONLINE.

[7] H. Kimura, K. Sakurama, S. Akiyama, and C. City, "Dynamic Walking and Running of the Quadruped Using Neural Oscillator," *Proc. of the 1998 IEEE International Conference on Intelligent Robots and Systems*, no. October, pp. 50–57, 1998.

[8] D. Papadopoulos and M. Buehler, "Stable running in a quadruped robot with compliant legs," *Proc. of the 2000 IEEE International Conference on Robotics and Automation*, vol. 1, no. April, pp. 444–449, 2000.

[9] F. Iida, G. Gabriel, and R. Pfeifer, "Exploiting Body Dynamics for Controlling a Running Quadruped Robot," *Proc. of the 2005 IEEE International Conference on Advanced Robotics*, pp. 229–235, 2005.

[10] U. Saranli, M. Buehler, and D. E. Koditschek, "RHex : A Simple and Highly Mobile Hexapod Robot," *The International Journal of Robotics Research*, pp. 616–631, 2001.

[11] T. J. Allen, R. D. Quinn, J. B. Richard, and R. E. Ritzmann, "Abstracted Biological Principles Applied with Reduced Actuation Improve Mobility of Legged Vehicles," vol. 1, no. October, pp. 1370–1375, 2003.

[12] A. M. Hoover, S. Burden, S. Shankar Sastry, and R. S. Fearing, "Bio-inspired design and dynamic maneuverability of a minimally actuated six-legged robot," *2010 3rd IEEE RAS & EMBS International Conference on Biomedical Robotics and Biomechatronics*, pp. 869–876, Sep. 2010.

[13] D. Jindrich and R. Full, "Many-legged maneuverability: dynamics of turning in hexapods," *The Journal of experimental biology*, vol. 202 (Pt 12, pp. 1603–23, Jun. 1999.

[14] R. J. Full, T. Kubow, J. Schmitt, P. Holmes, and D. Koditschek, "Quantifying dynamic stability and maneuverability in legged locomotion." *Integrative and comparative biology*, vol. 42, no. 1, pp. 149–57, Feb. 2002.

[15] F. I. Sheikh and R. Pfeifer, "Adaptive locomotion on varying ground conditions via a reconfigurable leg length hopper," *Proc. 15th International Conference on Climbing and Walking Robots*, pp. 527–535, 2012.

Appendix F

Preliminary Results of Dynamic Gaits

This appendix shows the preliminary results of dynamic gaits. We have implemented two types of dynamic gaits (pronk and bound) using an open-loop control of single-legged hopper. In pronk gait locomotion all four legs of the DTAR (Differential Terrain Adaptive Robot) moves in-phase, whereas in bounding gait the front pair of legs oscillates $180\,\mathrm{deg}$ out of phase from the hind pair of legs. Typical scientific method to quantify both gaits is to observe the foot-fall pattern. By measuring the foot-fall pattern of pronk and bound gaits (see Fig. F.1 and Fig. F.2), we conclude that the pronking and bounding motion of the DTAR robot seems remarkably similar to the pronk and bound observed in four-legged animal locomotion.

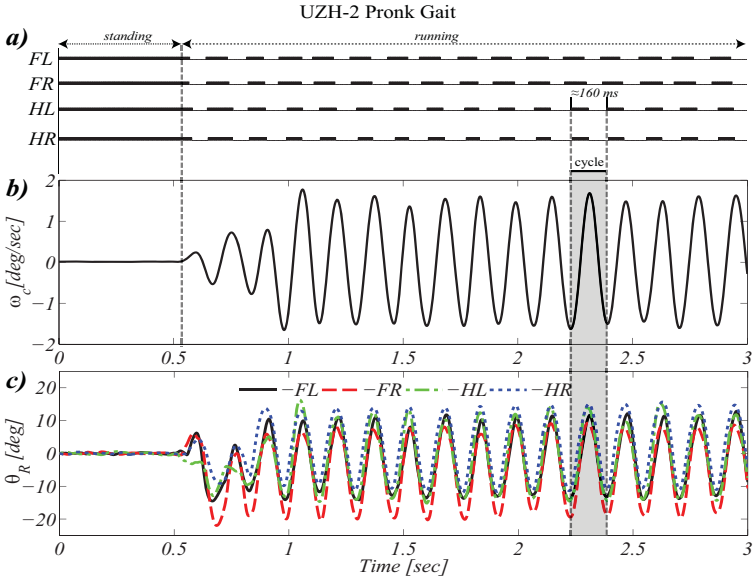

Figure F.1: Four-legged pronking. Plots a), b) and c) are synchronized in time; a) shows the foot-fall pattern of four legs: FL is the front-left leg, FR is the front-right leg, HL is the hind-left leg and HR is the hind-right leg; b) shows the angular rate of pitching of the trunk with respect to the foot-fall pattern and the oscillation of four legs (c); The duration of stride-length is approximately equal to 160 ms and it is indicated by the Gray highlighted area over plot b) and c).

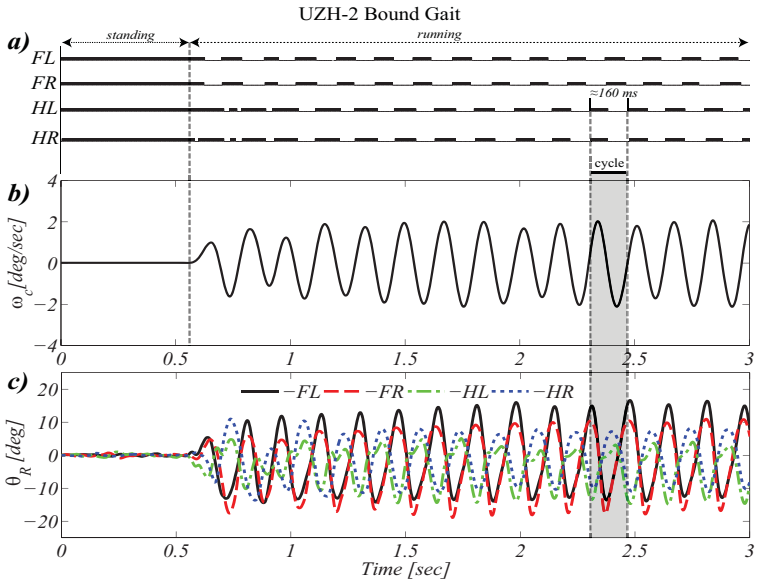

Figure F.2: Four-legged bounding. a) shows the foot-fall pattern of front and hind pair of legs: FL is the front-left leg, FR is the front-right leg, HL is the hind-left leg and HR is the hind-right leg; b) shows the angular rate of pitching in sync with the foot-fall pattern and the oscillation of each leg. The gray-highlighted area over b) and c) shows the duration of stride-length which is approximately equal to 160 ms. Moreover it indicates the effect of alternating leg oscillations between front and hind pair of legs with respect to the rate over which body pitches.

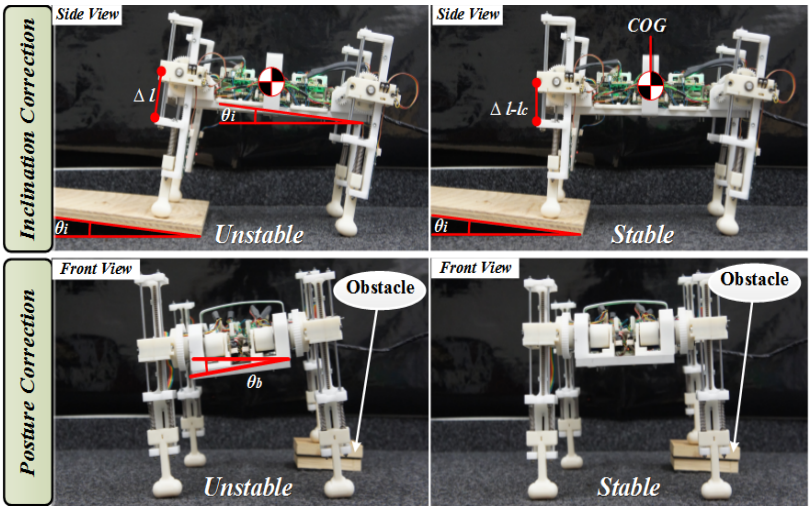

Figure F.3: Enhanced stability in the four-legged DTAR. The top shows the stability enhancement over an inclined surface through leg reconfiguration. The bottom depicts the gain in stability, when the robot encounters an obstacle.

Appendix G

Curriculum Vitae

Name	Farrukh Iqbal Sheikh
Date of birth	15th FEB 1982
Mail address	Lommisweg 12, 8048, Zürich, Switzerland.
Telephone	+41-(0)79-3747186
Email	farrukh.ssuet@gmail.com

Education

Doctor of Science (Ph.D.) **2009 - 2014**
Artificial Intelligence Laboratory (AI-Lab),
Department of Informatics, University of Zurich, Switzerland
Major: Artificial Intelligence, Robotics and Control.

M.Sc Master of Science in Space Science and Technology **2006 - 2008**

1st Semester	Department of Computer Science, Robotics and Telematics, Julius Maximilians University of Wurzburg, Germany.
2nd Semester	Space Science Department, Luleà University of Technology (LTU), Kiruna, Sweden.
3rd- 4th Semesters, and thesis work	Department of Automation and System Technology, Helsinki University of Technology (TKK), Finland.

Major: Space dynamics, robotics, automation and control

BS Bachelor of Science in Electronic Engineering **2001 - 2004**
Department of Electronic Engineering,
Sir Syed University of Engineering and Technology (SSUET)
Major: Analog, and digital electronics, automation and control.

Awards & Scholarships

- Silver medalist 2nd - position holder in BS degree program
- Erasmus Scholarship – MS degree program
- Best team project CAN-Sat
- Best team performance in control of the J2B2 mobile robot

List of Publications

[1]. Sheikh, F. I et al., "Significance of Foot Compliance for Fast and Energy Efficient Legged Robot Locomotion", is submitted to IEEE Transactions on Robotics and Automation.

[2]. Sheikh, F. I et al., "Dynamic Maneuverability through Voluntary Morphosis in a Four-Legged System", In Proceedings of 2013 IEEE International Joint Conference on Cybernetics and Intelligent Systems (CIS) & Robotics, Automation and Mechatronics (RAM), pages 49–54. Manila, Philippine.

[3]. Sheikh, F. I, "Towards Fast Running: Open-loop Speed and Direction Control of a Single Legged Hopper", In Proceedings of 2013 IEEE International Conference on Intelligent Robots and Systems (IROS), pages 5114–5120. Tokyo, Japan.

[4]. Sheikh, F. I. & Pfeifer, R, "Adaptive locomotion on varying ground conditions via a reconfigurable leg length hopper", In Proceedings of 15th International Conference on Climbing and Walking Robots (CLAWAR), pages 527-535. Baltimore, USA.

[5]. Sheikh, F.I., Q.H. Vu, H. Hauser, L. Aryananda, R. Pfeifer, SLIP-Model-Compatible and Bio-inspired Robotic Leg with Reconfigurable Length, In Proceedings of 5th International Symposium on Adaptive Motion of Animals and Machines (AMAM), pages 47–48. Awaji, Japan.

[6]. Sheikh, F.I, “Real-time human arm motion translation for the WorkPartner robot”, M.Sc thesis work in Aalto University, Finland, 2008.